

DOI: <https://doi.org/10.24297/jap.v20i.9268>

A Unifying Theory for Quantum Physics, Part 2:

Exit from the Labyrinth of Quantum Strangeness

Author: Jeffrey H. Boyd*

Affiliation: * Retired. 57 Woods Road, Bethany, CT, 06524-3103 USA

Jeffrey.Boyd@alumni.harvard.edu

Abstract:

The quantum world is allegedly strange. But is it? What if there's a simple mathematical explanation, and a simple solution? The success of quantum mechanics (QM) arises from the accuracy of its probability predictions, which are obtained by squaring amplitudes (the Born rule). Suppose for a moment that nature uses the negative of QM's equations. When squared they would yield the same probabilities, confirmed by the same experiments and technological triumphs. If that were true, if nature uses the negative of QM's equations, then the quantum world would become transparent, easy to understand. No more Schrödinger's-cat. No quantum-eraser. No backwards-in-time cause-and-effect. No paradoxes nor enigmas. But, what's a negative quantum equation? It could mean that particles follow zero-energy waves backwards, instead of forwards. That's still an eccentric idea, a residual strangeness. Overall, it's a bargain. We could swap one odd idea for another, because wave-particle duality is odd. We are accustomed to wave-particle duality. But we'll show that experiments support the other arrangement: quantum particles follow zero-energy waves backwards. How could that possibly be true? We present substantial experimental evidence, new mathematics, and six dozen colorful illustrations. This is the Theory of Elementary Waves (TEW).

Academic Discipline and Sub-Disciplines: Alternative Quantum Physics,

I. Introduction

There is a mountain of experimental data and technological triumphs, that say the quantum world would make perfect sense if we could accept two difficult-to-understand ideas:

- a) Nature uses the negative of our quantum equations, and
- b) Quantum particles follow zero-energy waves backwards.

This proposal is called the Theory of Elementary Waves (TEW). We review that mountain of empirical evidence in vivid detail.

If you would rather read a brief synopsis, each section of the article starts with a short, one or two paragraph "**Thumbnail Sketch**" that provides an executive summary. Those sketches are demarcated in red typeset, easy to find, easy to understand, and they cover the whole territory. In today's video-game world some readers get bored and stop reading anything that takes longer than sixty seconds, so these Thumbnail Sketches are an accommodation to that reality.

Consider Richard Feynman's idea of path-integrals. A law of calculus is that if you swap the bounds of integration, you get the negative of the integral. This means that if you integrate in the opposite direction, then you would get the negative of Feynman's path-integrals. That ties our two main themes together: nature using the negative of QM's equations, and quantum particles following zero-energy Elementary Waves backwards. The integration proceeds in the same direction as the waves.

The idea around which this article is organized is amazingly simple. The spectacular success of Quantum Mechanics (QM) is based on the accuracy of its probability predictions. The Born Rule says they are derived by squaring quantum amplitudes. Every probability has two square roots. This article proposes that nature uses the other square root, hitherto ignored. Both square roots ($+\psi$ and $-\psi$) are confirmed by the same lab data. Both could take credit for our high-tech economy. We call it the Max Born asymmetry: $Probability = |+\psi|^2 = |-\psi|^2$. With one square-root ($+\psi$) the waves and particles travel in the same direction (wave-particle duality). With the other ($-\psi$) they travel in opposite directions.

Even if this article is wrong, or partly wrong, it contains thought-provoking clever new ideas that might awaken physics students out of their slumber if you give them this article, with the assignment, "Prove that this theory is wrong!"



The strongest proof of our idea (TEW, $-\psi$), aside from the mountain of evidence we are about to present, is that the quantum and classical worlds would then be governed by the same rulebook. Except for the strange idea that “particles follow zero-energy waves backwards”, there is nothing unimaginable, or even peculiar about the quantum world. Enigmas such as the quantum-eraser, Wheeler’s *Gedanken*-experiment, and Schrödinger’s cat disappear in simple and logical ways, as you will see.

Comparing our theory to garden-variety QM ($+\psi$), what is the same, versus different? TEW ($-\psi$) will not significantly change bound particles, harmonic oscillators, the Periodic Table, nor chemical compounds, because if particles and waves gyrate around each other, it doesn’t matter if they travel in the same or opposite directions. The Standard Model won’t change, because in it there are no particles, just fields. But free particles will be dramatically different. With TEW ($-\psi$) they will follow backwards zero-energy Elementary Waves coming from the detectors. Therefore, interferometer and double-slit experiments will be central to our discussion.

It is astounding how many people think that all waves must carry energy, and therefore our ideas are wrong. They forget that Schrödinger waves carry no energy. They may carry a Hamiltonian or momentum operator, but not raw energy. They cannot push or pull particles, nor do any work. Quantum equations concern probability amplitudes, which are different from energy. Even an amplitude for energy is different from energy. Schrödinger waves and Elementary Waves travel in opposite directions. Energy and Elementary Waves travel in opposite directions.

Some scholars reject our theory on the grounds that they accuse it of being “metaphysics.” But wave-particle duality is also metaphysics, it just happens to be metaphysics you have grown accustomed to. So why is the metaphysics of wave-particle duality OK and then you accuse us of metaphysics? We challenge you, if you think this way, to open your mind long enough to examine the empirical evidence before you decide what is science and what is metaphysics.

Thomas Kuhn, in the *Structure of Scientific Revolutions*, says that when a new paradigm emerges in science, it sounds like unintelligible gibberish to established scientists. For example, Alfred Wegener proposed in 1912 that there had once been a supercontinent for which he coined the name Pangaea {from Ancient Greek pan (all, entire, whole) and Gaia or Gaea (Mother Earth, land)}. The supercontinent fragmented and drifted to become today’s continents. In 1912 no one knew there were mountain ranges beneath the oceans. India slid north, collided with Eurasia, and uplifted the Himalayas. All experts agreed that there was no force strong enough to move continents. Therefore, Wegener’s ideas were banished from science until 1960 because they were said to be preposterous. This article seeks to be to quantum physics what Pangaea was to geology. Pangaea led to plate tectonics, and this article will probably lead to technology and science that cannot yet be imagined.

2. The First Three Experiments

We now present the first three out of a mountain of experiments from leading scientific journals. These demonstrate our thesis that quantum particles and zero-energy waves travel in opposite directions. After this section we will address and solve some of the mysteries of QM: the quantum eraser, Wheeler’s thought experiment and Schrödinger’s cat.

2.1 A Neutron Interferometer Experiment

2.1.1 Thumbnail Sketch of This Neutron Interferometer Experiment, in Two Paragraphs

Figure 1 shows the neutron interferometer experiment we will discuss. Something called the “NP Analyzer Crystal” (at the red arrow), downstream from the interferometer, changes the interference upstream, inside the interferometer. That is an unexpected outcome. So, there you have the whole experiment in a nutshell. Somehow that NP Analyzer Crystal restores robust interference upstream inside the interferometer!

The experimenters say that neither they nor QM can explain this experiment. **Reiterate: this is an experiment that QM cannot explain.** The only coherent explanation anyone has suggested is that zero-energy waves travel from the detector, backwards through the interferometer, up into a nuclear reactor. Then neutrons follow those Elementary Waves backwards. It is a complicated experiment, but it produces clear results for which TEW is the only known explanation. This description is six pages long, and frankly, you can skip the equations because they won’t tell you anything decisive. How often does a QM article tell you, “Frankly, you can skip the equations”?



2.1.2. The Kaiser Neutron Interferometer Experiment

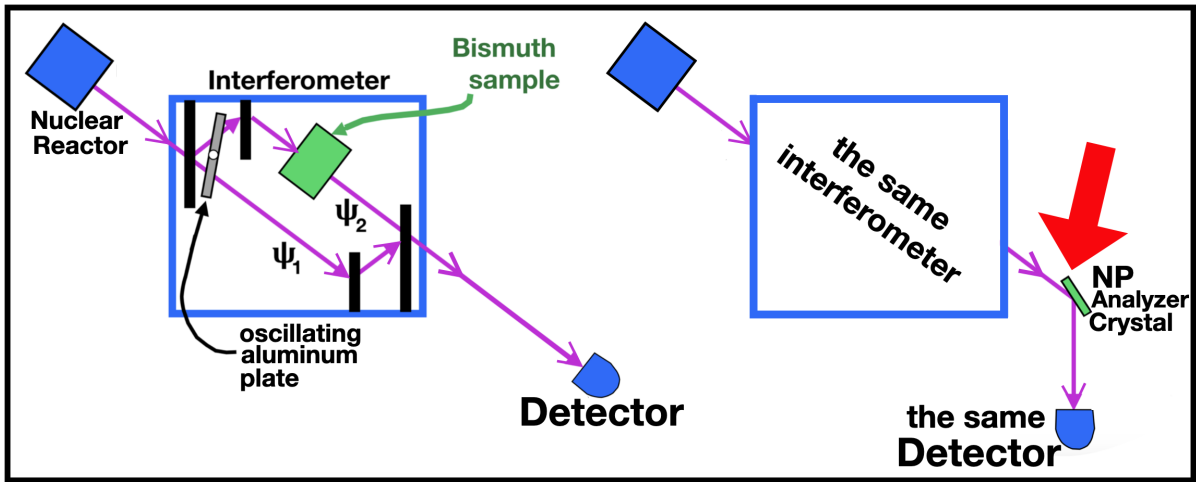


Fig. 1. Left: A perfect-silicon-crystal Neutron Interferometer (NI) with two arrangements of the detector. Left: Incoming neutrons are divided by silicon blades (black) into two beams (purple arrows). An oscillating ($\pm 1^\circ$) aluminum plate induces a phase shift so when ψ_1 and ψ_2 are recombined, the ^3He detector records a sinusoidal curve. A sample of bismuth is inserted (green), slowing ψ_2 but not ψ_1 . When ψ_1 and ψ_2 are recombined the interference diminishes as more-and-more bismuth is added. This means flattening sine waves, measured as decreasing relative contrast. Right: A “nearly-perfect” (NP) silicon-crystal is inserted (at the red arrow) outside and downstream. The data will show that the insertion of that NP Analyzer Crystal downstream restores robust interference upstream inside the interferometer!

A research team founded by Helmut Rauch in Austria did the basic research that created the field of neutron interferometry. We will discuss one aspect of one article published by that team. The experiment was conducted at the University of Missouri Research Reactor. The publication was authored by Helmut Kaiser, Russell Clothier, Samuel Werner, Helmut Rauch, and H. Wölvitsch and published in *Physical Review A* in 1992. (36)

The Kaiser research team sends a beam of neutrons from their reactor into an interferometer (Figure 1 left), within which the beam is divided by silicon blades (black rectangles) into two beams ψ_1 and ψ_2 , then re-combined into one beam that exits the interferometer through an exit beam called C3 and measured by a ^3He detector. All the data comes from that detector. Where ψ_1 and ψ_2 bifurcate there is an oscillating aluminum plate that creates a phase difference between ψ_1 and ψ_2 , so when they rejoin there is a sinusoidal curve (interference pattern), the height of which is measured by a metric called “Relative Contrast (%)”

Then in Figure 1 right, at the red arrow, an NP Analyzer Crystal is inserted downstream, prior to the detector.

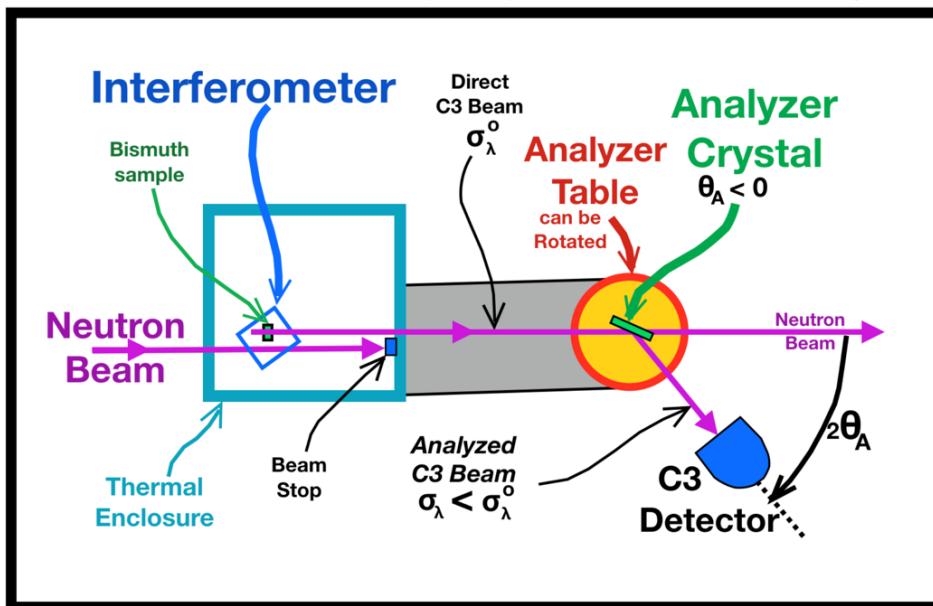


Fig. 2. The interferometer (a small square in blue on the left) is dwarfed by its surroundings. The analyzer table (yellow), which can be rotated, is 60 centimeters downstream from the interferometer. The ^3He Detector (blue) can be rotated into the Direct C3 Beam without an Analyzer Crystal, or (as in this diagram) into the (111) Antiparallel Configuration of the NP Analyzer Crystal. The Bragg angle of the Analyzer Crystal is $\theta_A = -22.0^\circ$ and therefore the angle is $2 \times \theta_A = -44.0^\circ$ in this diagram.

Bismuth is a metal of atomic number 83, which slows neutrons and neutron waves. They insert a sample of bismuth of various widths (D goes from 0 to 20 mm) in the upper path Ψ_2 but not the lower path Ψ_1 . As they increase the width of the bismuth sample from $D = 0$ mm to $D = 5, 10$ mm, etc, the upper wave packet no longer overlaps neatly with the lower Ψ_1 wave packet when they are recombined in the final silicon blade inside the interferometer, so there is a diminishing amount of interference: the sinusoidal curves flatten out toward a straight line. With 12 or more mm of bismuth there is almost no interference, interpreted as meaning that the upper wave packet is so delayed that the lower wave packet Ψ_1 leaves the interferometer before the Ψ_2 wave packet arrives at the reunion point, which is the fourth and final silicon blade inside the NI.

The wave packet of neutrons has a coherence length Δx of 86 Å. A full sample of $D = 20$ mm of bismuth causes a 435 Å delay in Ψ_2 , which is five times the coherence length Δx .

Then the researchers repeat the same experiment, with only one tiny change. Outside and downstream from the interferometer, in front of the detector, they insert a “nearly perfect” (NP) Analyzer Crystal of silicon: $\Delta\theta = 0.02^\circ$ full width at half maximum (FWHM), $\eta_A = 0.00015$ rad. The letters “NP” are important because the researchers also report data from another analyzer crystal of pressed silicon, and those data are not pertinent to this article. Any analyzer crystal data with the name “PR Analyzer Crystal” (“PR” for “PRessed”), are not included in this article, because they are irrelevant to this discussion.

That NP crystal is shown as a thin green rectangle in the Figures. It is expected to decrease the scatter of wavelengths of the neutron beam, and increase the center of the Gaussian, so the beam will penetrate the ^3He detector better. The Analyzer Crystal is expected to have no effect on the interference occurring upstream inside the interferometer. Nothing said by the researchers indicates that they ever thought about the unusual idea that waves might be traveling in a direction opposite to the neutrons.

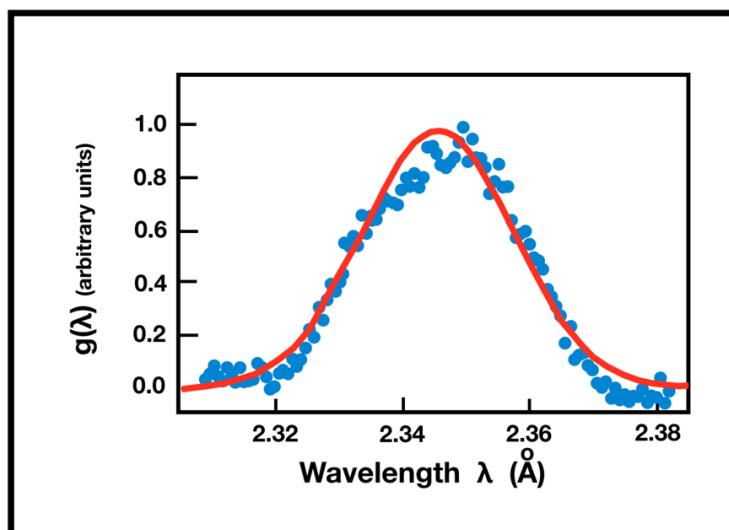


Fig. 3. The wavelength (λ) of incoming neutron waves forms a Gaussian curve. When an NP Analyzer Crystal is inserted into this beam, the horizontal spread of wavelengths decreases, and the height of the peak of the Gaussian increases greatly.

2.1.3 Mathematics of the Kaiser Neutron Interferometer Experiment

The researchers begin their report with a 5–page discussion of mathematics before they discuss the experiment. We presume that this long mathematical introduction is motivated by the unsuccessful desire to find a reason for data (discussed below) that they cannot explain. Some of that mathematics we will reproduce here, but it doesn't explain what happens in this experiment. In the end they blame their data on “Wheeler's smoky dragon,” referring to a cartoon John Wheeler once published showing a dragon inside a research apparatus, but the dragon is obscured by a cloud of smoke so you can't figure out what it is up to, until suddenly it pops out of the cloud and bites one of the detectors.

Kaiser's article emphasizes that a neutron wave packet depends on a Fourier sum of plane waves. They say that a Fourier sum of plane waves alters the coherent overlap of two wave packets (Ψ_1 and Ψ_2) traversing a perfect silicon crystal neutron interferometer (NI) by placing a sample of bismuth in the upper of the two paths. The

optical potential of bismuth is positive, so it causes a delay in the wave packet traversing it, so that when that when the wave packets (Ψ_2 and Ψ_1) re-join there is a loss of fringe visibility.

The Kaiser team says that the superposition principle is the most important assumption in QM. It allows us to use a Fourier sum of plane waves with a spectrum $a(k)$:

$$\Psi(r, t) = \int a(k) e^{i(k \cdot r - \omega_k t)} dk.$$

The plane waves add constructively in certain restricted areas since the phases are correlated by $a(k)$, as everyone knows.

After the neutrons enter the NI they encounter an oscillating aluminum plate which they call a “phase rotator.” It induces a variable phase difference between Ψ_1 and Ψ_2 , of value $\phi_p(\alpha)$, given by this equation:

$$\phi_p(\alpha) = N_p b_p \lambda d \frac{\sin^2 \theta_1 \sin \alpha}{\cos^2 \theta_1 \sin^2 \alpha}$$

where α is the oscillating angle of the slab, the neutron wavelength is λ , and $N_p b_p$ represents the density of the atom and the scattering length of the neutron. The thickness of the aluminum slab is d , and θ_1 is the Bragg angle of the NI.

The bismuth is called the “sample.” It induces a spatial delay

$$\Delta l = -\frac{DV_{op}}{2E}$$

in Ψ_2 , where E is the kinetic energy of the neutron, and its optical potential is

$$V_{op} = 2\pi \hbar^2 N b / m$$

and the neutron’s mass is m . They assume that the beam is not attenuated by the bismuth sample.

If a detector is placed in an exit beam, it will measure a time-averaged intensity of

$$I(D, \alpha) = A \int_{-\infty}^{+\infty} |a(k)|^2 dk + B \int_{-\infty}^{+\infty} |a(k)|^2 \cos[\phi_o + \phi_p(\alpha) + \chi_S(D)] dk$$

where ϕ_o is a constant that starts with a value $\phi_o = 0$. The counting rate $I(D, \alpha)$ is affected by the value of D and α . The variable B is for exit beam C3 and depends on how well the NI is functioning that day. Interferometers undergo subtle changes of shape over the course of a day. With the C3 exit beam usually $BC_3 \approx (0.5)AC_3$, the first integral in the previous equation

$$A \int_{-\infty}^{+\infty} |a(k)|^2 dk$$

is a constant. The second integral oscillates as they vary $\phi_p(\alpha)$. For example, if $|a(k)|^2$ is a Gaussian with standard deviation Σ_k then the equation gives us an intensity of:

$$I(D, \alpha) = A + B[\cos \phi_o + \phi_p(\alpha) + \chi_S(D)] e^{-(N_b D \Sigma_\lambda)^2 / 2}$$

where $\Sigma_\lambda = 2\pi \Sigma_k k^2$ is the width in wavelengths of the spectral distribution.

$$C_R(D) = e^{-(N_b D \Sigma_\lambda)^2 / 2}.$$

As they vary $\phi_p(\alpha)$ they trace out the sinusoidal pattern $I(D, \alpha)$ of an interferogram.

They define the “contrast” of the interferogram to be the amplitude of the oscillations (from bottom to top of the sinusoidal curve) divided by the mean value. The maximum contrast occurs when there is no bismuth: i.e. $C_{C3}(0)$.

The contrast $C(D)$ decreases as the sample thickness D increases. **The symbol “0” in their equations means “no bismuth sample”** and will be visible in many of their equations.

The equipment is imperfect, and they adjusted their equations to fit that reality. While in theory the C_{C3} varies from 0% to 100%, actually $C_{C3}(0) \approx 50\%$. To adjust to this imperfect equipment, they focus on the **relative contrast** $C_R(D) \equiv C(D)/C(0)$. They can calculate the relative contrast from the complex mutual coherence function $\Gamma(D, \alpha)$ as follows:

$$C_R(D) \equiv \frac{C(D)}{C(0)} = \frac{|\Gamma(D, \alpha)|}{|\Gamma(0, 0)|}$$

where they define

$$\Gamma(D, \alpha) \equiv \langle \Psi_1^*(0) \Psi_2(\Delta l) \rangle = \frac{1}{\sqrt{2\pi}} \int_{-\infty}^{+\infty} |a(k)|^2 e^{i\phi_o + i\phi_p(\alpha) + i\chi_S(D)} dk.$$

Note that of $\Gamma(D, \alpha)$ depends only on $|a(k)|^2$. If the displacement Δl is parallel to k , one can replace $|a(k)|^2$ by the wavelength spectrum $g(\lambda)$ in the equation to calculate $\Gamma(D, \alpha)$:

$$\Gamma(D, \alpha) = \frac{1}{\sqrt{2\pi}} \int_{-\infty}^{+\infty} g(\lambda) e^{i\phi_o + i\phi_p(\alpha) + i\chi_S(D)} dk.$$

In this experiment $\phi_p \ll \chi_S$, so the oscillating aluminum plate has a negligible effect on the contrast. Thus, with a Gaussian distribution $|a(k)|^2$, the contrast diminishes as a function of the thickness D of bismuth as follows:

$$C_R(D) = e^{-(N_b D \sum \lambda)^2 / 2}$$

The goal of Kaiser and his team is to study a coherent neutron beam and observe changes in the contrast of the interferogram detected in the C3 output beam. Unfortunately, there are other factors that also decrease the contrast. This must be corrected for. First, the beam is attenuated as it passes through the bismuth sample, although they did not mention it heretofore. The Ψ_2 wave is attenuated by $\exp(-\zeta)$ because of the absorption and scattering cross sections of the material. In previous research with this same equipment these researchers found the following loss of contrast with increasing sample thickness:

$$\left[\frac{C(D)}{C(0)} \right]_{att} = \frac{e^{-\zeta}}{a_1 + e^{-2\zeta} a_2}$$

Where the subscript “att” means “attenuated,” and a_1 and a_2 are the fractions of the beam intensity on the lower and upper path through the interferometer, where ($a_1 + a_2 = 1$). Thus, if they want to know what the contrast would be without the attenuation by the sample of bismuth, then they multiply their measured results (C_{meas}) by a factor f_{att} as follows:

$$C = C_{meas} \cdot f_{att}$$

where

$$f_{att} = C_{meas} \cdot e^{\zeta} (a_1 + e^{-2\zeta} a_2).$$

In addition to attenuation, there are other factors that make their equipment less than perfect: thermal gradients, gravitational warping of the crystal, vibrations, and imperfect machining of the crystal. In view of these defects, it is understandable that they would achieve a maximum of 50 % rather than 100 % contrast.

2.1.4 Theory of Crystal-Analyzed Coherence Measurements

They place their NI in a beam of neutrons with a Gaussian distribution of $\sum \lambda$ and a distribution of wavelengths

$$g_0(\lambda) = \frac{1}{\sqrt{2\pi} \sum \lambda} e^{-(\lambda - \lambda_0^2 / 2(\sum \lambda)^2)}.$$

Now consider placing the NP Analyzer Crystal in the exit beam C3. The Analyzer Crystal has a mosaic width of η_A and reflects out an exit beam with spectral width Σ_λ with a Gaussian distribution of wavelengths. Because the NP Analyzer Crystal decreases the scatter of wavelengths and increases the central peak of the Gaussian, the contrast could be higher in that beam than in the unanalysed C3 exit beam.

The NP Analyzer Crystal accepts a Gaussian window of wavelengths

$$W(\lambda) = e^{-(\lambda-\lambda_0^2/2(\Sigma_\lambda^0)^2)}$$

of width Σ_λ^0 as follows:

$$\Sigma_\lambda^A = \lambda_0 \eta_A \left| \frac{\cos(\theta_I) \cdot \cos(\theta_A)}{\sin(\theta_I - \theta_A)} \right|$$

where θ_I is the interferometer Bragg angle ($\theta_A = -22^\circ$). The analyzer Bragg angle θ_A is negative for an antiparallel configuration such as the one used here. The letter A in the variable θ_A refers to the Bragg angle of the “Analyzer.”

Table S1. Spectral widths expected in C3 Direct, and NP analyzed beams:

Beam	η_A (rad)	Σ_A	$\Delta\lambda/\lambda_0$
C3 Direct	_____	0.0120	1.20 %
NP Analyzed	0.00015	0.00030	0.03 %

Table S2. Signal and background counting rates per minute.

Beam	Signal	Background	Time
C3 Direct	1030	49.1 ± 1.2	5
NP Analyzed	32	61.2 ± 1.1	40

The spectrum $g(\lambda)$ reflected off the Analyzer Crystal is the product of the analyzer window $W(\lambda)$ and the incident spectrum $g_0(\lambda)$.

As we said, the term “ $C_{C3}(0)$ ” is defined as the amount of contrast in the C3 exit beam leaving the interferometer, when there is no bismuth sample. That is the state of the interferometer which they refer to as “**sample out.**” Every time they had a run of data, they would repeat that run with the sample of bismuth “out” so they could calculate the amount of contrast relative to how much contrast there would have been if there were no bismuth. It was tedious because the bismuth was a tiny, soft slice of metal inside a tiny box (the NI), in a lab that became hot in the late afternoon.

$$g(\lambda) = g_0(\lambda)W(\lambda) = \frac{1}{2\sqrt{2\pi} \Sigma_\lambda} e^{-(\lambda-\lambda_0^2/2(\Sigma_\lambda)^2)}$$

where the width Σ_λ is given by

$$\Sigma_\lambda = \Sigma_\lambda^0 \frac{\Sigma_\lambda^A}{[(\Sigma_\lambda^0)^2 + (\Sigma_\lambda^A)^2]^{1/2}}$$

The form of this equation insures that $\Sigma_\lambda < \Sigma_\lambda^0$ which is what they need a crystal with an antiparallel configuration.

$$C_A(D) = e^{-(NbD \Sigma_\lambda)^2/2} \geq C_{dir}(D)$$

How does this affect their measurements? The direct C3 exit beam coming out of the NI has a spectral width of Σ_λ^0 . As they increase D (increase the sample thickness of bismuth) its contrast $C_{dir}(D)$ diminishes with $\Sigma_\lambda < \Sigma_\lambda^0$.



2.1.5 The Experiment

Kaiser, et.al. report on four runs of data, of which our article reports only two. They have a run of data with no Analyzer Crystal, one with a “Pressed Silicon” (PR) crystal in a 111 anti-parallel position, a third run with a PR Analyzer Crystal in a 111 parallel position, and the fourth run of data was the “Nearly Perfect” (NP) Analyzer Crystal in the 111 anti-parallel position. They tend to emphasize the PR Analyzer Crystal data (presumably because those data made sense), and they tend to de-emphasize the NP Analyzer Crystal data (presumably because those data made no sense to them). By contrast, we have completely ignored all the PR Analyzer Crystal data and emphasized the NP Analyzer Crystal data precisely because it cannot be explained by QM.

The research team had to decide what analyser crystals to use, and what Bragg angles. As we said, we will report only data gathered from a “nearly perfect” (NP) silicon crystal: $\Delta\theta = 0.02^\circ$ full width at half maximum (FWHM), $\eta_A = 0.00015$ rad. They used this NP Analyzer Crystal in the (111) antiparallel configuration. With an incoming neutron beam of $\lambda = 2.35 \text{ \AA}$ the Bragg angle that they use is $\theta_A = -22.0^\circ$.

They machine bismuth to different thicknesses. It is a soft metal and difficult to work with. A slice of soft metal 5 mm thick is extremely delicate and demands utmost attention to insert that delicate slice into the tiny interferometer. The NP Analyzer Crystal is mounted on a goniometer (see Figure 2), the tilt and rotation of which are controlled by a step motor. That apparatus is called the “analyser table” and is located ~ 60 cm downstream from the interferometer. When the crystal is placed in the C3 beam its tilt and position are optimized for obtaining the (111) Antiparallel Configuration.

The detector is black to thermal neutrons, and consists of three detectors, each of which is a 0.5 inch, cylindrical, 20-atm ^3He detector mounted on a neutron-shielding B4C-epoxy cassette with a one-inch by one-inch collimated opening. This makes the probability of detection constant in a horizontal plane. To see all parts of the neutron beam spectrum, all the C3 detectors are mounted horizontally.

Most neutrons coming through the interferometer are not refracted, because they fall outside the window. The “Direct Beam” also diverges and would spill into the C3 detector and would overwhelm the relatively weak C3 exit beam. So, they placed a “Beam Stop” consisting of a B4C-epoxy block inside the thermal enclosure (see Figure 2, left of center of the diagram).

As stated earlier, a NI operates far below 100 % efficiency. Dephasing causes a relative drop in contrast from a starting value of C_0 to $C(D)$.

Using standard statistical methods they calculate the sample-out contrast $C_o \pm \Sigma_o$ and the sample-in contrast $C_{in} \pm \Sigma_{in}$ and then use those numbers to calculate the relative contrast, which is their main statistic $C_R \pm \Sigma_R$ using the equation:

$$C_R = \frac{C_{in}}{C_o},$$

where

$$C_R = C_R \left| \left[\frac{\Sigma_o}{C_o} \right]^2 + \left[\frac{\Sigma_{in}}{C_{in}} \right]^2 \right|^{1/2}$$

They calculate the relative contrast at a full range of D (thickness of bismuth). Then they insert the NP Analyzer Crystal in the (111) Antiparallel Configuration ($\theta_A = -22.0^\circ$). Because of the long run times for this configuration, they collect less data, meaning that they collect data for D at values 4, 8, 12, 16 and 20 mm. Therefore, the data are slightly thinner for that run, but there are nevertheless adequate data for use in Figure 3.

2.1.6 Results

The experiment presents astonishing results. Figure 4 (blue sinusoidal curves) shows the dampening effect of bismuth on the wave interference inside the interferometer. Figure 5 (red sinusoidal curves) shows that somehow, against all reason, the NP Analyzer crystal at the red arrow in Figure 1, restores robust wave interference (tall sine waves), as if the bismuth were invisible. Then Table 1 gives you statistics from the article, which say the same thing.

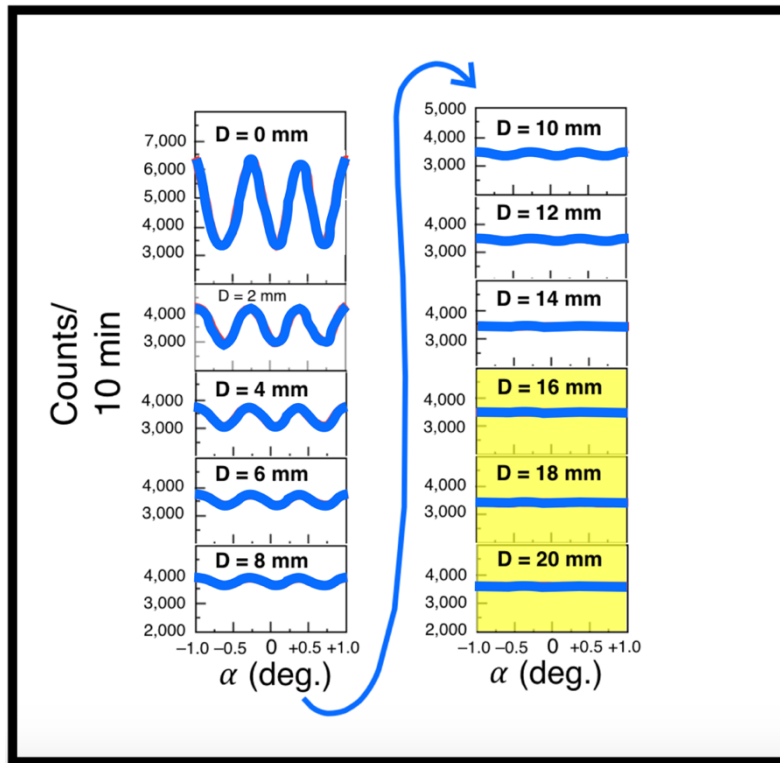


Fig. 4. This shows the interferograms with no Analyzer Crystal. We added the yellow highlight to call attention to the loss of Relative Contrast with enough bismuth. (Data from p.37, Figure 8, “Direct C2”)(37)

When a Nearly Perfect (NP) Analyzer Crystal is inserted outside and downstream from the interferometer, robust interference is restored upstream, no matter how much bismuth is used. The experimenters say that neither they nor QM can explain these data.

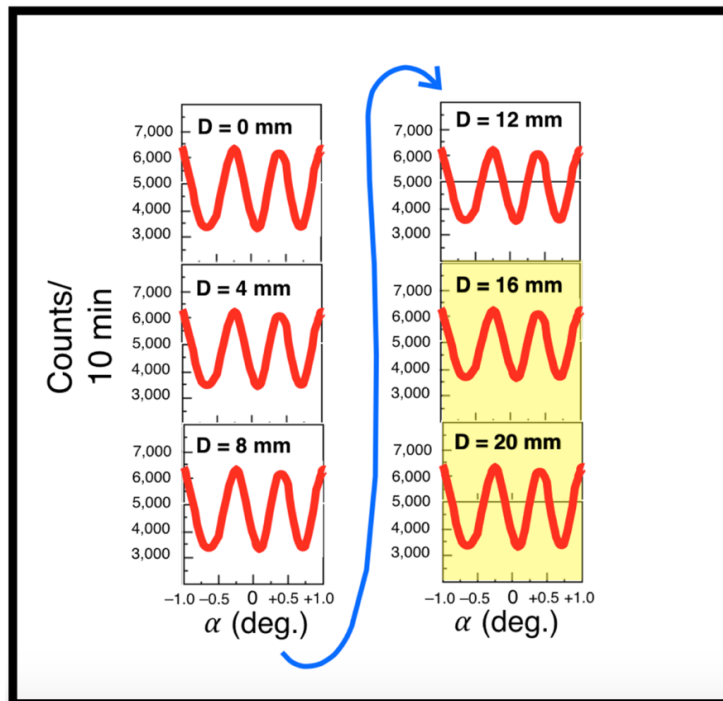


Fig. 5. This shows the robust interferograms with an NP Analyzer Crystal inserted outside and downstream from the interferometer. This diagram is dramatically different from the preceding one. We added the yellow highlight to call attention to the loss of Relative Contrast with enough bismuth. (Data from Figure 9 top and bottom, p. 40)(36)

Somehow the NP Analyzer Crystal reinstates full-bodied interference even though it is downstream! (Table 1).

2.2.1 Thumbnail Sketch of This Reversal of Feynman's Path-Integrals, in 2 Paragraphs

TEW says that Elementary Waves start at the detector in an experiment with a free particle, and travel to the photon source, and then a photon follows the wave back to the detector. Thus our waves and particles travel in opposite directions, which is different from Feynman's way of thinking. For this reason we develop new path-integral equations which start earlier, and travel in the opposite direction as Feynman's path-integrals. Because of that reversal, our equations are the negative of Feynman's path-integral equations.

That explains the equations you are about to encounter. But then the question is, why bother overhauling Feynman's equations in this way? The answer to that question depends on whether or not it is important to you to develop a logically self-consistent model, or whether you are content with the illogicality of Feynman's approach. What illogicality? Feynman requires his students to agree to the proposition that every single photon traveling from any point **a** to any point **b**, takes an infinite number of pathways simultaneously! His students didn't agree. They said one photon can only take one trajectory. The only mathematical way to reconcile the two viewpoints, is the TEW equations we are about to derive. Figure 6 is interesting to look at, if you want to understand what we are talking about..

2.2.2 Derivation of Reverse-Path-Integral Equations

When considering Feynman's path integrals, our "Max Born asymmetry" ($|-ψ|^2 = |+ψ|^2 = \text{probability}$) needs to be rewritten $|K_R|^2 = |K|^2 = \text{probability}$, where K_R is the "reverse-path integral", and K is the "path integral" or amplitude. (33)

We will integrate Feynman's path integral in the opposite direction as Feynman, as we said, starting at detector **b** and moving continuously across all pathways to a photon source **a** (**b**→**a**). We derive our equations from Feynman and Hibbs' equations 2.17-2.25, by **swapping the bounds of integration**. (33)

As we said, and as you already know, when you swap the bounds of integration you get the negative of the integral. Therefore, our TEW functionals are the negative of the functionals of Feynman and Hibbs. We will use subscript "r" to indicate our Reverse functionals. For example, our

$$\mathbf{R-path\ integral} \equiv K_R(a, b) = -K(b, a) \equiv \mathbf{Feynman's\ path\ integral}$$

$$\mathbf{R-action} \equiv S_R = -S \equiv \mathbf{Feynman's\ "action"}$$

$$\mathbf{R-Lagrangian} \equiv \mathcal{L}_R = -\mathcal{L} \equiv \mathbf{Feynman's\ "Lagrangian"}$$

What Feynman and Hibbs' path integral measures is the amplitude for a particle moving from the source **a** to a detector **b** in a fixed time-period. By this they do not refer to any one specific path. It was the particle's amplitude across **all** possible pathways, of which there were an infinite number.

Because Feynman's integrals embrace all pathways, he is forced to say that every photon always takes an infinite number of routes simultaneously, an idea that only makes sense to him. How else could he justify K embracing all pathways unless the photon does likewise? That illogical idea arises from the mathematics of wave-particle duality, which we regard as false.

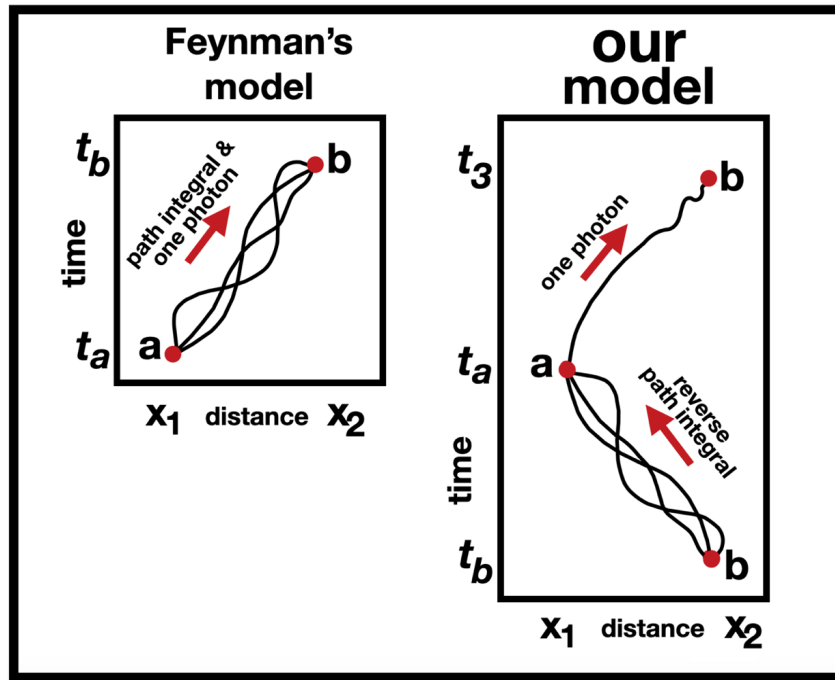


Fig. 6. Left: Feynman’s model for how a path integral K and photon travel from a to b . Right: Our model for how a reverse path integral K_R travels across multiple pathways in Phase 1, then a single photon selects one pathway to follow to the detector in Phase 2. Our model starts earlier than Feynman’s.

Many of the equations in this article are also found in Part 1 of this article, in *Journal of Advances in Mathematics*. For a trajectory $x(t)$ we define the reverse-action S_R as follows:

$$S_R = \int_{t_b}^{t_a} \mathcal{L}_R(\dot{x}, x, t) dt$$

where \mathcal{L}_R is the reverse-lagrangian for the system. For a particle of mass m subject to a potential energy $V(x, t)$, which is a function of position and time, the reverse-lagrangian is

$$\mathcal{L}_R = \frac{m}{2} \dot{x}^2 - V(x, t)$$

We call the trajectory $\bar{x}(t)$ that goes from b to a with a minimum of action “ S_R .” If we keep the endpoints fixed, but otherwise displace the path away from $\bar{x}(t)$ by an increment of $\delta(t)$, then we have defined

$$\delta x(t_b) = \delta x(t_a) = 0$$

The fact that $\bar{x}(t)$ is an extremum of S_R implies that, to the first order in $\delta x(t)$

$$\delta S_R = S_R[\bar{x} + \delta x] - S_R[\bar{x}] = 0$$

So, plugging in the equation defining the reverse action S_R we can say:

$$S_R[x + \delta x] = \int_{t_b}^{t_a} \mathcal{L}_R(\dot{x} + \delta \dot{x}, x + \delta x, t) dt$$

$$\begin{aligned}
 &= \int_{t_b}^{t_a} \left[\mathcal{L}_R(\dot{x}, x, t) + \delta\dot{x} \frac{\partial \mathcal{L}_R}{\partial \dot{x}} + \delta x \frac{\partial \mathcal{L}_R}{\partial x} \right] dt \\
 &= S_R[x] + \int_{t_b}^{t_a} \left[\delta\dot{x} \frac{\partial \mathcal{L}_R}{\partial \dot{x}} + \delta x \frac{\partial \mathcal{L}_R}{\partial x} \right] dt
 \end{aligned}$$

Upon integration by parts the variation in S_R becomes

$$\delta S_R = \left[\delta x \frac{\partial \mathcal{L}_R}{\partial \dot{x}} \right]_{t_b}^{t_a} - \int_{t_b}^{t_a} \delta x \left[\frac{d}{dt} \left(\frac{\partial \mathcal{L}_R}{\partial \dot{x}} \right) - \frac{\partial \mathcal{L}_R}{\partial x} \right] dt$$

Since $\delta S_R(t)$ is zero at the end points, the first term on the right-hand side of the equation is zero. Between the end points $\delta S_R(t)$ can take on any arbitrary value. Thus the extremum is that curve along which the following condition is always satisfied.

$$\frac{d}{dt} \left(\frac{\partial \mathcal{L}_R}{\partial \dot{x}} \right) = \frac{\partial \mathcal{L}_R}{\partial x}$$

The **path of least action** $\bar{x}(t)$ always satisfies the following condition:

$$\frac{d}{dt} \left(\frac{\partial \mathcal{L}_R}{\partial \dot{x}} \right) - \frac{\partial \mathcal{L}_R}{\partial x} = 0$$

which is the Euler-Lagrange equation.

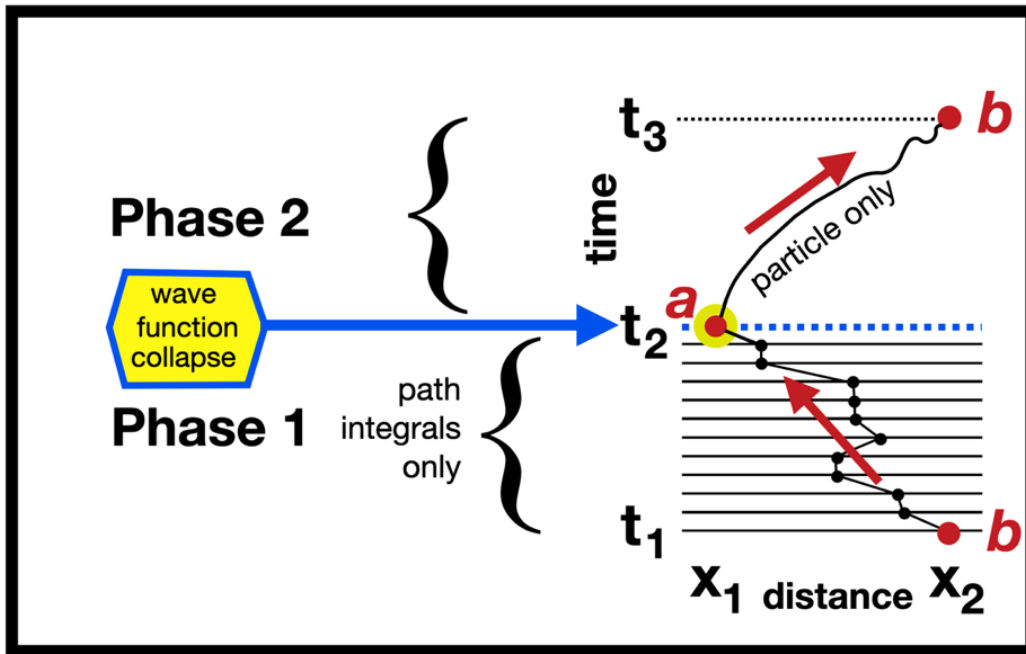


Fig. 7. Compared to the right side of the previous Figure, we have sliced the time in Phase 1 into increments of duration ϵ . Only one path (named “ x_n ”) is diagrammed here. It consists of dots connected by straight lines crossing a stack of time slices. As ϵ diminishes towards zero, this choppy path approaches a smooth path x_n .

When we sum across all the paths x_n from “b” to “a”, we arrive at a first approximation of the R-path integral:

$$K_R(a, b) = \sum_{\text{All paths from } b \text{ to } a} \phi_R[x(t)]$$

where $\phi_R[x(t)]$ is the phase of a path. In Feynman’s work is is the **phase** of the path which is most important variable in deriving the total path-integral. The contribution of a path to the total phase is proportional to its reverse-action S_R :

$$\phi_R[x(t)] = \text{constant } e^{(i/\hbar)S_R[x(t)]}$$

We need a constant that will normalize these equations. Following the lead of Feynman and Hibbs, we define:

$$\mathcal{A}_R = \left(\frac{2\pi i \hbar \epsilon}{m} \right)^{1/2}$$

We may write (F&H Eq. 2.22):

$$K_R(a, b) = \lim(\epsilon \rightarrow 0) \frac{1}{\mathcal{A}_R} \int \dots \iint e^{(i/\hbar)S_R(a,b)} \frac{dx_1}{\mathcal{A}_R} \frac{dx_2}{\mathcal{A}_R} \dots \frac{dx_{N-1}}{\mathcal{A}_R}$$

where the action

$$S_R(a, b) = \int_{t_b}^{t_a} \mathcal{L}_R(\dot{x}, x, t) dt$$

is a line integral taken over the trajectory passing through the points of x_n (Figure 7). We define the reverse path integral to be

$$\mathbf{K}_R(a, b) = \int_b^a e^{(i/\hbar)S_R(a,b)} \mathcal{D}[x(t)]$$

This is F&H’s equation 2.25 after we swap the bounds of integration. The negative sign of our integral is embedded inside the subscript “R”. (33)

2.2.3 Feynman Diagrams

The most famous application of Feynman’s path integral approach is the Feynman diagrams, which are a way of summarizing and cataloging intricate mathematical equations.

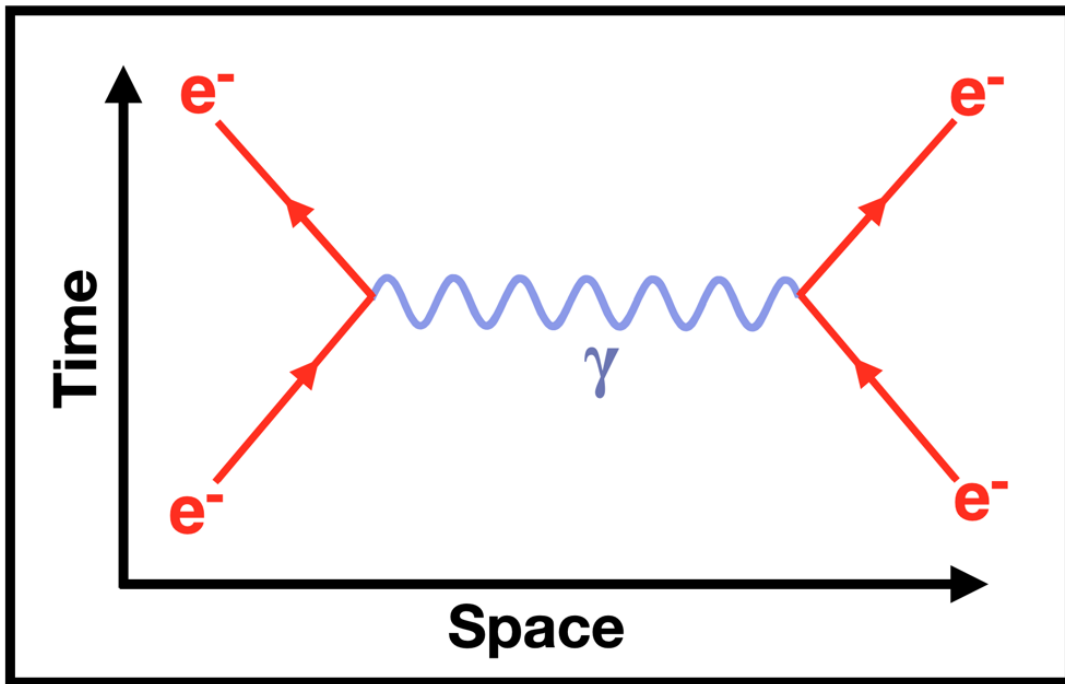


Fig. 8. This Feynman diagram shows two electrons approaching one another in space, then exchanging a virtual photon, and repelling one another.

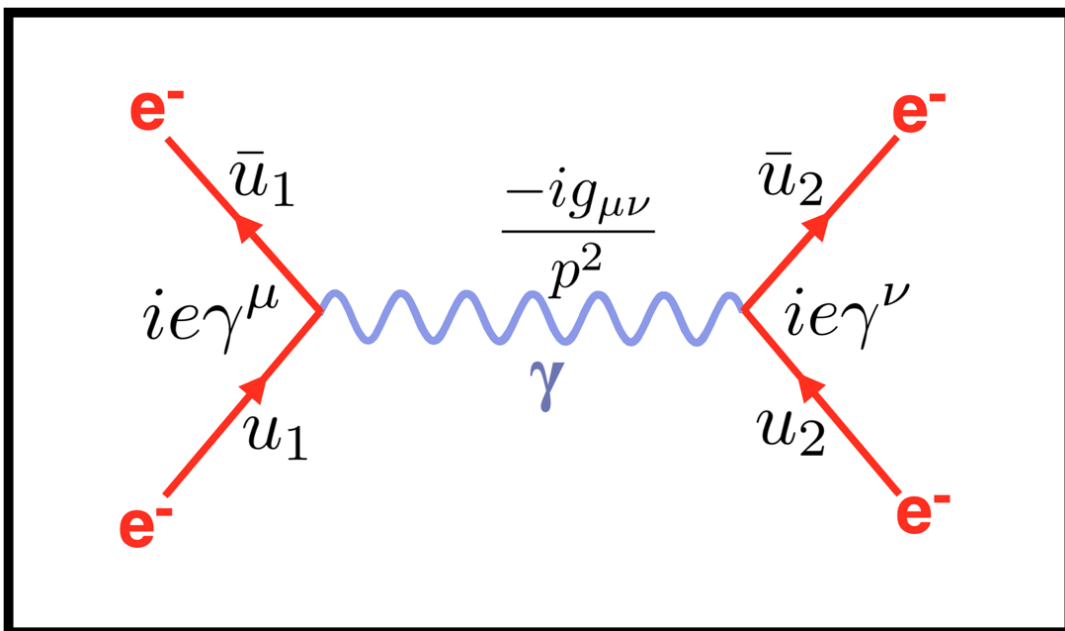


Fig. 9. Every line and every 3-way juncture in a Feynman diagram has an equation that represents the amplitude of that event occurring.

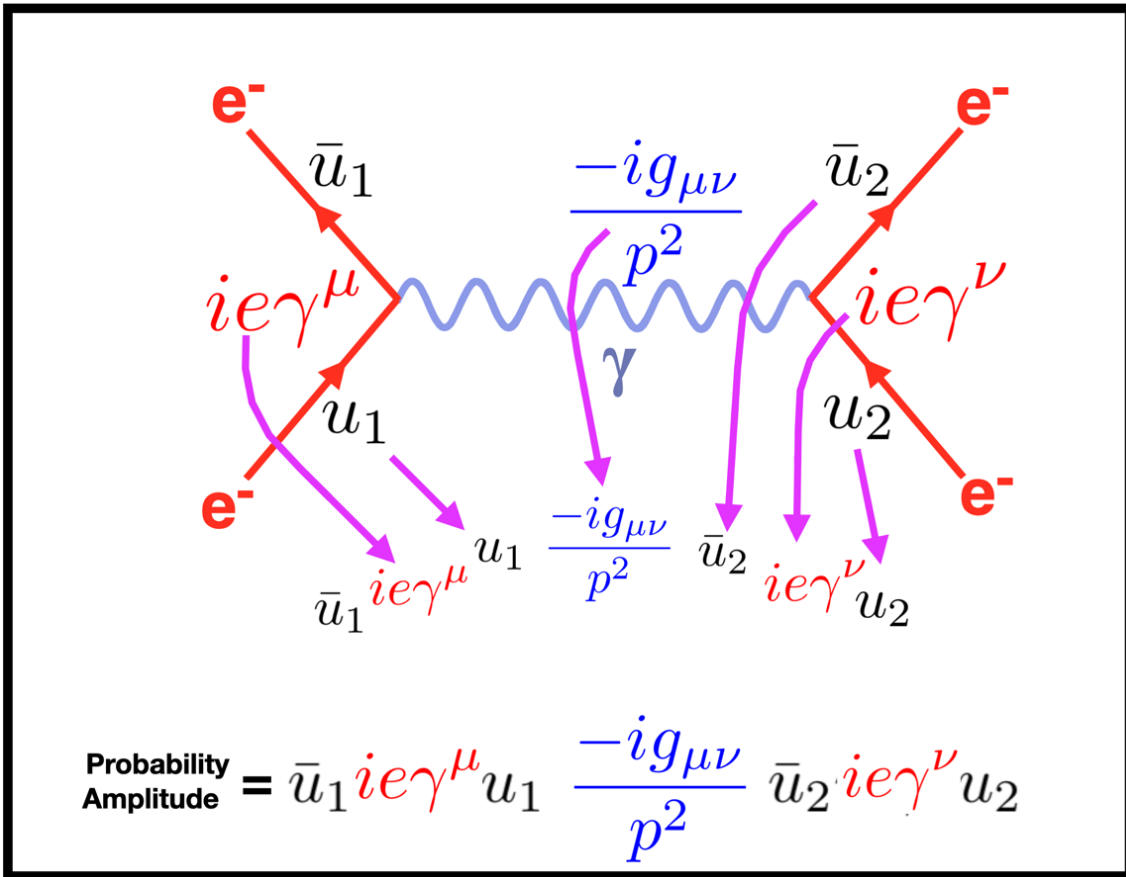


Fig. 10. The amplitude equations from the preceding diagram can be harvested into the equation at the bottom of this Figure. The original Feynman diagram (Figure 8) is more intuitively satisfying than the equation at the bottom of this Figure. Both say the same thing, but Figure 8 says it in pictures.

The point of these three Feynman diagrams is that these diagrams are a visual way of cataloging equations that are otherwise too complex to think about.

2.2.3.1 The Gerald Gabrielse Study Using Feynman Diagrams

They are so accurate, flexible, fun, and brilliant that it is not immediately evident that Feynman diagrams contain an unscientific flaw. We will illustrate this in an international study led by Gerald Gabrielse at Harvard University, published in *Physical Review Letters* in 2006.

Feynman is fond of saying that his QED provides the most accurate science that humans ever had. For example, he says that if the distance from San Francisco to New York City were measured with the accuracy of his equations, the calculated distance would differ from the measured distance by less than the width of a human hair. In five paragraphs we will discuss the “inconsistency” to which we referred in the previous paragraph.

The Gabrielse multinational study focuses on the electromagnetic fine structure constant α , which measures the strength of electromagnetic interactions and is one of the fundamental constants in physics. The electron’s g value is a measure of the magnetic moment in terms of the Bohr magneton and is a fundamental property of the simplest elementary particles. QED provides a precise relationship between α and g .

Gabrielse’s team uses a single electron caught for months in a cylindrical Penning trap in a cyclotron, as one of the sources of empirical data. The QED mathematical data are based on studies of Feynman diagrams with increasingly complicated branch points. The probability amplitudes are generated by many supercomputers all over the world working collaboratively for more than a decade.

The next Figure, which is from Gabrielse’s article, shows a photon traveling from point **a** to **b** with several branch points to accommodate virtual particles.

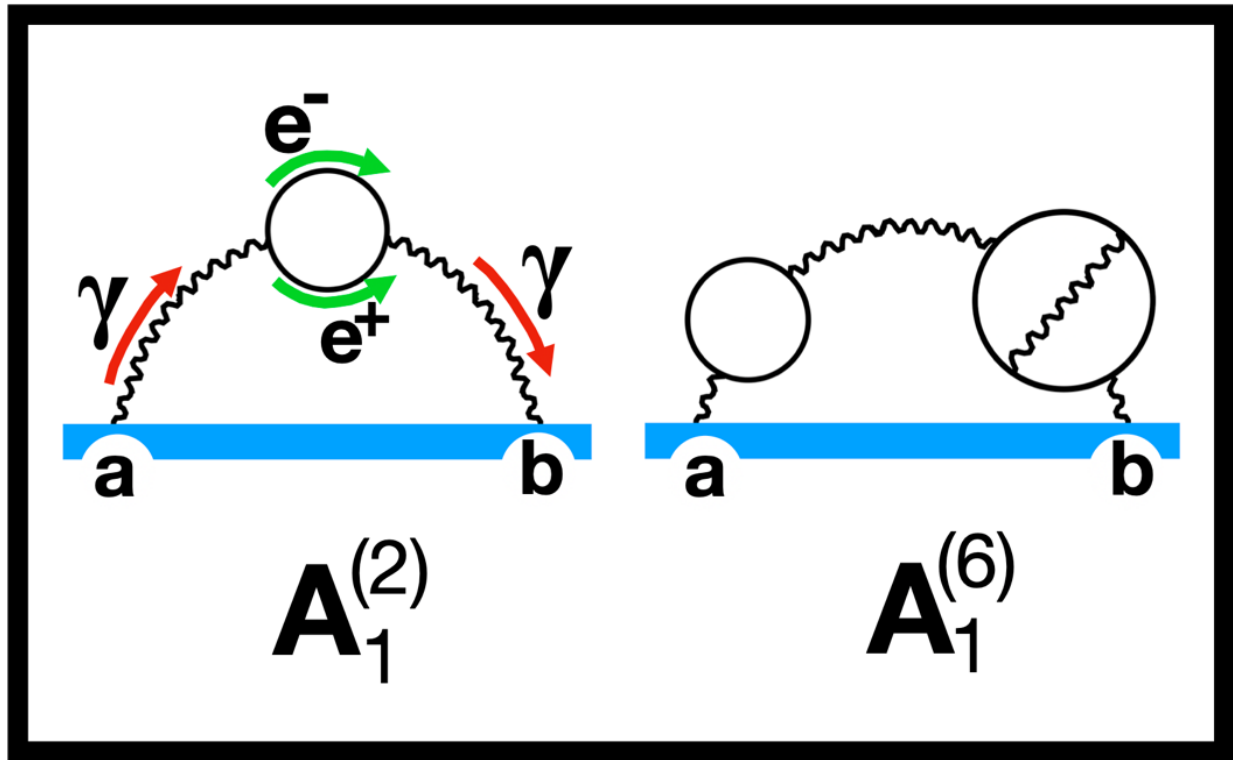


Fig. 11. These are two of the Feynman diagrams which look different than the previous ones, but the principles are the same: every line or 3-way juncture represents an equation. This diagram comes from a study published by the Gabrielse study, in which solid and wiggly curves represent electrons (**e**) and photons (**γ**) respectively. Left: photon leaves point **a**, moving up an arc. Before it gets to the top of the curve, it splits into a virtual electron-positron pair. They zip around the small circle, then collide and annihilate each other. A photon emerges on the right to arc down to point **b**. There are two branch points in the left diagram (photon to electron-positron, and electron-positron to photon) which makes it a second order Feynman diagram, which is denoted $A_1^{(2)}$. The right-hand diagram which has more virtual particles, displays six branch points and is therefore a sixth order Feynman diagram: $A_1^{(6)}$.

Gabrielse’s group reports on 891 eighth-order Feynman diagrams, which allows them to calculate α with a precision of 0.70 parts per billion. Alpha is $\alpha = 137.035,999,710$. This means that QED is extremely accurate.

This is so impressive that it is easy to lose sight of the fact that their work suffers from a contradiction, which they never mention. Gabrielse et.al., assume that every single photon crosses every single Feynman diagram, and there are an infinite number of those. Within each Feynman diagram, every photon crosses every virtual circuit inside, and there can be dozens of those. We are talking about a single photon that accomplishes all this simultaneously!

Our Reverse Path Integral (K_R) travels in the opposite direction (from **b** to **a**), backwards across all the same diagrams and backwards across every virtual circuit inside each Feynman diagram.

As we said, our approach allows a compromise between Feynman and his students, giving us the best of both viewpoints. Our approach integrates across all pathways and therefore calculates as accurately as Feynman the amplitude of a particle traveling from **a** to **b**. Our approach agrees with Feynman’s students that one photon should be limited to one pathway, but we don’t know which one. When we square our K_R we calculate exactly the same probability prediction as Feynman when he squares his K .

We present this as evidence that our K_R is more trustworthy than Feynman’s K .



2.3. Davisson-Germer Experiment



2.3.1 Thumbnail Sketch

Here we consider the first and most famous experiment that allegedly “proves” wave particle duality, namely the Davisson–Germer experiment. We reject wave–particle duality, and we claim this famous experiment can be explained by either model: QM or TEW. The experiment provides no way of deciding which of these two approaches is better. If you want a simple summary of what we are about to say, look at Figure 16 and read the last paragraph.

2.3.2 Description of the Experiment

In 1927 Clinton Davisson and Lester Germer at Bell Labs, which at that time were in Manhattan, studied the surface of a crystal of nickel by firing slow electrons at it. (29) The angle at which electrons reflected off the crystal showed a pattern reminiscent of the X-Ray diffraction of crystals discovered by William Bragg and Max von Laue in 1913.

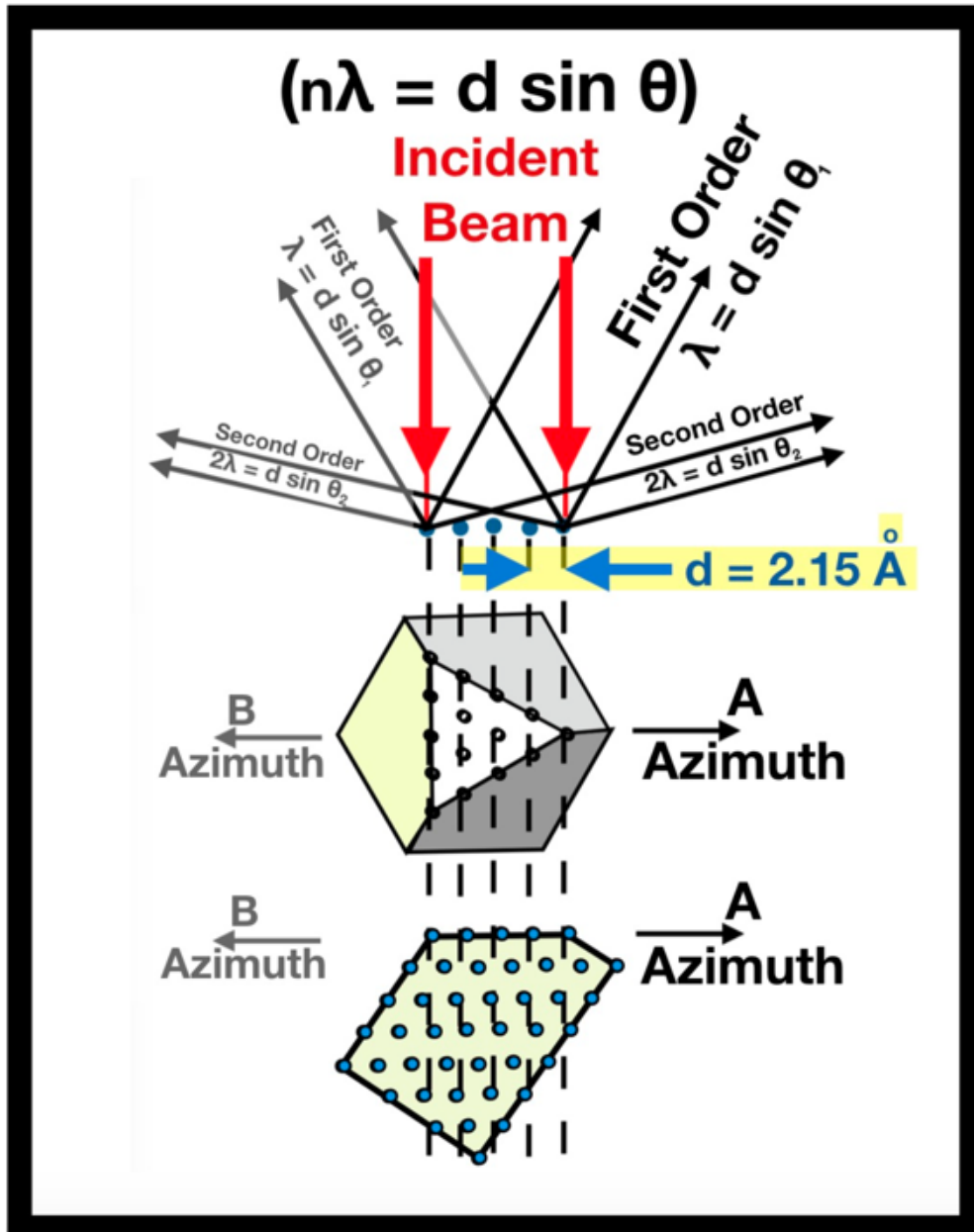


Fig. 12. Davisson’s diagram of electron refraction in a Nickel crystal. The constant “d” has a value 2.15 Å when $\theta = 50^\circ$ and 54 volts so $n\lambda$ has a value $2.15 \times \sin 50^\circ = 1.65$.

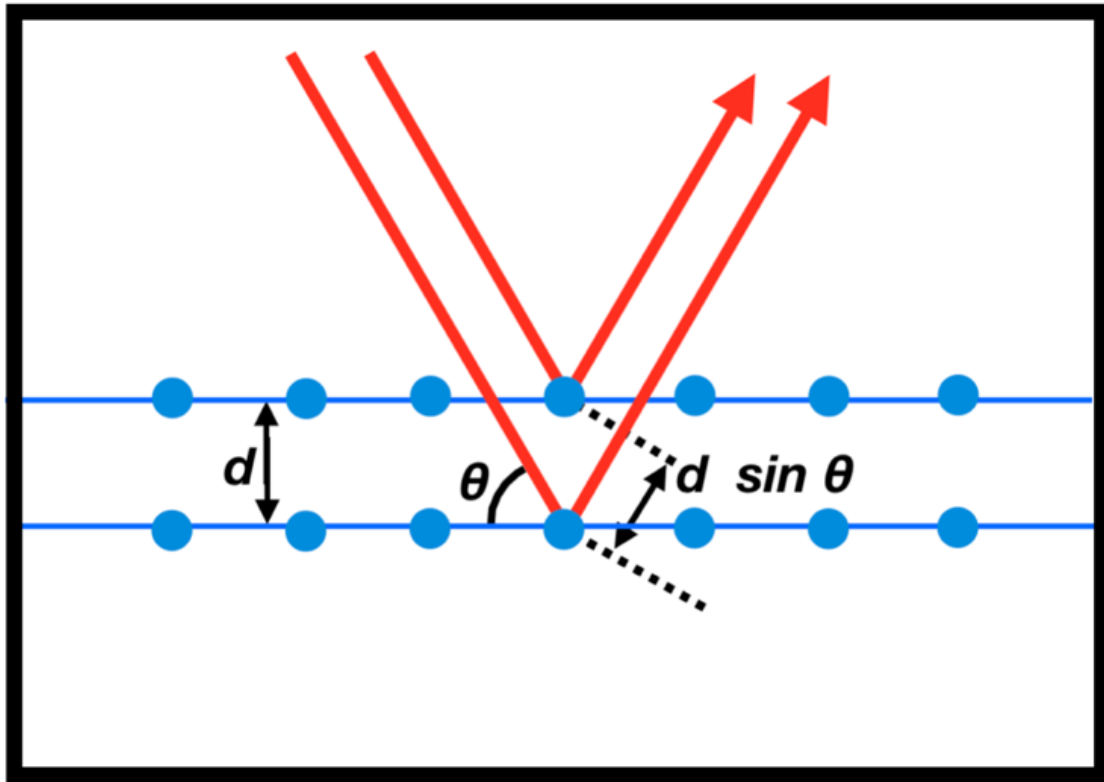


Fig. 13. Bragg diffraction. Two beams with the same phase impinge on a crystal and are scattered off two atoms. The lower beam travels an extra length of $2d \sin \theta$. Constructive interference occurs when this length is equal to a multiple of the wavelength: $n\lambda = 2d \sin \theta$.

When Davisson and Germer fired an electron gun at 54 volts at a crystal of nickel, they found an unusual “spur” in the data at 50° , as evident in Figure 15. In their article in *Nature* they also referred to this “spur” as a “hump.” All discussion of “wave-particle duality” arises from a discussion of the meaning of that “spur.” That spur could only be explained if a wave of $\lambda = 1.67$ were refracting through the crystal, and the electrons were interacting with such a wave. (29)

Davisson writes “ $n\lambda$ has a value $2.15 \times \sin 50^\circ = 1.65$.” He says this is very close to the de Broglie equation:

$$\lambda = h/mv = \sqrt{\frac{150}{V}}$$

and the length of a phase wave of a 54-volt electron is about

$$\sqrt{\frac{150}{54}} = 1.67$$

Because there are different Azimuths inside the nickel crystal, the optimal wave for some Azimuths is 1.67 \AA , and for others 1.65 \AA . With each Azimuth there is a “spur” or “hump” and it is that phenomenon that is the center of focus.

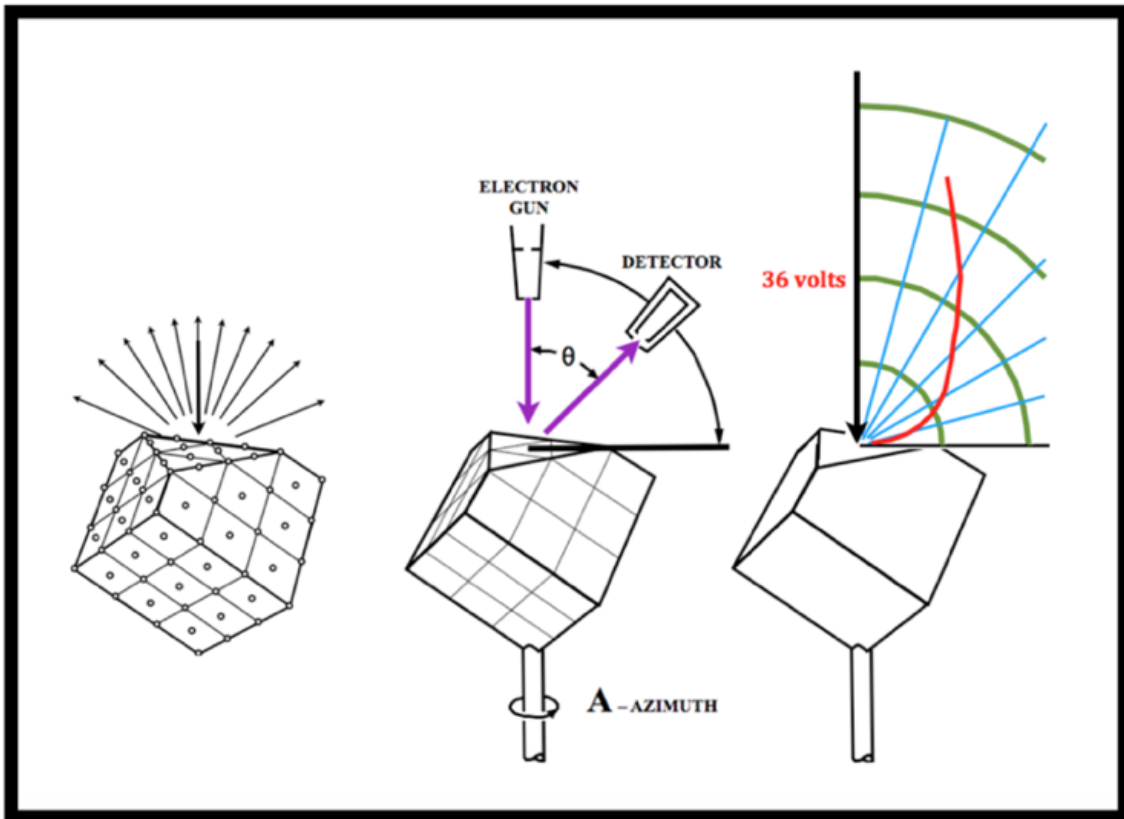


Fig. 14. Diagrams from Davisson and Germer, to which we added color. Electrons shot down from a gun at various voltages, come off the nickel crystal at angle θ . Scientists can control the voltage and the angle θ at which the detector is set. They can also measure the amount of current coming through the detector. Those 3 variables are plotted on the graph above the right-hand diagram, using polar coordinates.

Davisson said, "There are circumstances in which it is more convenient to regard electrons as waves than as particles. We will allow perhaps that electrons have a dual nature. When they produce tracks in a cloud chamber, they are particles. When they refract through crystals, they are waves. A similar situation exists with X-Rays. When they refract through crystals, they are waves, but when they give rise to the Compton effect or cause emission of electrons from atoms, they are particles: quanta of photons."

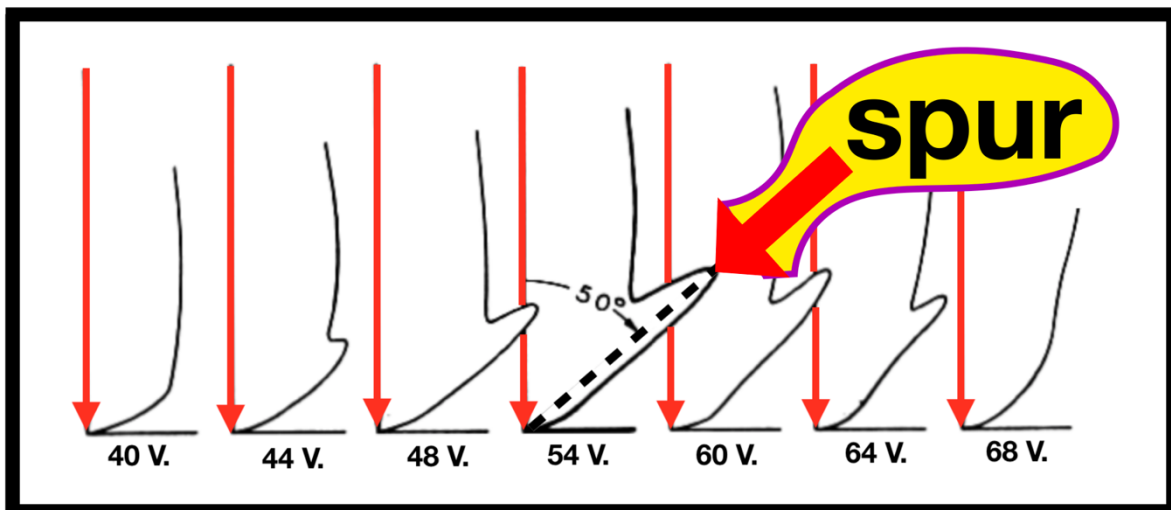


Fig. 15. The unusual spur or hump noted by Davisson and Germer, is visible only at a few voltages (V). It is greatest at 54 volts. It indicates electrons are interacting with waves of 1.67 Å.

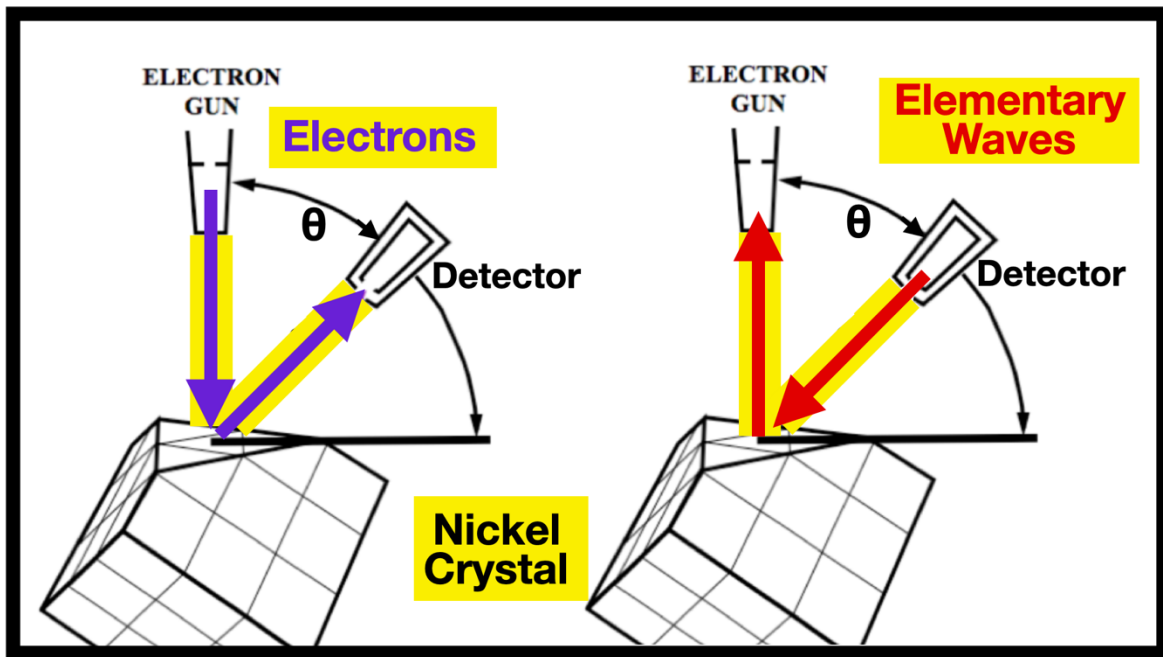


Fig. 16. Left: electrons target a nickel crystal. Right: Elementary Waves of 1.67 \AA travel in the opposite direction, and electrons follow them backwards. This explains the data equally well.

The 1920's was a remarkable decade for quantum mechanics. In 1926 Schrödinger invented his wave equation. Everyone was looking for a way to relate a wave-packet to a particle. Einstein and Bohr suggested a duality. That idea was in the air. Everyone was talking about it in the mid-1920's. When the Davisson-Germer study was published in 1927 it caused an enormous stir.

The Davisson-Germer experiment proved wave-particle interaction. Elementary Waves would not be discovered for another 69 years. Davisson and Germer did not know that the same data could be explained by zero-energy waves of 1.67 \AA emanating from the detector (Figure 16), refracting backwards through the crystal, so electrons of corresponding de Broglie wavelength (voltage and velocity) were following those waves backwards to the detector.

Think of it this way: Davisson and Germer could only detect electrons. Their data about electrons is superb and cannot be faulted. But they have no information about zero-energy waves. If the electrons behave the same, their experiment cannot distinguish between theories in which waves are traveling in the same, or in the opposite direction as the electrons.

Thus, TEW can explain the spur (Figure 16) with as much accuracy as wave-particle duality explains the spur. The electrons act the same with both theories. The waves, which travel in opposite directions in the two theories, are invisible and, as we said, the Elementary Waves were not discovered until seven decades after the work of Davisson and Germer (see Figure 16). Therefore Davisson and Germer had no way of knowing that there were two explanations of their data.



3. Untangling the Mysteries of QM

In this third section, we will examine five experiments in which the illogicality of QM vanishes when we change from the positive to the negative square root of a probability (i.e., when we change from $+\psi$ to $-\psi$). This is strong evidence for the validity of our thesis. Reminder: $\sqrt{\text{Probability}} = \pm\psi$ and we are investigating $-\psi$.

We will also examine what the phrase “wave-function-collapse” means in section 3.3.

3.1 Quantum Eraser

There are two quantum experiments that convince scientists that the quantum world is bizarre, different from the world of everyday experience: the quantum eraser and Wheeler’s thought experiment. We will now consider them in sequence and show that when we change to the assumptions of TEW, neither experiment proves that.

3.1.1 Thumbnail Sketch of the Quantum Eraser Experiment

This “quantum eraser” is a double-slit experiment in which each photon is split in half. One half goes to a target-screen. The other half goes to some complicated equipment. They claim if the latter half-photon tells us which slit was used in the double-slit experiment, then the target screen data will be erased backwards-in-time. They pay zero attention to the laser. Our theory (TEW) totally disagrees with their explanation. The TEW perspective is so radically different from the QM perspective, that it is as if we are discussing different experiments. We claim Elementary Waves start at all the detectors and travel backwards through the equipment, converging on the laser. The only place any decisions are made is at the laser where each photon makes a choice of which Elementary Wave it wants to follow backwards. After that choice it is a deterministic experiment. According to TEW, the experiment shows no quantum eraser, no backwards-in-time cause-and-effect, no backwards-in-time anything, and no evidence of Complementarity. You can skip the equations because they won’t tell you anything interesting. Often in this article, but not always, Figures are provide more insight than do equations.

3.1.2 Description of the Experiment

In a double slit experiment, you see an interference fringe pattern on the target screen only if you do not know which slit the particle went through. If you discover which slit, the interference pattern vanishes. This phenomenon is called “Complementarity” in QM. We will delay until later our reason for rejecting the doctrine of Complementarity.

Kim, Yu, Kulik, Shih and Scully published an experiment allegedly showing that you can have an interference fringe pattern on the target screen, but if you subsequently learn which slit was used, then that interference data will be erased backwards-in-time! (37)

We will re-analyze the data from a TEW viewpoint and show that this experiment does NOT show any erasure of data, nor backwards-in-time cause-and-effect. We will show that the allegedly “erased data” never existed in the first place. Furthermore, we will show that the decisive events in this experiment occur two dozen nanoseconds earlier than Kim, et.al. know. They think the decisive events occur at the beam-splitters or detectors. We say they are located at the laser.

Kim et.al., have **zero** interest in the laser. They never include it in their diagrams, equations, nor text. They refer to it with the vague term “pump.” Yet that laser is the location where everything important happens, according to TEW. It is an irony.

This experiment takes the output from a double slit apparatus and splits each photon into two entangled photons. The photons are split by a β – BaB₂O₄ (beta-barium-borate, BBO crystal), which Kim, et.al. call “type II SPDC” (spontaneous parametric down-conversion). One of the photons, called the “signal photon” etches an interference wave pattern on a target screen. Later, the “idler photon” is randomly assigned either to a detector that allows us to know which slit was used, or to another detector that prevents us from knowing which slit was used.

If the idler photon reveals which slit is used, then the interference wave pattern on the target screen is allegedly erased, backward in time. If the idler photon does not disclose which slit is used, then the interference wave pattern on the target screen persists. Because of this focus on time, the equipment is carefully constructed so that the detector D₀ that encodes the interference-fringe wave-pattern, is closer to the BBO crystal than are the several detectors that disclose whether we know or do not know which slit is used. Because it is closer, they insert a lens (a yellow ellipse near the top of Figure 17) to bring the image into focus at less distance.



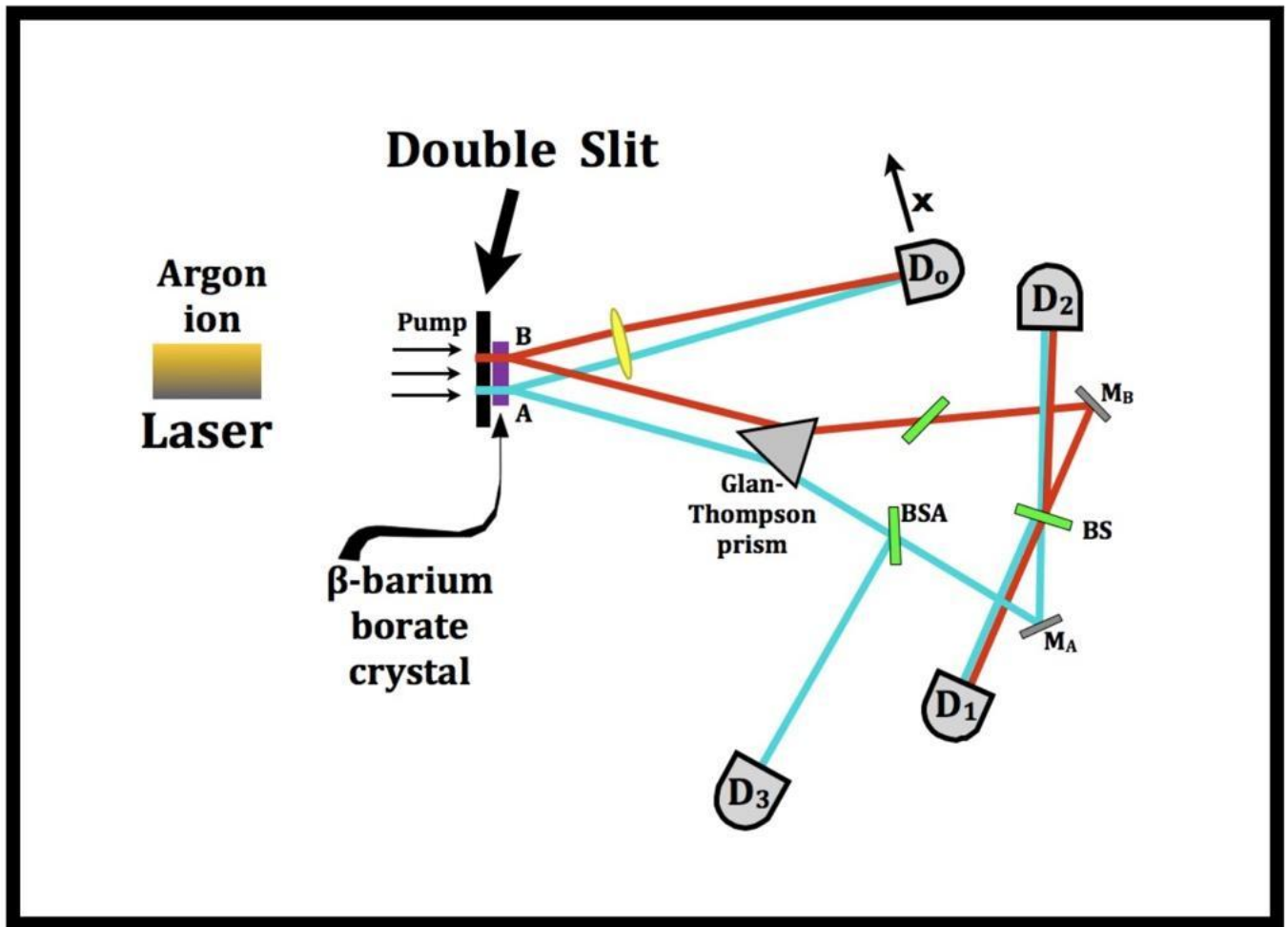


Fig. 17. This is the experiment as published, except that the experimenters excluded the laser from their diagrams and used no color in their diagrams. A laser on the left sends photons through a double slit barrier, after which each photon is split into a “signal” and “idler” photons by a BBO crystal. This crystal causes type-II spontaneous parametric down conversion (SPDC), meaning that the crystal takes each photon of 351.1 nm and splits it into two offspring photons of 702.2 nm each, orthogonal to one another. Traditionally these are called the “signal” and “idler” respectively.

The colors red and aqua in our diagrams refer to which slit the parent photon came through: aqua for slit A and red for slit B. So, there are four photons to keep track of, a “signal” and “idler” from slit A, and a “signal and idler” from slit B. Those four photons all have wavelength 702.2 nm. In this diagram, the “signal” always heads up (north) to detector D₀, and the “idler” south to other detectors.

To add more complexity, there are four detectors. The top one (D₀) moves up and down in the “x” direction, with a step motor to sweep out the area of interference of photons coming out of the two slits of the double slit apparatus. Since the diagram is so complicated, we display it again in the next two figures.

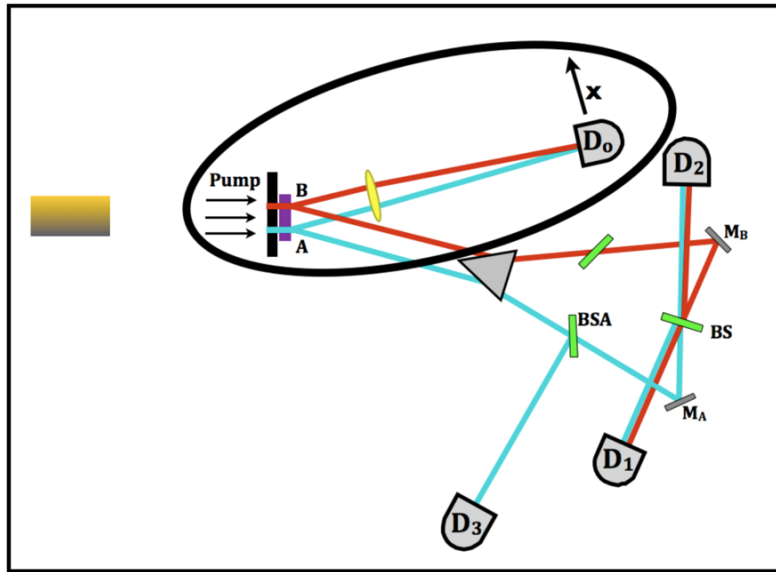


Fig. 18. This diagram is the same as the previous one, with an ellipse drawn around the equipment at the top. This ellipse contains the place where interference fringe data is recorded using “signal” photons. If you had a double slit experiment with a target screen, the screen would be located where the D_0 detector is located. But there is no target screen. The D_0 detector sweeps across the interference fringe area as it moves up and down the “x” axis, so D_0 collects the same data that a target screen would collect.

All data is stored in a computer not shown in these diagrams.

Their plan is to collect data from D_0 on whether there is an interference fringe pattern before a decision is randomly made whether other detectors can “see” which slit was used. Therefore, as we said, detector D_0 is closer to the double slit barrier than are the other three detectors. The yellow ellipse is the lens that brings D_0 into focus.

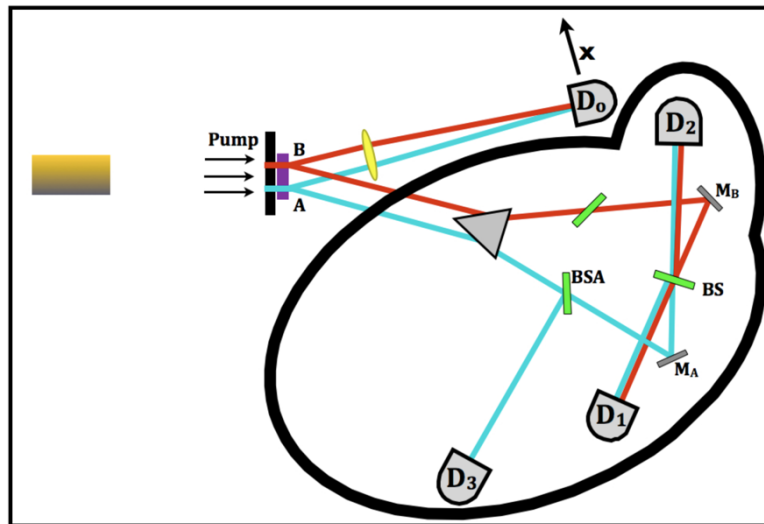


Fig. 19. This diagram is the same as the previous two, except that a black line has been drawn around the lower part of the equipment. The two idler photons (red line = slit A, and aqua line= slit B) go through a Glan-Thompson prism (gray triangle) which slightly changes their direction of flight, to make more room for all the equipment. Detectors D_1 , D_2 and D_3 are stationary, not moving. The thin green rectangles marked “BS” are beam splitters. The thin gray rectangles are mirrors (M_A and M_B). Therefore, if detectors D_1 or D_2 “click”, you do not know which slit was used, because the idler photon enters those detectors as **both** a red line and an aqua line. But if detector D_3 “clicks”, you know the parent photon came through slit A, since only an aqua colored line enters D_3 .

As we said, the hypothesis which this equipment is designed to test is that data are “erased” from the target screen (meaning the D_0 detector) backwards-in-time if we subsequently know (from detector D_3) which slit was used.

Kim, et.al. do not provide a photograph or graph of the interference fringe pattern during that nanosecond when it allegedly exists before erasure. That is a flaw in their experimental design. **They assert that data was “erased” but they provide no evidence that the data ever existed.** We will demonstrate below that it never existed. This is a fatal flaw for a “quantum ERASER” experiment.

3.1.2 Mathematics from Kim et.al.

In the equations of Kim, et.al., there is another detector D_4 not shown in the diagrams. D_4 would be symmetrical with D_3 . It would receive an idler photon from BS_B (beam splitter B) so that only a red line would enter D_4 , no aqua line.

Kim et. al. say they have predicted results using standard QM equations. Data are based on a pair of detectors clicking simultaneously. For example, if D_0 clicks a few picoseconds before D_1 , that means that a signal photon has been detected at D_0 , and the idler has been detected at D_1 . Therefore, for the D_0 & D_1 pair, the variable R_{01} would count “one click.”

The variable R_{0i} represents the variable counting the combination of detectors D_0 and D_i both clicking during time T . Let $T = 0$ be the time when photons leave the SPDC (i.e., BBO crystal). Then the Glauber equation is:

$$R_{0j} \propto \frac{1}{T} \int_0^T \int_0^T dT_0 dT_j \langle \Psi | E_0^{(-)} E_j^{(-)} E_j^{(+)} E_0^{(+)} | \Psi \rangle$$

$$= \frac{1}{T} \int_0^T \int_0^T dT_0 dT_j | \langle 0 | E_j^{(+)} E_0^{(+)} | \Psi \rangle |^2$$

where T_0 is the detection time for D_0 , and T_j is the detection time for D_j where $j = 1, 2, 3, 4$, and where $E_{0,j}^{(\pm)}$ are the positive and negative frequencies at detector D_0 and D_j . The entangled state of the type II SPDC (which is what we call the “BBO”) is denoted $|\Psi\rangle$.

$$|\Psi\rangle = \sum_{s,i} C(k_s, k_i) \alpha_s^\dagger(\omega(k_s)) \alpha_i^\dagger(\omega(k_i)) |0\rangle$$

where

$$C(k_s, k_i) = \delta(\omega_s + \omega_i - \omega_p) \delta(k_s + k_i - k_p)$$

for the SPDC and ω_j and k_j where $j = 1, 2$, or 3 are respectively the frequency and wave vectors for the $s =$ signal, $i =$ idler and $P =$ pump (i.e. laser), and they assign ω_p and k_p to be constants. The creation operators for the signal and idler photons are denoted α_s^\dagger and α_i^\dagger . The δ functions are calculated for infinite interaction time for an infinitely large SPDC.

$$\Psi(t_0, t_j) \equiv \langle 0 | E_j^{(+)} E_0^{(+)} | \Psi \rangle$$

where $\Psi(t_0, t_j)$ is the wave function, and where $t_0 \equiv T_0 - L_0/c$ and $t_j \equiv T_j - L_j/c$ where $j = 1, 2, 3, 4$ and where L_0 or L_j is the optical distance from the BBO crystal to detectors D_0 or D_j .

Kim, et.al. say that four wave functions correspond to four combinations of detectors D_a as follows:

$$\Psi(t_0, t_1) = A(t_0, t_1^A) + A(t_0, t_1^B)$$

$$\Psi(t_0, t_2) = A(t_0, t_2^A) - A(t_0, t_2^B)$$

$$\Psi(t_0, t_3) = A(t_0, t_3^A)$$

$$\Psi(t_0, t_4) = A(t_0, t_4^A)$$



Detector D_4 is implied in the bottom equation, but, as we said before, the authors did not include D_4 in the published diagrams nor mention it in their text. In the equations just itemized, the upper index of t (A or B) indicates which slit in the double-slit the photon came through. For simplicity they used only the longitudinal integral, and wrote the two-photon state in terms of k_e and k_o in the following equation:

$$|\Psi\rangle = A'_0 \int dk_e \int dk_o \delta(\omega_e + \omega_o - \omega_p) \times \Phi(\Delta_k L) \alpha_{k_e}^\dagger \alpha_{k_o}^\dagger |0\rangle$$

where $\Phi(\Delta_k L)$ is a sinc-like function:

$$\Phi(\Delta_k L) = (e^{i(\Delta_k L)} - 1)/i(\Delta_k L).$$

Combining equations, they find that

$$A(t_i, t_j) = A_0 \int dk_e \int dk_o \delta(\omega_e + \omega_o - \omega_p) \times \Phi(\Delta_k L) f_i(\omega_e) f_j(\omega_o) (e^{-i(\omega_e t_1^e + \omega_o t_2^o)}).$$

where $f_{i,j}(\omega)$ is assumed to be a Gaussian of a hypothetical spectral transmission filter in front of detector $k_{i,j}$. To complete the integral they define Ω_e and Ω_o to be the center frequencies of the SPDC, $\Omega_e + \Omega_o = \Omega_p$ and they define ν to be a small tuning frequency, such that when they define $\omega_e = \Omega_e + \nu$ and $\omega_o = \Omega_o - \nu$, the relationship $\omega_e + \omega_o = \Omega_p$ is true. Therefore they can expand k_e and k_o around $K_e(\Omega_e)$ and $K_o(\Omega_o)$ respectively.

Completing the integral, the wave packet for the two photons coming from the SPDC is:

$$A(t_i, t_j) = A_0 \Pi(t_i - t_j) e^{-i\Omega_e t_i} e^{-i\Omega_o t_j}.$$

They dropped the e, o indices.

The shape of $\Pi(t_i - t_j)$ is determined by the bandwidth of the spectral filters and the parameter DL of the SPDC, where $D \equiv 1/u_o - 1/u_e$. If the filters are removed they obtain a rectangular pulse function $\Pi(t_1 - t_2)$. By “rectangular” they mean: $\Pi(t_0 - t_j) = 1$ if $0 \leq (t_0 - t_j) \leq DL$ and is otherwise 0.

Kim, et.al. say “Clearly the two amplitudes $\Psi(t_0, t_1)$ and $\Psi(t_0, t_2)$ overlap at both $t_0 - t_j$ and $t_0 + t_j$. Therefore interference is expected in both the counting rates of coincidences R_{01} and R_{02} , but the different sign will result in a phase shift of π .”

$$R_{01} \propto \cos^2(x\pi d/\lambda f) \text{ and} \\ R_{02} \propto \sin^2(x\pi d/\lambda f)$$

For R_{01} and R_{02} they will have a standard interference and diffraction pattern:

$$R_{01} \propto \text{sinc}^2(x\pi a/\lambda f) \cos^2(x\pi d/\lambda f) \\ R_{02} \propto \text{sinc}^2(x\pi a/\lambda f) \sin^2(x\pi d/\lambda f)$$

where d is the distance between slits A and B, a is the width of each slit (equal widths) and $\lambda = \lambda_s = \lambda_i$ is the wavelength of the signal and idler photon, and f is the focal length of the lens between the BBO crystal (SPDC) and the D_0 detector. As we mentioned, a lens is used to bring the detector D_0 closer to the BBO crystal, to force the D_0 detector to collect data picoseconds earlier than any of the other detectors. As we noted earlier, their experiment was designed to collect data on an interference fringe pattern (D_0 detector) before they determined which slit was used (detectors D_1, D_2, D_3 , and D_4)

The final data confirm their hypothesis. The data stored inside the computer show that there is or is not an interference pattern from detector D_0 depending on which detector the idler photon strikes.

The researchers conclude that they have created a quantum eraser like that proposed by Scully and Drühl in 1982. Marlan Scully is an author of both the 1982 and the 2000 articles, the connecting link between the original idea and its fulfillment.



3.2.3 Our Model of How This Experiment Works

According to TEW, zero-energy Elementary Waves start at the detectors and move backwards through the equipment and go into the laser. All wave interference is at the laser. Our assumptions are so drastically different than the assumptions of Kim, et.al., that it is as if we are analyzing at a different experiment than theirs.

As a rule, TEW claims things happen **long before** QM is aware of it. As a rule, if there is an interference fringe pattern on a target screen, TEW tries to show that interference of Elementary Waves impinging on the photon source, is indirectly the cause of that pattern on the target screen. From the viewpoint to QM, this way of thinking makes no sense. Thomas Kuhn describes paradigm shifts in science. He says that a new paradigm usually sounds like unintelligible gibberish to those trained in the old paradigm.

According to our viewpoint what the D_0 detector measures is reality. If detector D_0 sees an interference pattern, that means waves are interfering as they impinge on the laser. If detector D_0 sees no interference pattern, that means waves did not interfere at the laser.

We make the controversial claim that detector D_0 never tells us a lie. A general observation about TEW is that we believe what detectors tell us. Our approach never alleges that detectors are duplicitous by showing us a wave pattern, then erasing it before we can observe it.

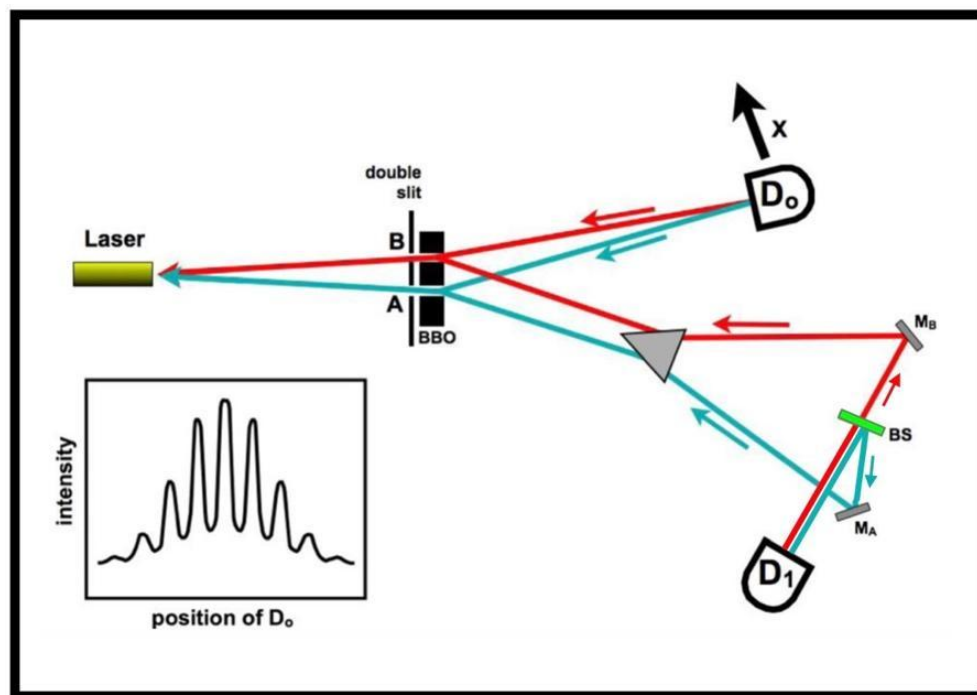


Fig. 20. TEW model: Elementary rays of 702.2 nm (red or aqua) originate from the detectors and move to the BBO crystal, where they combine into red or aqua rays of 351.1 nm heading toward the laser. Since two rays (red and aqua) impinge on the laser, there is wave interference as D_0 moves along the "x" axis. The intensity of the interference impinging on the laser is shown in the small graph in the lower left (hypothetical data). Some detectors are omitted from this diagram, for simplicity.

Remember: any trajectory connected to slit B (the upper slit) is colored red. Any trajectory connected to slit A (the lower slit) is aqua blue.

Figures 20 and 21 present pictures of the elementary rays traveling from the detectors through the BBO crystal, backwards through the double slits, and impinging on the laser. The previous Figure pertained to times when there is interference impinging on the laser. Now we will turn to the circumstance in which there is no interference impinging on the laser.

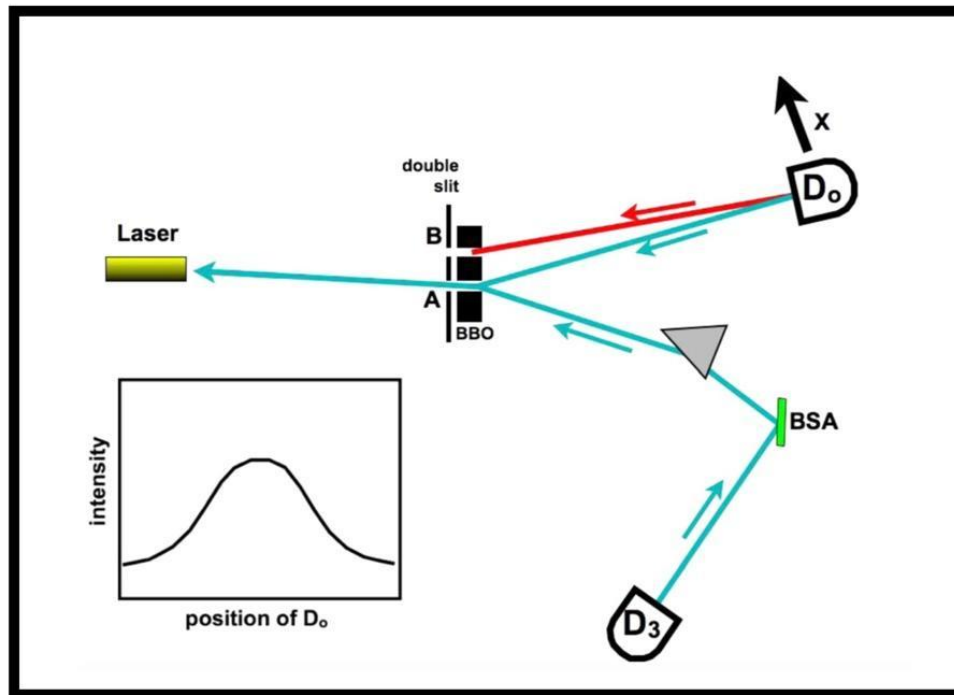


Fig. 21. TEW model: Detector D_3 puts out an aqua elementary ray of 702.2 nm, but no red ray, for the simple reason that it cannot “see” slit B (the upper slit) because of how the equipment is constructed.

In this Figure the BBO crystal is unable to produce a red ray of 351.1 nm going toward the laser because of lack of ingredients (one of the two red rays of 702.2 nm is missing). Therefore, there is no wave interference. Therefore, the final dataset reports NO INTERFERENCE, because there is no superposition of waves in proximity to the laser, as shown in the small graph at the lower left (hypothetical data). Some detectors are omitted from this diagram, for simplicity.

To reiterate, for there to be wave interference, there need to be two elementary rays of 351.1 nm impinging on the laser: one red, the other aqua. If there is no interference pattern in the final dataset, that means one of those two rays is absent. That is the key to understanding this experiment. It explains **all** the data.

Each detector emanates elementary rays of 702.2 nm, and those waves follow the trajectories (red or aqua), moving towards and through the BBO crystal. If you compare Figures 20 and 21 you will see that in the first case a 351.1 nm red ray can form inside the BBO crystal, but in the second it cannot, because half of its ingredients are missing. Specifically, the red ray of 702.2 nm is not coming up from below, for the simple reason that detector D_3 cannot “see” the BBO crystal because of how the equipment was designed and built.

A photon in the laser makes a random choice which in-coming Elementary Wave it will follow backwards. After that choice, there are no other decisions. The outcome of the experiment is 100% determined once a photon leaves the laser, which is dozens of nanoseconds earlier than what Kim, et.al. realize.

At the laser the photon must make one of four choices:

- Waves from D_0 and D_1 coming through both slits and interfering.
- Waves from D_0 and D_2 coming through both slits and interfering.
- Waves from D_0 and D_3 coming only through slit A: no interference.
- Waves from D_0 and D_4 coming only through slit B: no interference.

If the photon randomly chooses # a or # b then the final data will show an interference pattern on the target screen (D_0). If the photon randomly chooses # c or # d, then the final data will show no interference pattern on the target screen (D_0).

Once a photon leaves the laser, it is split into a signal and idler photon because it is following backwards signal and idler Elementary Rays of 702.2 nm flowing backwards through the BBO crystal.

At each beam splitter an idler photon follows its predetermined trajectory in one direction or the other. Following an Elementary Ray backwards constitutes a trajectory. After a photon leaves the laser, the final data are 100% determined.

When we presented this to a meeting of the American Physical Society (APS), someone in the audience said, "You are making this into a deterministic experiment!" That person was limiting his attention to what happens after the photon leaves the laser. From his viewpoint the random decisions that Kim, et.al., portray as occurring when an idler photon confronts a beam-splitter, were transformed by our model into deterministic decisions, thus eliminating randomness from the experiment.

Our reply was that our theory endorses randomness but reassigns when and where the randomness occurs. Those random decisions that Kim, et.al., say happen at a beam-splitter, happen at the laser, according to our view. After the photon leaves the laser, it is indeed a deterministic experiment.

This is a typical dispute between TEW and QM. We reassign most of the decisions for free particles, locating them at the particle source. Therefore, our way-of-thinking sounds bizarre to audiences trained in the QM way-of-thinking. On those dozen occasions when we presented TEW to the APS the audiences had blank faces, and usually made no comments. They were polite and applauded at the end. But there were no questions asked by either the audience or the moderator. It was as if the APS audiences were saying to themselves, "What on earth is this?"

We claim TEW has explained the quantum eraser experiment of Kim, et.al., in a straightforward and easy-to-understand way. Our explanation makes it clear that the quantum world follows the same rulebook as the world of everyday experience. There is no evidence of backwards-in-time cause-and-effect in either world. Data cannot be erased backwards-in-time in either world. We find nothing unusual about the quantum world, except for size.



3.2. Wheeler's "Gedanken Experiment"

We turn now to the other experiment that convinces physicists that the quantum world is bizarre. Once again we will show that, with the assumptions of TEW, there is nothing bizarre about the quantum world.

3.2.1 Thumbnail Sketch of the Wheeler Thought-Experiment of Jacques, et.al.

This is an interferometer experiment (see Figure 22) in which allegedly the human decision how to test the quantum of energy coming out the exit door of the interferometer, has an effect backwards-in-time at the front door of the interferometer. They allege that the quantum of energy as it enters, becomes a wave or a particle inside the interferometer, in anticipation of how it will later be tested. As was the case in the quantum eraser experiment, so again here, the TEW perspective is dramatically different from the QM perspective. So much so that it is as if we were investigating different experiments. From the TEW perspective, the only thing they prove is that when they look for a wave they see a wave, and when they look for a particle they see a particle. That proves that both waves and particles are **always** present at the same time, which is what TEW predicts. The Elementary Waves are always present, traveling backwards from what the researchers assume. And photons are always present when data is collected, because it is the photons which make a detector "click." The experiment shows no backwards-in-time cause-and-effect, no backwards-in-time anything, no evidence of wave-particle duality, and nothing mysterious.

3.2.2 Description of the Experiment

John A. Wheeler proposes a thought (German "*gedanken*") experiment to investigate the mysteries of wave particle duality. A photon is put into an interferometer where it is forced to become either a wave (traveling around both arms of the interferometer), or a particle (traveling on one arm or the other).⁽³⁵⁾

If the device is in an "open" configuration, and one of the two detectors "clicks", we know it is a particle. If the device is in a "closed" configuration (meaning that the two arms intersect at the exit door, Figure 22-right) then we look for wave interference which would tell us that the quantum chose to be a wave.



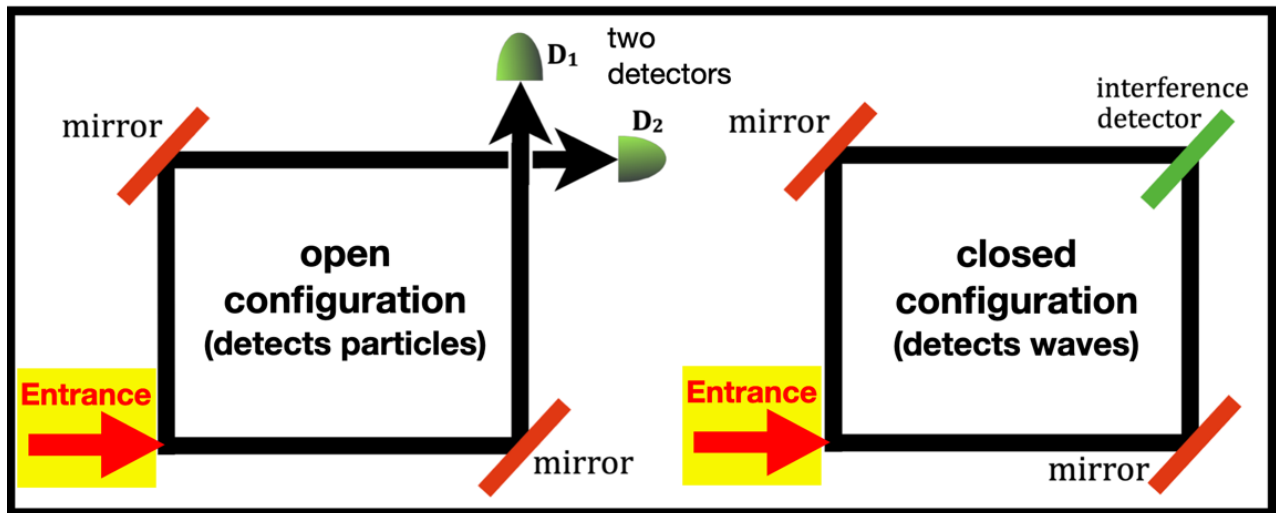


Fig. 22. Wheeler’s two arrangements of an interferometer. Left: an open configuration tests for a particle causing either detector D1 or D2 to “click.” Right: a closed configuration looks for interference caused by a wave crossing both sides of the interferometer.

Then Wheeler went further with his thought experiment. He wondered if this mechanism would operate backwards in time? Once a photon is inside an interferometer, committed to acting like a wave or particle (i.e., crossing the interferometer on both arms (as a wave) or just one arm (as a particle)), then we decide to test it one way or the other. Wheeler’s hypothesis is that the photon would know in advance and would have entered the front door as a wave or a particle in anticipation of how it would later be tested.

In other words, backwards-in-time cause-and-effect. The effect would predate the cause. The “effect” is the photon’s decision at the entrance to be a wave or a particle, and the “cause” is our decision how to test it at the exit.

Vincent Jacques, E. Wu, F. Grosshans, et.al., published a study in 2007 in which they built the interferometer described by Wheeler and confirmed Wheeler’s predictions.(35)

This is another one of the experiments which convince people that the quantum world is bizarre.

The next Figure shows the Mach Zehnder interferometer built by Jacques et al. It is 48 meters wide (half a football field), which causes the photon to take 160 ns to cross it, which gives the researchers time to have a random number generator (which takes 40 ns) determine whether the equipment will subsequently test the quantum as a particle (open configuration) or as a wave (closed configuration). The switch that determines this is an Electrical Optical Modulator (EOM), which is controlled by the random number generator. The EOM can switch positions very rapidly.

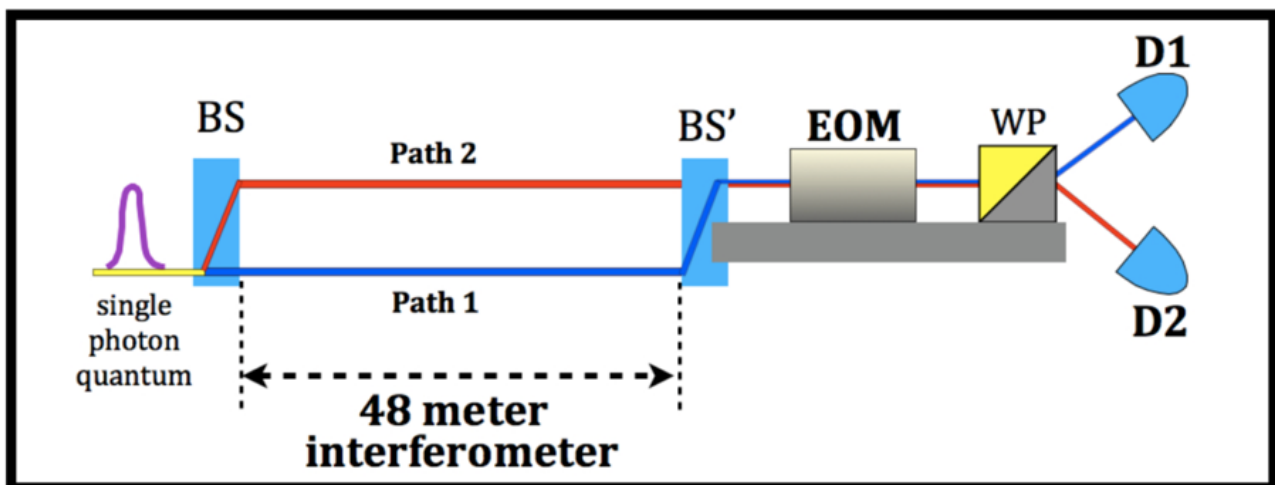


Fig. 23. The Mach-Zehnder interferometer used by Jacques et. al. is as wide as half a soccer field. BS and BS’ are an Yttrium Orthovanadate (YVO₄) beam splitter and reverse beam splitter. The lower path (Path 1, which is blue) has a horizontal polarization; the upper path (path 2, which is red) has a vertical polarization. Paths 1 and 2 are

separated by 4 mm. EOM is Electrical Optical Modulator, WP is a Wollaston prism, and D1 and D2 are silicon avalanche photodiode detectors.

After a photon enters the interferometer (lower left) and makes its decision about how to cross the interferometer, a random number generator (not shown) causes the EOM to determine the angle of polarization (see Figure 25), which establishes how the results are measured.

3.2.3 Their Technology Was Developed in a Previous Study

Perhaps the most remarkable feature of this experiment is that they have a single quantum of energy enter the front door of the interferometer. To understand how it is possible to create and control a single quantum of energy, we need to pause and go back to a previous study, published in the *European Physical Journal* in 2005, in which the authors developed the technology used in this 2007 study.

They stored a single photon quantum of energy inside a cavity in a diamond: a nitrogen (N) vacancy (V) inside a diamond nanocrystal. They used a pulsed laser at a wavelength of 532 nm with an 800-picosecond pulse duration to excite a single photon stored in such an N-V vacancy. The 50 pico-Joules energy per pulse was high enough to pump the defect in the diamond to an excited level, so that a photon popped out. Thus, they were able to generate a single quantum of energy, one photon at a time. The time duration for such an N-V center is 45 ns. They used the laser to bump out a photon once every 436 ns. Thus, they can emit one single quantum of energy at a time, and the long duration (436 ns) between photons means that they are studying only one photon at a time.

They needed to prove mathematically that they had been successful in generating one single photon. They used the following equation to assure themselves that they were dealing with a single photon. A single quantum photon should violate this equation:

$$\alpha = \frac{N_C \times N_T}{N_1 \times N_2} \geq 1$$

Where N_T is the number of trigger pulses applied to the N-V diamond emitter, and N_C is the count of control photons. If they force the photon to go through a Fresnel biprism and measure it with two detectors, D1 and D2, then N_1 and N_2 are the count of photons going to those detectors respectively. If light behaves like a classical wave, with many photons then the equation $\alpha = (N_C \times N_T)/(N_1 \times N_2)$ is ≥ 1 . However, if they are dealing with only a single photon at a time, then α is approximately zero, or in any case significantly less than one, which violates the equation above.

Their control ("C" in N_C) was low intensity laser light, that they used as a sample of multiple photons simultaneously. The number of photons in such a laser pulse is determined by a Poisson distribution:

$$P(k) = e^{-\lambda} \frac{\lambda^k}{k!}$$

They found $\alpha = 1.00 \pm 0.06$ for the dim laser light, which was significantly higher than $\alpha = 0.13 \pm 0.01 < 1$ for the single photon they produced from the N-V cavity in a diamond. Thereby they proved that their technology could produce a single photon, one at a time.

In that earlier study they showed that a single photon can generate an interference pattern with a Fresnel biprism. This convinced them that they had proved that a single photon is both a particle and a wave that can interfere with itself. (We have a different interpretation.)

That previous study by Jacques, et.al., emboldened them to undertake this experiment.

3.2.4 Back to the Wheeler Gedanken Experiment

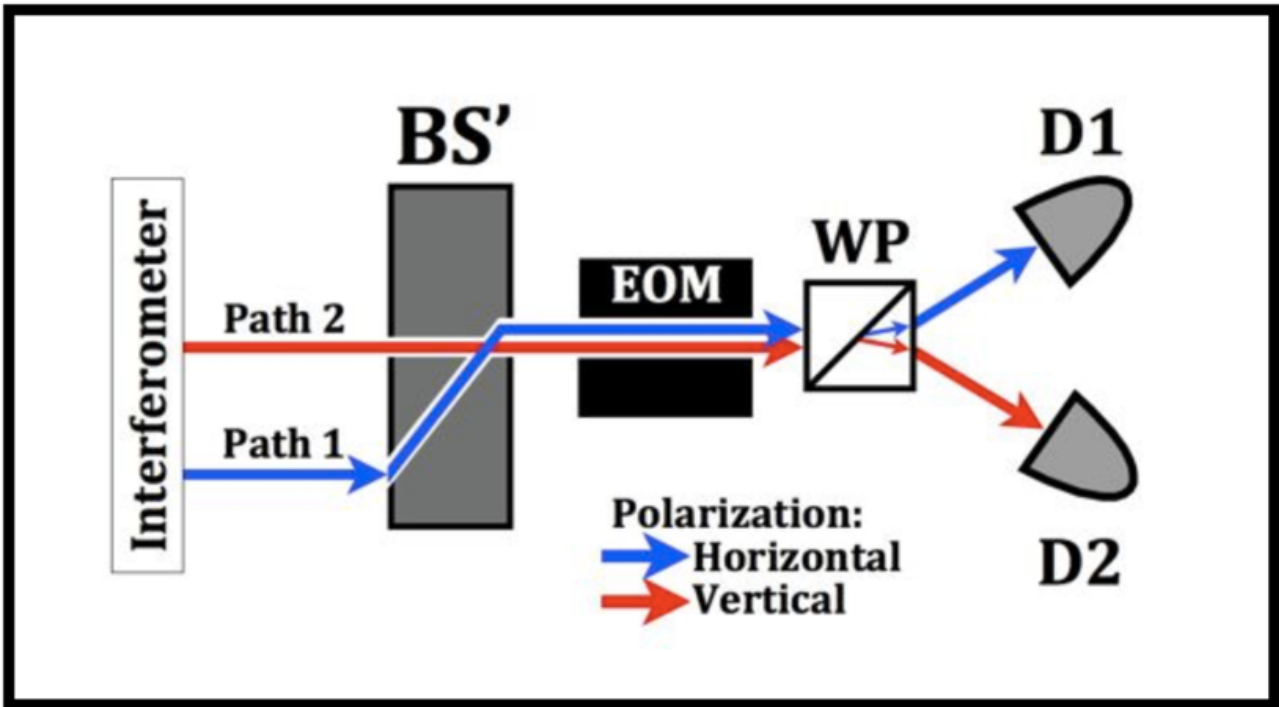


Fig. 24. This shows the output area of the Jacques experiment. In the second beam splitter BS' the horizontal and vertically polarized photons are recombined. That device (Yttrium Orthovanadate (YVO_4) reverse beam splitter BS') rocks back and forth to create a phase shift and interference of Ψ_1 and Ψ_2 . If the EOM is "OFF" it (the EOM) acts as if it were absent. The photons then enter the Wollaston prism where they are assigned to one detector or the other, depending on their polarization.

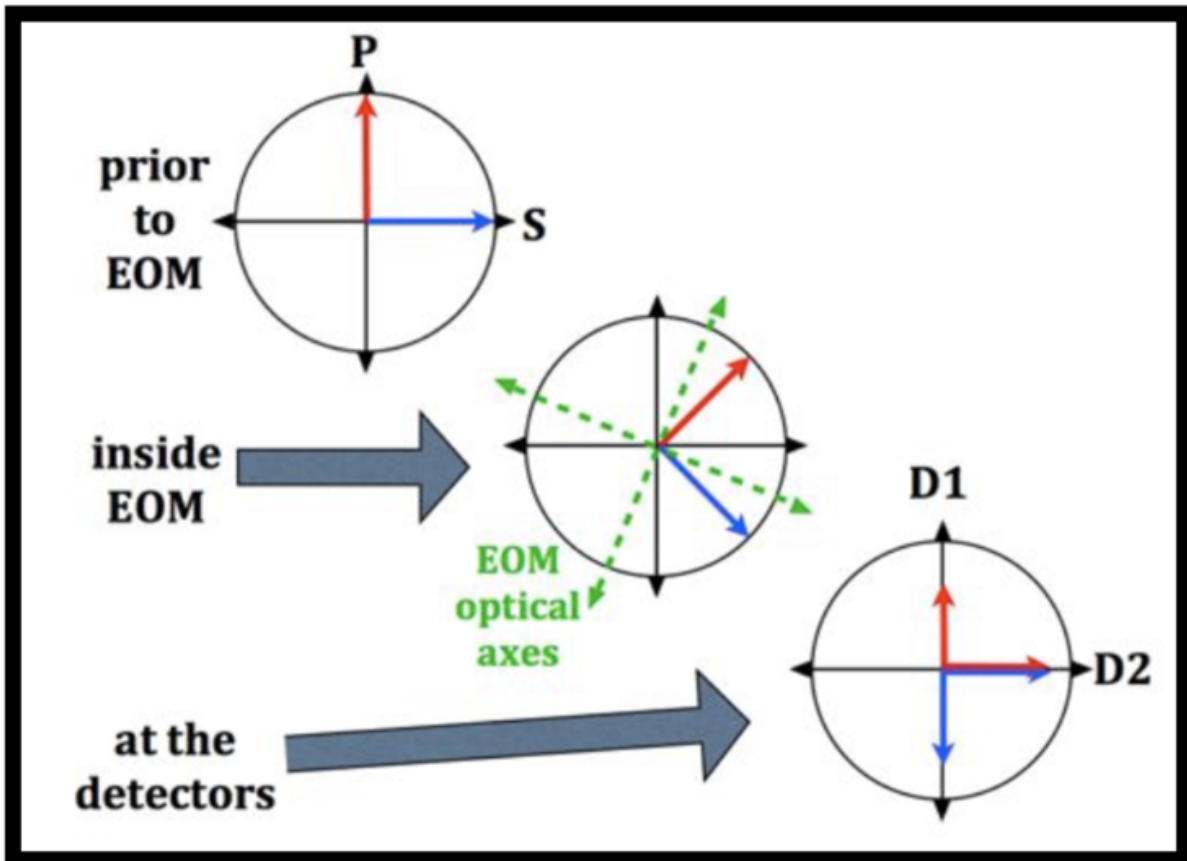


Fig. 25. How the EOM affects angle of polarization. If the EOM is "OFF" (top diagram) it acts as if it is not present. If it is "ON" it rotates the polarization by $\pi/4$ (middle diagram). Bottom: at the detectors, D1 accepts all horizontally polarized photons, D2 accepts vertically polarized.

A phase shift ϕ was implemented between the two pathways by having the reverse beam splitter rock back and forth, as we said. Therefore, if the quantum was crossing the interferometer as a wave, there would be a phase difference between the two paths, and therefore interference inside the WP prism. This would register at the detectors (D1 and D2) as $Y = \pm \cos^2 \phi$ (see Figure 26).

3.2.5 Conclusions in the Jacques, et.al., Publication

Jacques et.al., say the graphs below proves that Wheeler's hypothesis was correct. Shortly we will explain why we disagree.

Jacques et.al., say the random choice in the output area whether to test the quantum as a wave (EOM is "ON") or as a particle (EOM is "OFF") causes the quantum of energy to enter the front door of the interferometer as a wave or a particle. Cause and effect are reversed in time. The state of the EOM is the "cause" whereas the earlier decision of the photon as it entered the front door of the interferometer as a wave (crossing both arms of the interferometer) or as a particle (crossing only one arm) is the "effect."

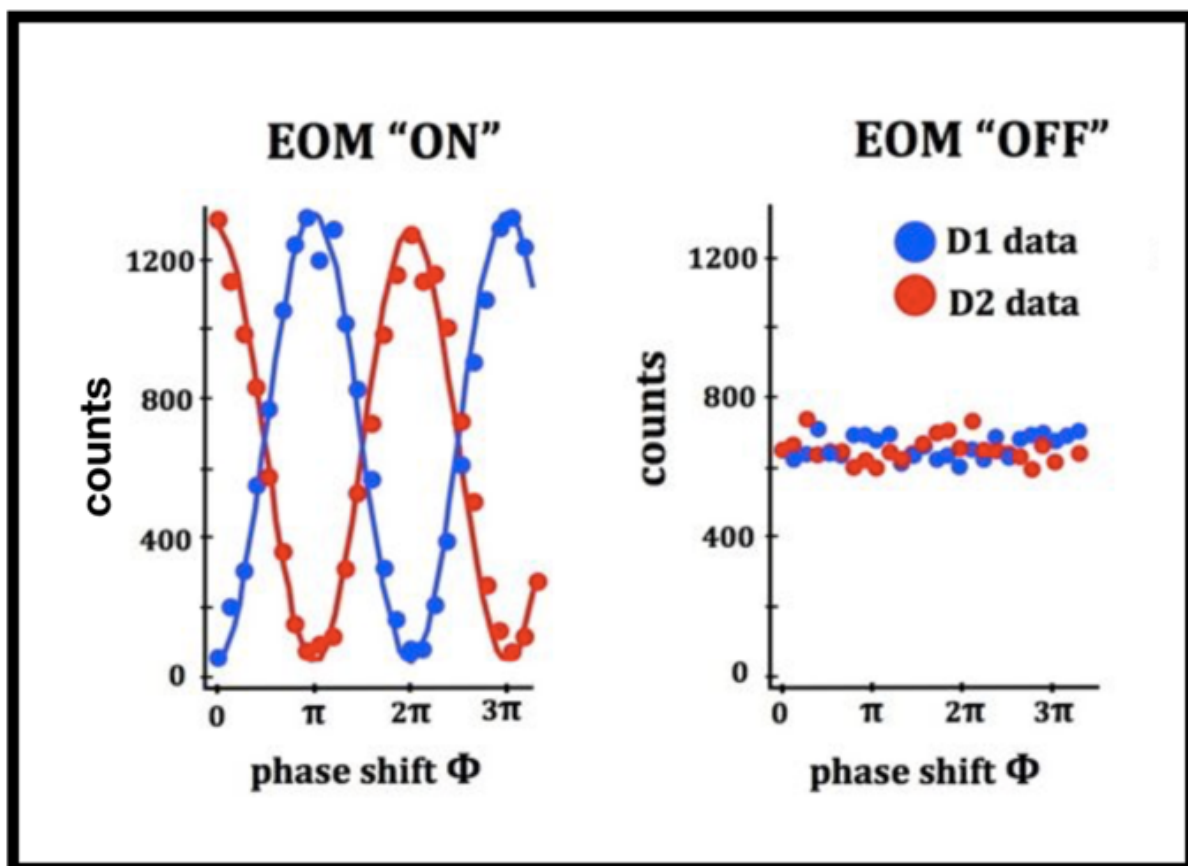


Fig. 26. Output data upon which the entire Jacques experiment pivots. On the left the equation is $Y \approx \pm 650 \times (\cos^2 \phi) + 700$. On the right it is $Y \approx 700 \pm 70$. When the EOM is "ON" they are testing for waves, and the sinusoidal waves on the left show that they see waves. When the EOM is "OFF" they are testing for particles, and the pattern on the right shows that they see particles.

They conclude that when they look for a wave, they find a wave, and when they look for a particle, they find a particle.

That last sentence usually would lead someone to conclude, "So, therefore both waves and particles are always present." But Jacques *et al.*, don't follow that logic. They interpret that sentence as if it said, "Therefore, if a wave is seen it means there is no particle, and if a particle is seen, it means no wave."

Their equipment is so designed that if you find a particle you cannot also test whether a wave is present, and vice-versa. The EOM can only be "ON" or "OFF." There is no third option. The idea that the quanta were either waves or particles is an **assumption** that cannot be tested by the equipment they built and used.

They say they prove Wheeler’s idea, yet that “proof” is an assumption and not based on empirical evidence. If you doubt it, then ask yourself this: If there were both waves and particles always present, then how would their equipment discover that? To restate the obvious: if you build experimental equipment that can test for either waves (EOM is “ON”) or particles (EOM is “OFF”) but not both, and waves and particles both exist simultaneously, what conclusions can you legitimately draw?

Here is an analogy. Imagine that you have a camera with two lenses, one of which can only see men, and the other lens can only see women, and you are blind except when you look through your camera. You go into a busy city and take photographs of people walking on the sidewalks. With one lens you only see men, and with the other lens you only see women. You conclude that your choice of lens is **causing** the men to become women and the women to become men. This is an astonishing scientific discovery.

You wonder if this effect could work backwards-in-time. You find a way to use an EOM to switch lenses after the photons from the people across the street have started their flight and before the photons enter your camera. You still find that your choice of lens causes the men to become women and the women to become men. You have now proved that this effect operates backwards in time!

In defense of Jacques et.al., we must look at the experiment from their viewpoint. They believed that a quantum of energy was enough to create either a wave or a particle, but not both. We start with a different assumption about how much energy is needed for a wave (none).

According to our theory there are both Elementary Waves and photon particles present simultaneously throughout the experiment, just as there are always women and men walking on the sidewalks of an average city.

Our view is that every quantum of energy that enters the interferometer becomes a particle that can only cross the interferometer on one arm or the other, not both. Waves of zero-energy are always present, crossing the interferometer in the opposite direction. The energy of the photon is needed to make a detector “click” no matter whether the EOM is “on” or “off.” If you look carefully at Figure 26, every single red or blue dot represents the impact of one single photon. So, their data is collected as discreet bits, each “bit” being a single photon. To say that they sometimes found waves is an inference they made from the sinusoidal curves on the left side of Figure 26. That sinusoidal curve is made of discreet dots.

Therefore, the Vincent Jacques’ experiment can be explained by TEW. This experiment contributes to our conviction that the quantum world is governed by the same rulebook as the world of human experience. Time always goes forwards in both places. Cause always precedes effect. There is no reason to believe that the quantum world is in any way bizarre or even strange. The difference between the quantum and classical worlds is limited to size.



3.3. Wave-Function-Collapse

3.3.1 Thumbnail Sketch of the Phrase “Wave-Function-Collapse”

QM and TEW have such different ways of thinking that they can’t communicate. So, we will build a bridge by using the term “wave-function-collapse.” The QM side of the bridge is the teaching of Professor Robert Jaffe from the Massachusetts Institute of Technology, his 6 postulates of QM. His core idea is that when you measure or observe a quantum system, wave-function-collapse occurs so that you find only one value for your measurement. TEW has no interest in measurement. It says wave-function-collapse occurs earlier. In a double-slit experiment it occurs when a particle is fired from the gun, because at that moment the particle chooses which of many Elementary Waves it will follow backwards. The single eigenvalue that Jaffe measures at the target-screen is already determined earlier, when the particle leaves the gun. QM and TEW have a difference of opinion about whether a quantum observable has, or does not have definite characteristics before it is measured. QM says “No.” TEW says “Yes.” This has implications for the Schrödinger cat paradox. QM says the cat has no definite properties (“dead” or “alive”) until it is observed. TEW says that the life or death issue was settled before the cat was observed. Figure 27, which is interesting to look at, provides useful insight into this.

3.3.2 Robert Jaffe’s Idea of “Wave-Function-Collapse”

Our “wave-function-collapse” bridge will be supported by one abutment inside QM, and the other abutment inside TEW. On the QM side, our abutment will be the teaching of Jaffe of MIT about the “six postulates of QM.”



- a. “The space of states is a vector space with an inner product.
- b. “Every observable attribute of a physical system is described by an operator that acts on kets that describe the system.
- c. “The only possible result of a measurement of an observable A is one of the eigenvalues of the corresponding operator \hat{A} .
- d. “When a measurement is made, the probability of obtaining eigenvalue α_n is $|\langle \alpha_n | \Psi \rangle|^2$.
- e. “Immediately after the measurement of an observable A has yielded a value α_n , the state of the system is normalized to eigenstate $|\alpha_n\rangle$.
- f. “The time evolution of a quantum system preserves the normalization of the associated ket.”

Those six postulates are abstract. The basic idea is that when you measure an attribute of a physical system, the attribute corresponds to an operator defined in a vector space. A vector space with an inner product is a Hilbert space. Inside the operator are eigenvalues. When you measure the physical system, what you discover is one of the pre-existing eigenvalues of the corresponding operator. After you measured it, that value persists. If you measured it again, you would get the same answer.

This change in the eigenvalues, caused by measurement, is what we will call “wave-function-collapse” on the QM end of our bridge. The “collapse” means the infinite number of possible eigenvalues of that operator before measurement (sometimes called a superposition of eigenvalues) collapses to become one single eigenvalue because of the measurement. This is not just a mathematical change in Hilbert space. The real world also changes, because the characteristic “ A ” now has a fixed value, which allegedly was not true prior to measurement.

When we turn to the TEW side of the bridge, we need to establish an abutment in a system that doesn’t care about measurement. The decisive moment in TEW is when a quantum system is created. One example is when a particle α leaves the gun in a double slit experiment. As we said earlier, we have an unusual definition of this “quantum system”, namely a bonding of particle α and one specific Elementary Ray that is flowing continuously from point “ z ” on the target screen. The particle follows that wave backwards. That is what we call a “quantum system” for the sake of this rather simple-minded discussion.

According to the TEW way-of-thinking, whatever attribute the pairing of “ α and an Elementary-Ray” acquires at creation (as they leave the particle gun), they carry until α hits the detector and is measured.

For our linguistic bridge to work, we need to translate that last sentence into the postulates of Jaffe.

Let’s say that the union of particle α and an Elementary Ray (which we are calling a “quantum system”) has embedded inside an attribute A corresponding to operator \hat{A} .

We propose that when the quantum system was formed, the eigenvalues of \hat{A} collapsed to one specific eigenvalue α_n where n has a specific value, which we will call 7.

Later when we measure the system at the detector (target screen) we find that characteristic A has an eigenvalue of α_7 . In other words, that “wave-function-collapse” that Jaffe says happens at measurement, TEW says happened earlier, at the particle gun. Inside the

Elementary Ray and particle α union (“quantum system”) we find attribute A , which corresponds to operator \hat{A} which already has value α_7 after the particle leaves the gun. TEW and QM differ concerning when the quantum system acquired that value (α_7).

There is a dispute between TEW and QM concerning the characteristics of a quantum system before it is measured. TEW says it has definite characteristics. QM says it has none because measurement produces those characteristics. Before measurement there was a “superposition” which consists of mutually exclusive eigenvalues all existing simultaneously.

This is the Schrödinger cat paradox in disguise. This means that Schrödinger’s cat is a problem for QM but not for TEW.

3.3.3 A High-Energy Collision Experiment

When and where does wave-function-collapse occur in Figure 27?

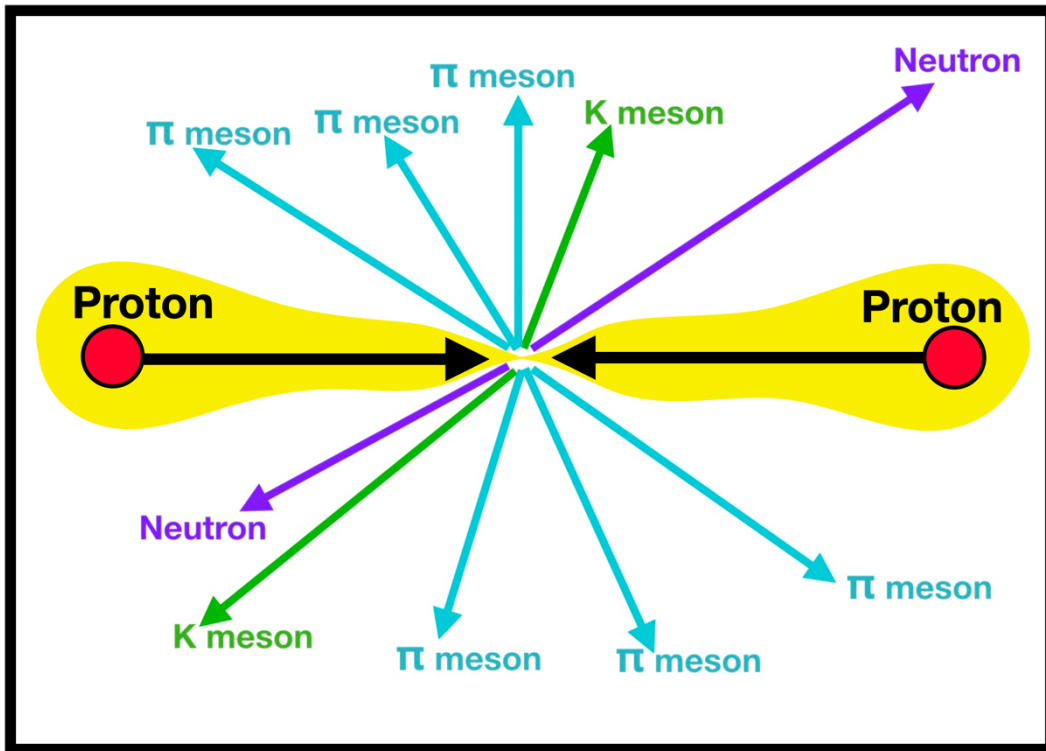


Fig. 27. If two protons collide at almost lightspeed, they annihilate. New particles spray out from inside the collider and are measured by detectors outside. When and where is wave-function-collapse located? TEW says it is at the center. QM says it is when the new particles are measured, later and outside the collider.

TEW says the decisive event is when newly created particles attach to Elementary Waves at the center of this Figure. The eigenvalues are settled long before the particles reach the detectors, which is where QM says wave-function-collapse occurs.

Our goal was to build a bridge to clarify the meaning of “wave-function-collapse.” We have now achieved that goal.



3.4. Double-Slit Experiments

In teaching people how to understand TEW, the most decisive lesson is the double slit experiment, to which we now turn. Feynman said that the double-slit experiment embodies what he called the “central mystery” of QM. All the mysteries of the double-slit experiment, including Complementarity, can be understood using TEW, without the need for human observers.

3.4.1 Thumbnail Sketch of the Beginning of the Section on Wave-Function Collapse

We will start this section with a little-known experiment by Robert Pfleegor and Leonard Mandel, that provides evidence that cannot be explained by wave-particle duality. Reiterate: this is another experiment that QM cannot explain! After Pfleegor and Mandel, we will show colorful pictures (Figures 30–32) displaying what allegedly happens inside a double-slit experiment, if wave-particle duality were true. The pictures are so self-contradictory that it isn’t possible that nature does it that way. Then we’ll explain why Einstein and a mathematician named John von Neumann would probably endorse our viewpoint.

3.4.2 The Pfleegor and Mandel Attenuated Laser Experiment

We start our discussion with a variation on a double-slit experiment that was built by Robert L. Pfleegor and Leonard Mandel of the University of Rochester, Rochester NY. They built a different kind of experiment and disproved wave-particle duality. This experiment is not mentioned in other discussions of double-slit-experiments. (39)

It is widely taught that when a single photon goes through a double-slit experiment, if there is an interference fringe pattern on the target screen, then that means the photon went through both slits and interfered with itself. Pfleegor and Mandel's experiment disproves that idea.

They replace the double-slits with two lasers. Each photon can come from one laser or the other, not both simultaneously. If the wave-particle duality theory were correct, this arrangement with two lasers should eliminate any interference wave pattern on the target screen. But Pfleegor and Mandel find such a pattern! Photons are emitted one-at-a-time. Yet there is an interference wave pattern on the target screen!

Since this is confusing, we will suggest one way in which this could happen. Suppose that zero-energy waves of one laser interfere with the zero-energy waves of the other, so there are already invisible standing waves inside the equipment before any photon arrives. Then when a photon is emitted from one laser or the other, we would expect the photon to behave as if it is experiencing wave interference, because the zero-energy waves were already present and interfering. An analogy would be that if we could see a kayak but could not see the river, and we saw the kayak bobbing up and down as it went down the river, we might conclude that there are standing waves on the invisible river.

3.4.2.1 Pfleegor and Mandel Materials and Methods

Pfleegor and Mandel use two independent Helium-Neon lasers producing attenuated light, with the two beams crossing at an angle that varied slightly $\theta \leq 2^\circ$. As we said, this is akin to a double slit experiment in which each photon comes from one slit (analogous to one laser) or the other but cannot come through both slits (analogous to both lasers). The light is so attenuated that having two photons in the experiment simultaneously is statistically improbable. A photon takes 3 nanoseconds to cross this apparatus, which is followed by 150 ns of darkness, with no photons.

The two He-Ne lasers cross paths (with polarization aligned), but the light is so diminished that a photon from one laser would register, followed by a long dark spell, then another photon, perhaps from the other laser. At risk of being repetitive, we say that since interference appears in the final data, one cannot attribute it to a wave-particle interfering with itself.

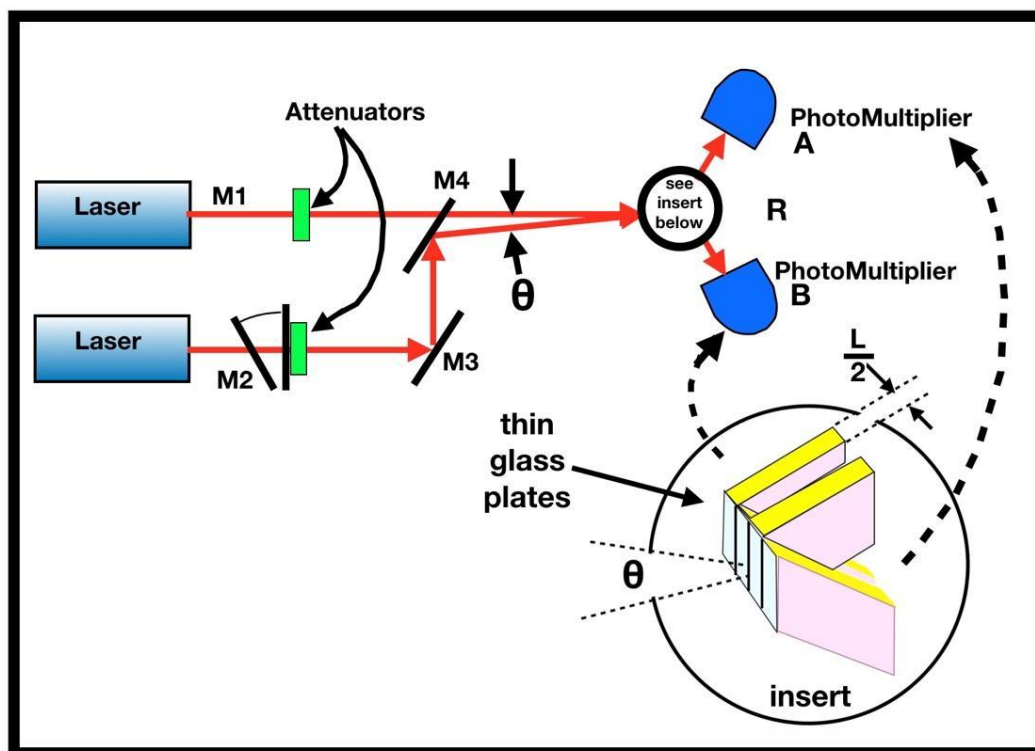


Fig. 28. Equipment used by Pleeegor and Mandel. Two He-Ne lasers (on left) with correlated polarization put out attenuated beams: one photon 2% of the time. The two beams (shown in red) have a small angle θ between

them. The contents of circle R are shown in an insert in the lower right: a stack of thin plates of glass. All the odd numbered plates (1, 3, 5 . . .) send photons to one photomultiplier and the even number send photons to the other.

The photons are triaged by that stack of glass plates, each of which has a thickness half an interference fringe width. When the half-fringe spacing coincides with the plate thickness, the fringe maxima fall on the odd numbered plates, at which time the even number plates should receive approximately zero photons. The position of the fringe maxima fluctuates slightly as θ changes. If the number of photons n_1 increases for detector A, the number of photons n_2 decreases for detector B.

This stack of glass plates aggregates data. Data from the peaks of several interference fringes are aggregated by the equipment and by the mathematical equations, thereby summing the interference information across all peaks. This is done by design, because this experiment has so few photons that there are not enough photons to make several peaks visible on graph paper.

3.4.2.2 Results of Pfleegor and Mandel Experiment

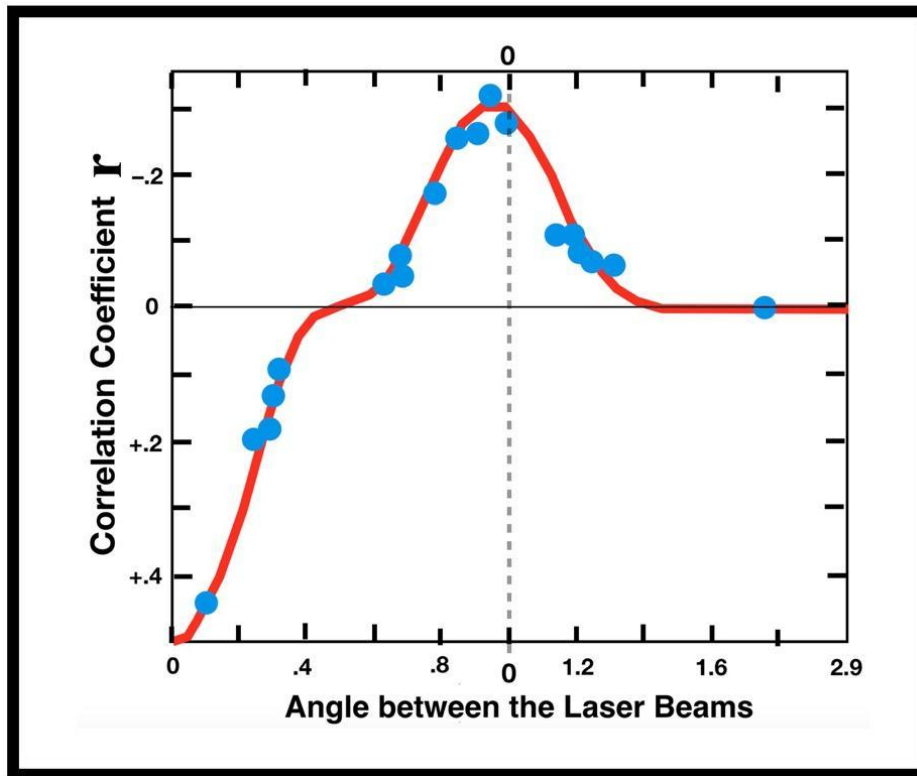


Fig. 29. Data from Pfleegor and Mandel for 19 photons, compared to the red line predicted by their equations. The interference fringe (proof of wave interference) is found in the peak at the center. Statistically the blue dots fall on the red line so accurately that Pfleegor and Mandel conclude that this graph proves the interference effect for which they were searching.

The correlation coefficient graphed on the vertical axis of Figure 29 is:

$$r = \frac{\langle \Delta n_1 \Delta n_2 \rangle}{\sqrt{\langle (\Delta n_1)^2 \rangle \langle (\Delta n_2)^2 \rangle}}$$

The authors develop an equation that predicts what the results should be, which yields the red curve shown on Figure 29. We will not further explain how their equation works, nor will we discuss the calibrations on the horizontal axis of Figure 29.

It is easy to see why Pfleegor & Mandel designed their experiment to produce only one interference peak, in contrast to most double-slit experiments that have at least a half dozen. The goal of Pfleegor and Mandel is to work with a small number of photons, to prove that almost no photons are needed to create an interference-fringe-pattern.

3.4.2.3 Conclusions from the Pfleegor and Mandel Experiment

This experiment disproves the QM thesis that a single photon interferes with itself in a double slit experiment. If a single photon demonstrates an interference fringe-pattern (i.e., the peak in the center of Figure 29) that implies that it is affected by zero-energy wave interference that is present even when there is no photon, which is most of the time.



3.4.3 Computer Generated Video of a Double Slit Experiment, Using QM Assumptions

We turn now to a garden-variety double-slit experiment. It is vitally important to distinguish between what we know versus what we think we know (i.e., what we fantasize). What we know is that particles leave a source (or gun), and a pattern appears on a target screen. We cannot see what happens in between. We cannot see the waves if there are waves. We might imagine that the waves are forming a probability cloud, but we can't see the alleged cloud, so we should keep an open mind about whether it exists.

The best approach is to hold the alleged cloud as a hypothesis and collect data that supports or undermines that hypothesis. With the beautiful pictures we are about to display, despite their beauty, the preponderance of evidence indicates the hypothesis is wrong. We should seek a better hypothesis.

The following sequence of pictures is produced by a computer making hundreds of Schrödinger time-evolution calculations for each point in a fine grid of locations in the x-y plane. The probability of a photon being found at each point will be graphed vertically on the z-axis using a rainbow of colors. The unstated assumption is that one Schrödinger equation has jurisdiction over the entire experiment, an assumption we disagree with.

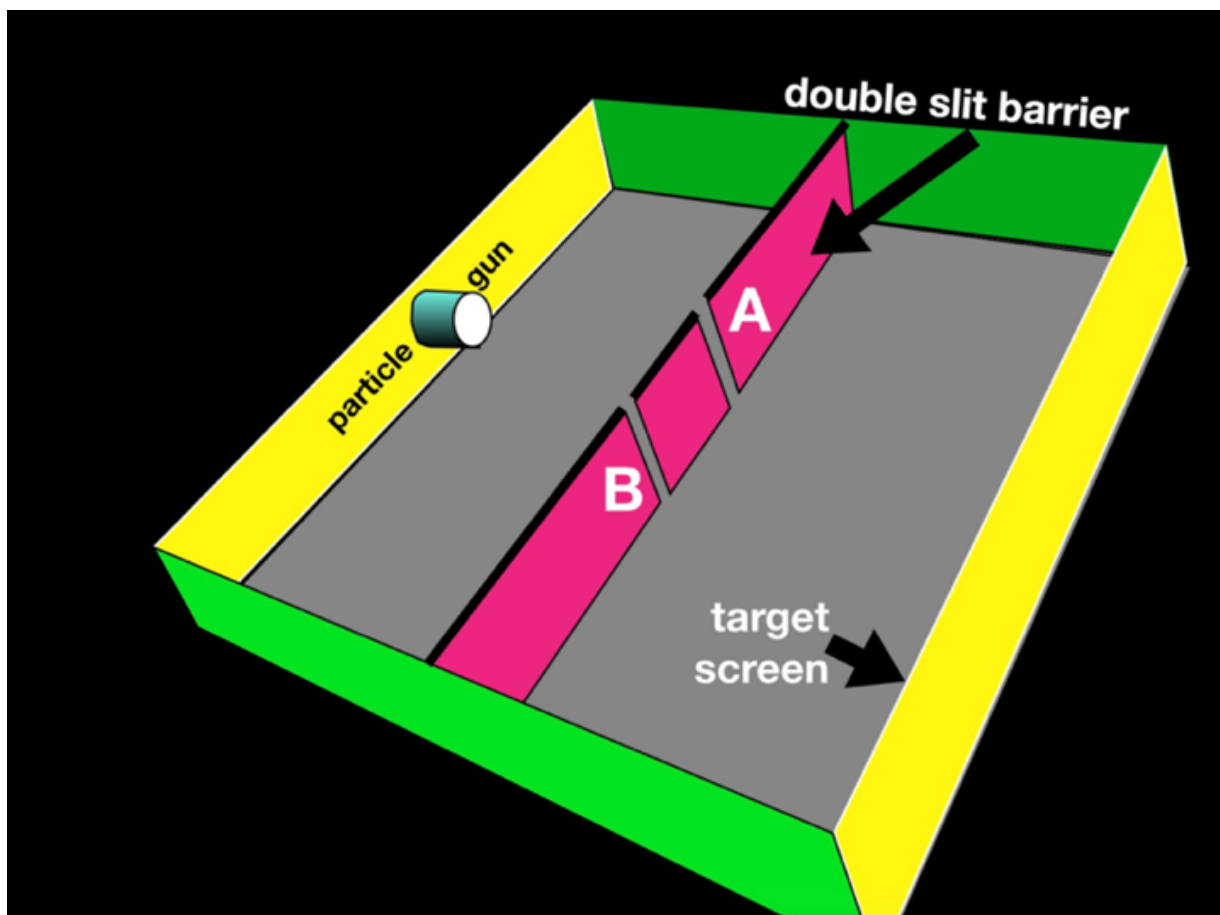


Fig. 30. This is the apparatus we will explore in the next two Figures. The x-y plane is shown in gray here but is black in the next two Figures.

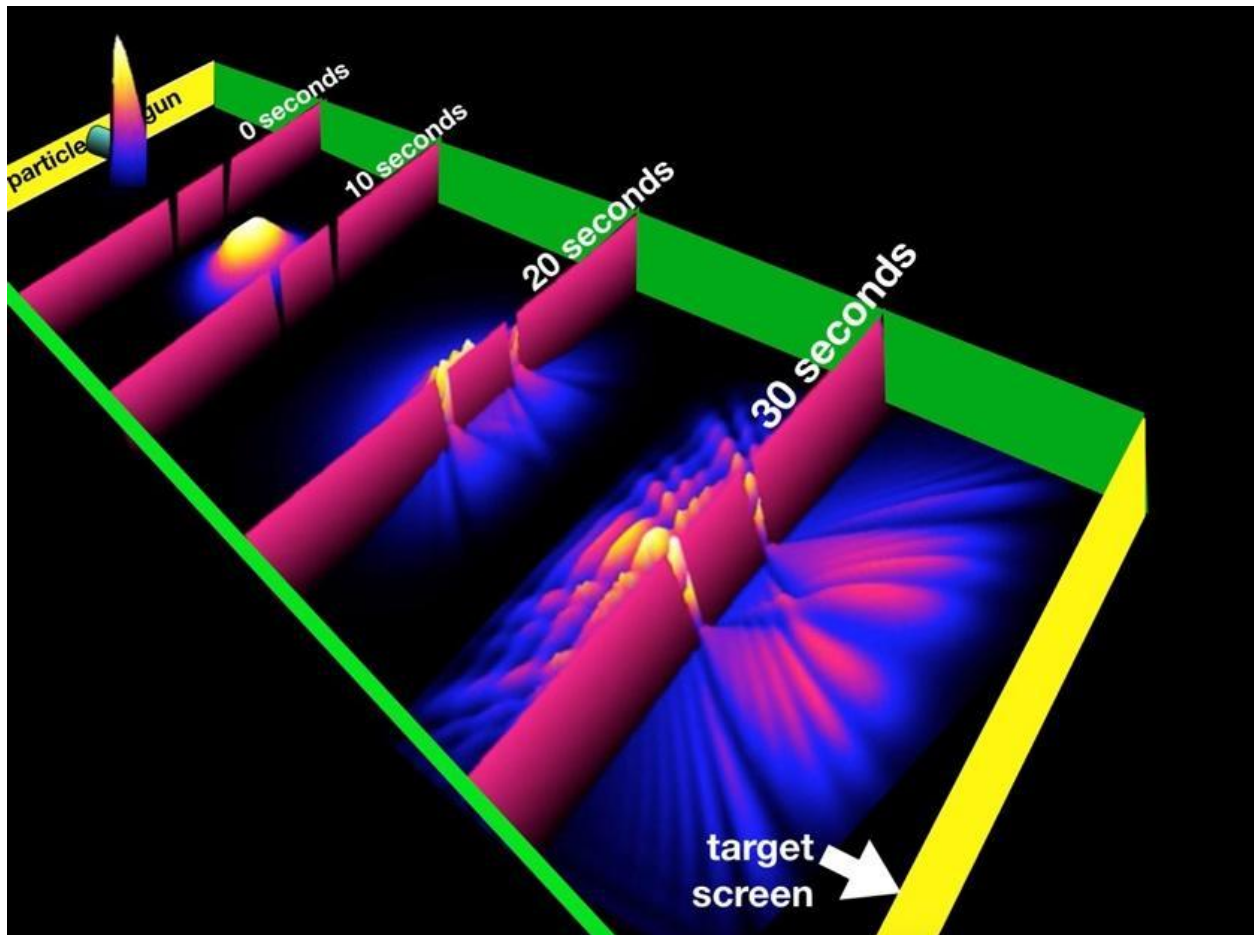


Fig. 31. This is a time-lapse photo (a computer screenshot every ten seconds) of the time-evolution. It is slow because the computer makes hundreds of calculations for each point on the x-y plane. The pink double-slit barrier is represented four times, depending on the time when the screenshot is taken.

At zero-seconds the Gaussian forms a sharp peak, meaning we know where the particle is located with a high probability. At 10 seconds the Gaussian spreads out and loses altitude. At 20 and 30 seconds the probability cloud begins to bounce off the pink barrier and recoil backwards toward the particle gun. Slivers of the cloud leak through the two slits (A and B). At 30 seconds, most of the probability is a backwash ricocheting off the double-slit barrier. A minority of the probability has passed the double-slit barrier and is streaming toward the target screen.

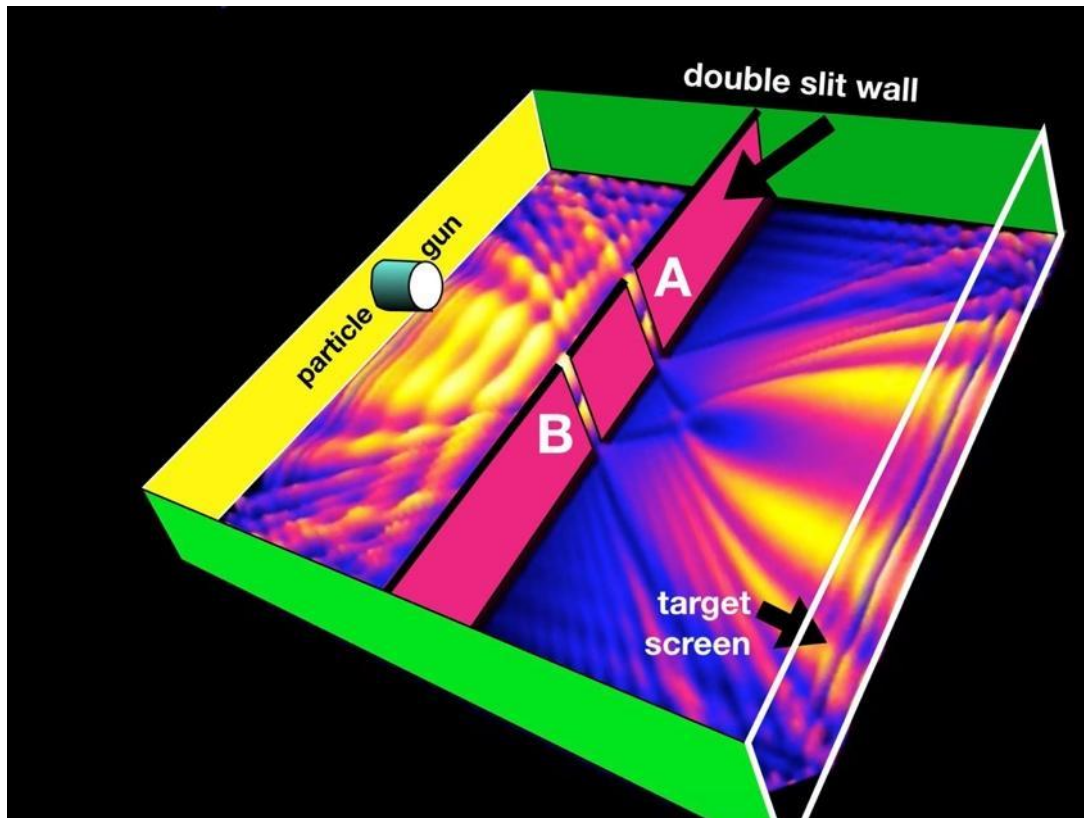


Fig. 32. By 40 seconds the probability cloud has reached the target screen.

Several things can be learned from Figures S31–32. First, most of the probability cloud remains on the gun side of the double-slit barrier, as a backwash. It never makes it through the two slits. Second, that minority of the probability that is streaming toward the target screen has ridges and valleys such that we would expect that it will make a wave-pattern on the target screen, although the central peak looks insufficiently represented. Third, the probability cloud is extensive, filling the box wall-to-wall and end-to-end. It is impossible to imagine how such an extensive cloud could instantly become one dot, when wave-function-collapse abruptly occurs.

When wave-function-collapse occurs, the entire cloud must instantly vanish everywhere because 100% of the probability is abruptly relocated from the cloud to the dot. It is impossible to imagine how this happens instantaneously. Most experts deal with this contradiction by avoiding it. They use words like “decoherence” to obfuscate the problem. We say the contradictions are real and cannot be covered up by using a word like “decoherence.”

If any part of the cloud were to continue to exist after a dot appears, it would be capable of creating a second dot, which would be impossible because the gun only fired one shot.

If you believe TEW, you will believe no such probability cloud exists. TEW says that there are Schrödinger equations governing the double-slit-experiments, but those equations (plural) do not function in the way that Figures 31–32 assumes. We envision many Schrödinger equations, not just one.

3.4.4.1 Comments by Albert Einstein and John von Neumann

Einstein says when a dot appears on the target-screen, the entire probability cloud needs to collapse to a single point, faster than the speed of light, which is impossible.

Mathematician John von Neumann has a different criticism of the garden-variety double-slit experiment. He says the Schrödinger equation is a deterministic equation. He asks, "How did randomness get into quantum mechanics?" Randomness cannot arise from a deterministic equation.

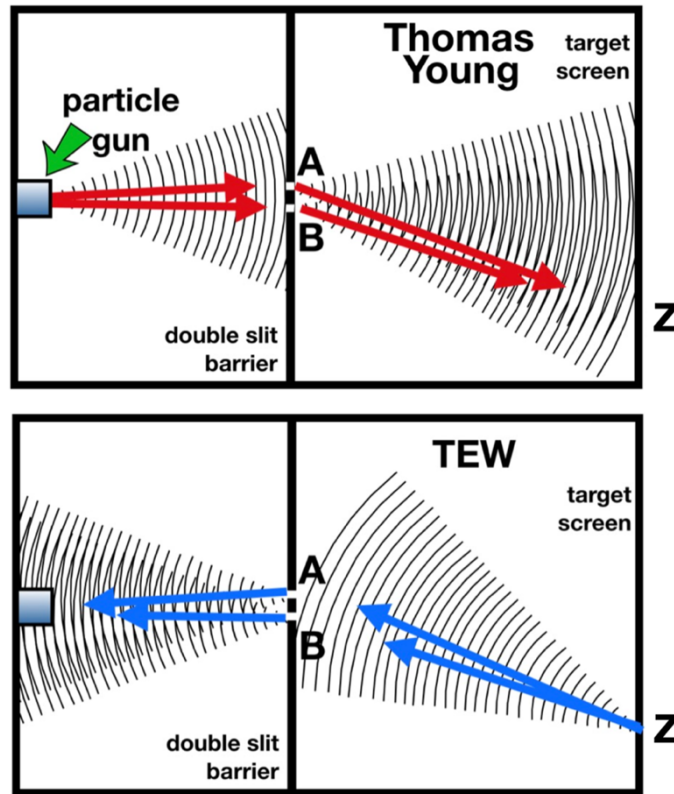


Fig. 33. Thomas Young's model of a double-slit experiment (top) compared to our model (bottom). "Z" is an arbitrary point on the target screen.

Our reply to Einstein is that his criticism does not apply to TEW's picture of the double slit experiment (Figure 33 bottom). In TEW nothing goes faster than the speed of light. As we said, there is no probability cloud in the double-slit experiment.

Our reply to von Neumann is that the source of randomness is the particle (α) inside the gun. We know from Brownian motion that particles are intrinsically erratic. It is the particle that makes a random choice among incoming Elementary Waves. After that decision is made, it is a Schrödinger wave that carries the particle to the target screen, and that is indeed a deterministic wave, as von Neumann said. At the instant we call "wave-function-collapse" the double-slit experiment changes from probabilistic to deterministic, which is when the particle is emitted from the gun.

The particle, before leaving the gun, selects which Elementary Wave it will follow backwards. As we will show below, the Elementary Wave, starting at point "Z" on the target screen, travels to the photon source, makes a sharp "U" turn at the particle, and as it does so it blossoms into a Schrödinger wave, which carries the particle to the same point "Z" on the target screen.

But, if the particle had chosen a different in-coming Elementary Wave, the quantum system (meaning the particle-wave-backwards union) would be different. There is a different Schrödinger wave for each quantum system, and there are as many quantum systems as there are points on the target screen.

Although it is repetitive (we apologize) we will state the same thing in a different way. Von Neumann is correct that each Schrödinger equation is deterministic. It only becomes relevant after the particle has made its choice. Schrödinger equations are not relevant to the first half of the experiment when plane waves ($\Psi_L = e^{(ik + \omega t)}$) from the target screen are coming backwards through the two slits and competing with one-another for the particle's

attention. As we said, randomness enters the double-slit experiment because of the unpredictability of a particle as it makes its erratic choice of which pathway to take away from the particle gun.



3.4.5 Complementarity

3.4.5.1 Thumbnail Sketch of Complementarity (Part of the Section on Double-Slit Experiments)

We will now give a sensible explanation of ‘‘Complementarity.’’ That word means that if you know which slit a particle went through then the wave-interference pattern on the target screen vanishes. We explain it based on Elementary Waves alone. QM says you need a human observer to explain complementarity. We say that it makes no sense to have a science that depends on human observers. Why does QM depend on human observers when nature doesn’t care about human observers? Nature has existed 13.8 billion years and is spread over billions of galaxies, and most of the time there are no human observers. So, the QM idea of ‘‘observers’’ is nonsense. It violates the postulate that the laws of nature are invariant in different locations. Our theory avoids the need for human observers.

3.4.5.2 Complementarity Is Due to Elementary Waves, Not Due to Human Observers

Complementarity is caused by mathematical rules we are about to state, not by human observation. The linear partial differential equations (PDEs) in this experiment can be added together if and only if they originate from the same point Z on the target screen. Two PDEs from different points (like Z₁ and Z₂) have no ability to add together.

To discover which slit a particle uses, researchers insert a detector. The energy from the lamp is infinitely more than the zero-energy of the Elementary Waves passing through the lamplight. It changes the waves, so they no longer act as if they originated at point Z. The wave passing backwards through A no longer adds together with the wave passing backwards through B, because of the PDE rules. There is no wave interference near the gun.

What does the wave interference pattern on the target screen mean? Indirectly it reflects the interference of Elementary Waves near the particle gun. If-and-only-if there is interference in proximity to the gun, will the screen display a wave interference fringe pattern (Figures 34 and 35).

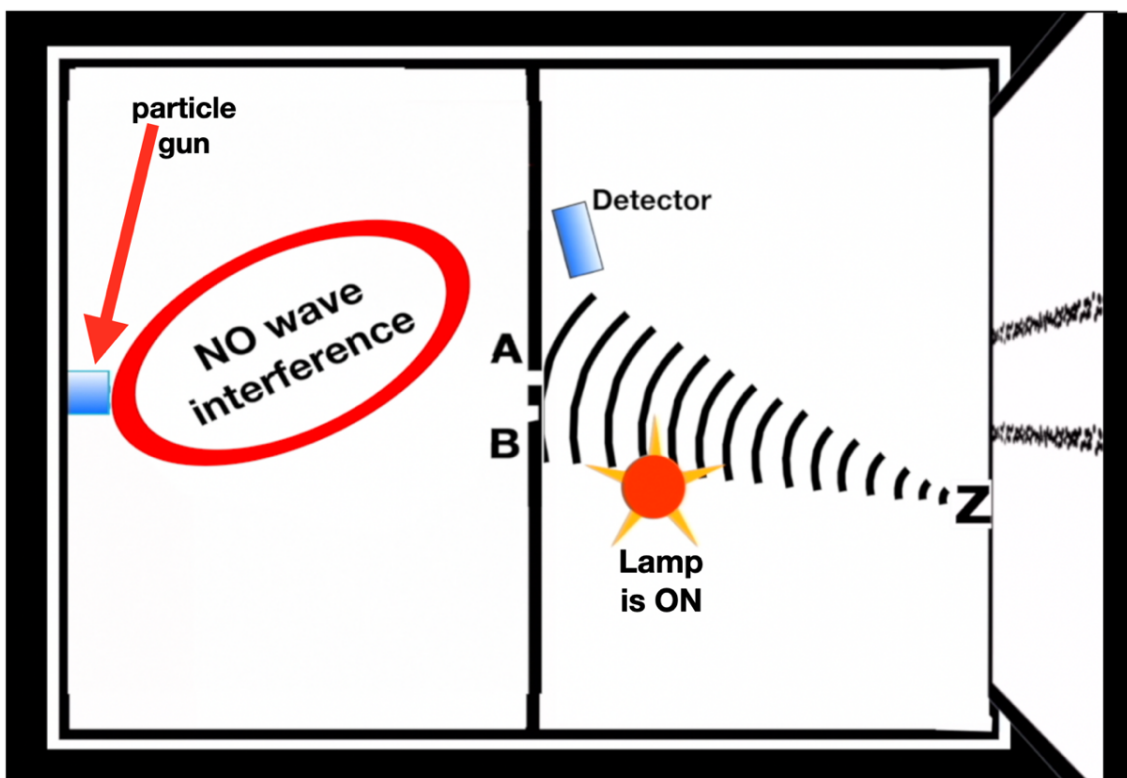


Fig. 34. Elementary Waves from point Z do not interfere after passing backwards through the two slits because the energy from the lamp modified them. The wave through A acts as if it originated at A. The other as if it originated at B. Because of the PDE rules they do not interfere. The absence of wave interference in proximity to the gun indirectly causes an absence of a wave pattern on the target screen on the right.

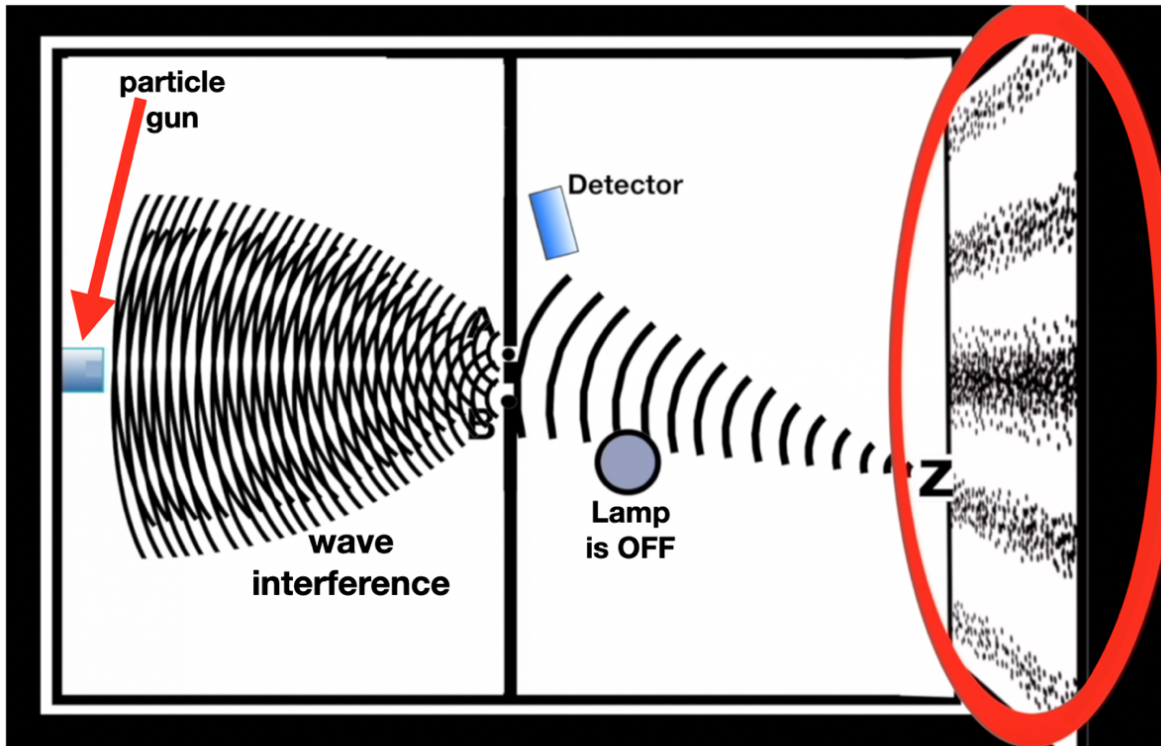


Fig. 35. With the Lamp OFF the waves from point Z through slit A form a superposition with those from Z through B, because of the PDE rules. Wave interference on the left indirectly produces the wave pattern on the target screen (right).

3.4.6 Wave Pattern on the Target-Screen

Does TEW produce the same wave interference fringe pattern on the target screen as QM does? We will now present two different Figures, using two different mathematical equations, to prove that the pattern on the target screen will be the same with TEW as with QM.

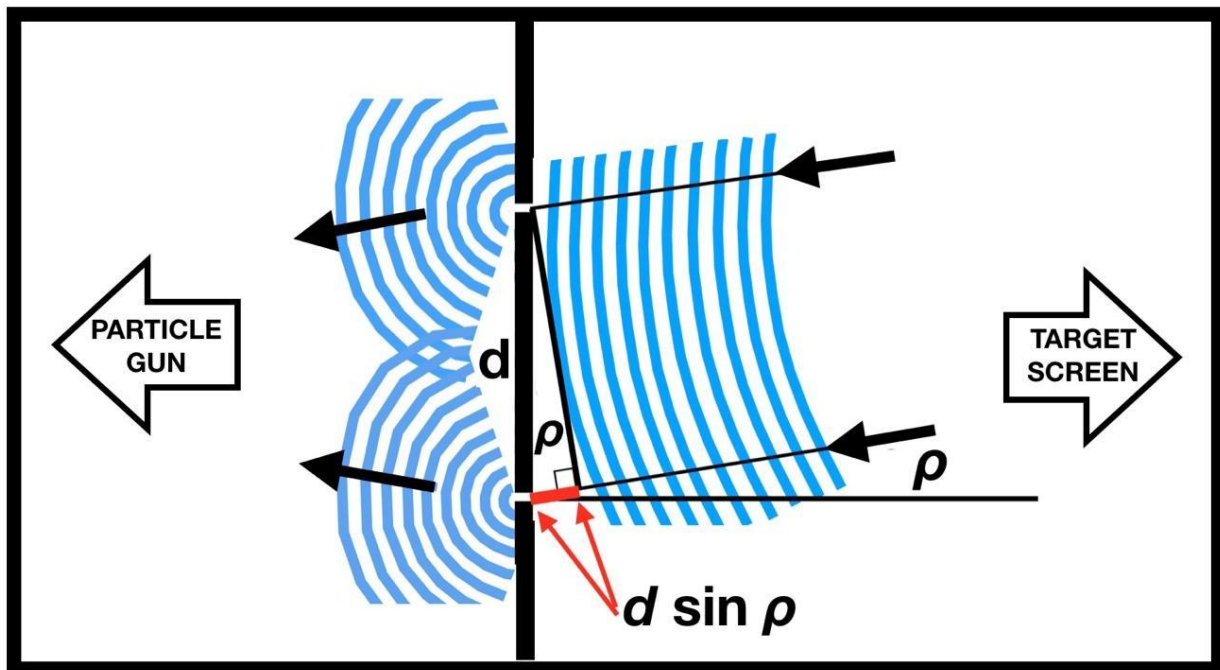


Fig. 36. This reverses the direction of the waves in Thomas Young's diagrams but keeps his triangle and equation intact.

This Figure shows that Young’s equation [$d \sin(\rho)=m\lambda$, for $m=0, \pm 1, \pm 2, \dots$] still predicts where the peaks will be located on the target screen.

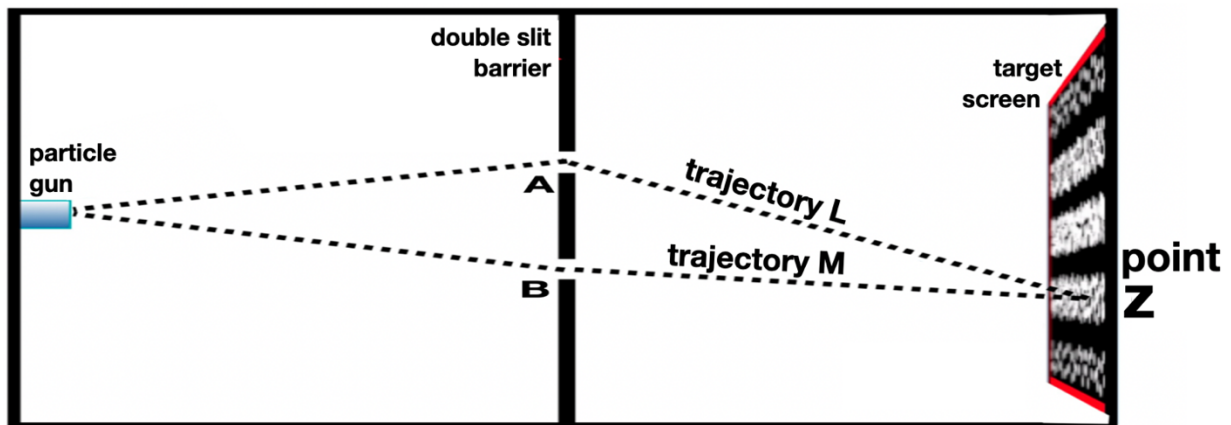


Fig. 37. This is another way to show that the pattern on the target screen will be the same with TEW as with QM. This diagram compares the length of two trajectories (“L” versus “M”) between the particle gun and point “z.”

If λ is the wavelength

$$\text{Phase of the wave} = \left[\left(\text{Length of “L”} - \text{Length of “M”} \right) \text{ modulo } \lambda \right] \times \left(\frac{2\pi}{\lambda} \right)$$

The phase of the wave, measured in radians, tells us the vertical position of a dot inside a wave interference fringe pattern. This equation does not mention whether the waves are traveling to the right or to the left. The equation means that the phase of the wave will be the same at the particle gun as at the target screen. With TEW the phase of the wave at the gun determines the likelihood that a particle will be fired in response to that wave. Therefore, the phase of the wave information will be transported by the particle from the gun to the target. The phase of the wave at the gun determines the phase of the wave pattern on the screen.

3.4.7 The Meaning of “Plane” Waves

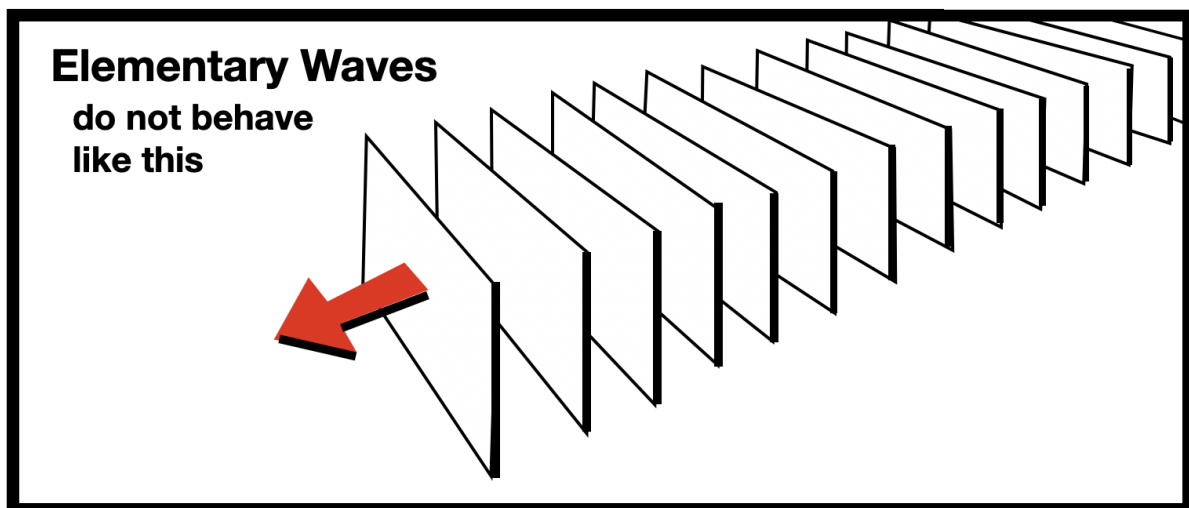


Fig. 38. Although we speak of them as “plane waves” ($\Psi_L = e^{(ik + \omega t)}$), nevertheless Elementary Waves coming from the target screen do not march across the space between the screen and the double slit barrier as a series of parallel planes.

This is because of the rules governing PDEs: two Elementary Wave PDEs cannot be added together if the wave PDEs originate from different points of origin (like z_1 and z_2) on the target screen. It would be clearer if we named them “plain” instead of “plane waves.”



3.5.1 Thumbnail Sketch of the Bell Test Experiments (Two Paragraphs)

It's complicated. John Bell proposed an experiment in 1964 to test an esoteric aspect of the quantum world. For more than fifty years quantum scientists did these experiments, proving that nature didn't work the way Einstein thought. From those experiments come quantum computers, cryptography, and communication. But the Bell test experiments cause havoc. Some quantum experts say, "Everything here on earth is immediately affected from the other side of the Milky Way galaxy, 106,000 light-years away." Other quantum experts say, "Nonsense!"

TEW has its own esoteric and hard-to-understand idea, called a "Theory of Bi-Rays", which generates equations that explain the Bell test experiments. Our approach avoids the local effect of anything 106,000 light-years away. Furthermore, our experiments start earlier than QM's experiments. Before a photon leaves its lamp, first an Elementary Wave travels from the detector to the lamp and triggers the photon to follow it backwards. Since TEW starts long before a particle (photon) starts to move, therefore we start our stopwatch long before QM starts its stopwatch. That means many phenomena that QM thinks are too far away ("nonlocal"), could have an influence because TEW classifies them as "local." That leads us to say that our Bi-Ray explanation of these experiments is a "local realistic" explanation but differs from Einstein's "local realism." That sentence grates on the ears of QM experts, because they define "local/nonlocal" differently than we do, due to the timing of our respective stopwatches.

3.5.2 The Theory of Bi-Rays

TEW has another level of sophistication, more advanced than what we mentioned so far. The advanced version of TEW is called "Bi-Ray Theory." TEW says, as you remember, that everywhere in space there are an infinite number of Elementary Waves traveling in all directions and at all frequencies. That, in turn, implies that every Elementary Ray, like the blue arrow in the next Figure, has a mate, namely the red arrow traveling coaxially in the opposite direction.

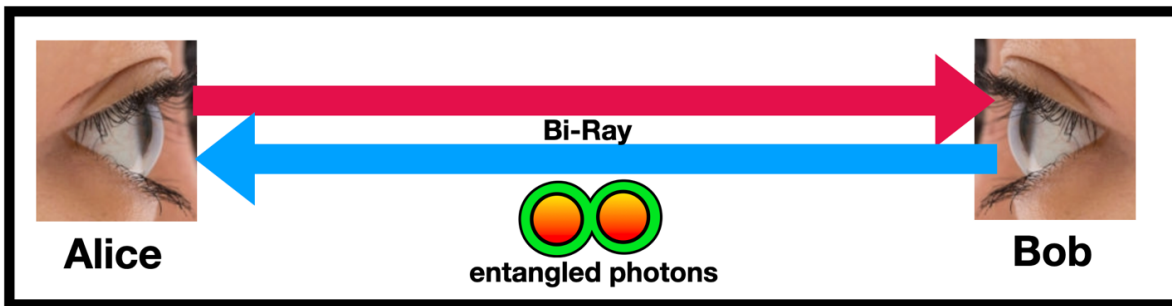


Fig. 39. A pair of entangled photons is emitted by a 2-photon Source (not shown) in the middle of a bi-ray. The two photons travel in opposite directions. Each photon follows both rays of the Bi-Ray.

We call this a "Bi-Ray", namely an Elementary Ray going in one direction, and an identical one traveling coaxially in the opposite direction. "What makes such countervailing rays coherent?" The answer is the photons or particles which are following the Bi-Rays. This is an assumption we make.

It is instructive to use an analogy that these Bi-Rays are like a train track with two rails. A photon is like an engine. It is the engine and not the railroad track which provides the energy. This analogy has two advantages: first, it clarifies that each photon travels on both tracks (both rays); second, it clarifies that the energy comes from the photon and not from the Bi-Rays.

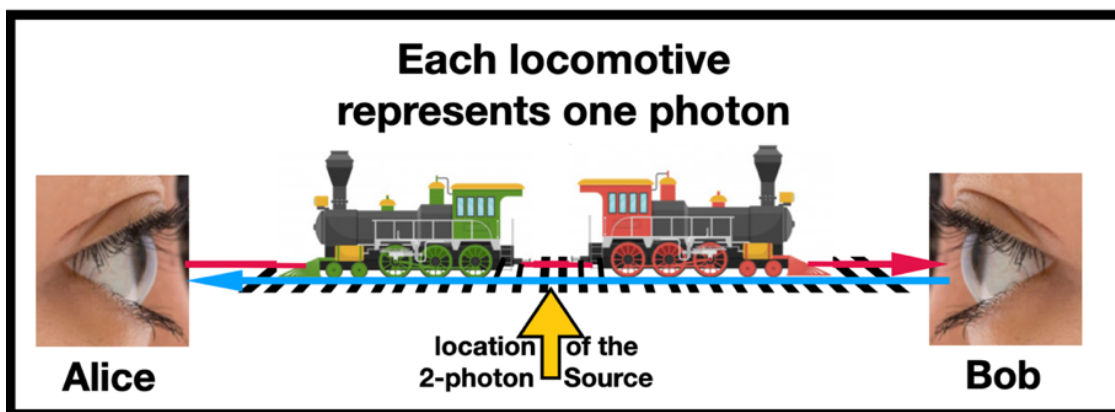


Fig. 40. The Bi-Rays are like railroad tracks which each of the photons follow. The railroad track metaphor emphasizes how each photon follows both rays (rails).

We assume that the probability of a locomotive (or photon) following the Bi-Ray (railroad track) is the amplitude of it following one ray times the amplitude of it following the other ray or rail.

Based on the equations below, we will derive a coincidence rate for Alice and Bob that will be $P = \cos^2(\varphi_2 - \varphi_1)$ or $P = \sin^2(\varphi_2 - \varphi_1)$, where “P” means “probability.” In the Bell test experiment literature, they use the term “coincidence rate” for that.

The difference between cosine and sine in the final data is that it depends on what technology is used to generate two entangled photons. For example, in Alain Aspect’s experiment (Figure 41) they used a calcium cascade source to generate 2-photons with the same polarization, and therefore the coincidence rate they discovered was $P = \cos^2(\varphi_2 - \varphi_1)$. If Aspect had used a different source that generated photons orthogonal to one another, then his coincidence rate would have been $P = \sin^2(\varphi_2 - \varphi_1)$.

One experiment found a coincidence rate of $\sin^2(\theta + x)$, where the variable “x” varied depending on the time of the day, as the temperature of the equipment changed. The variable $\theta = \varphi_2 - \varphi_1$. That entire family of sinusoidal squared curves violates Bell’s inequality.

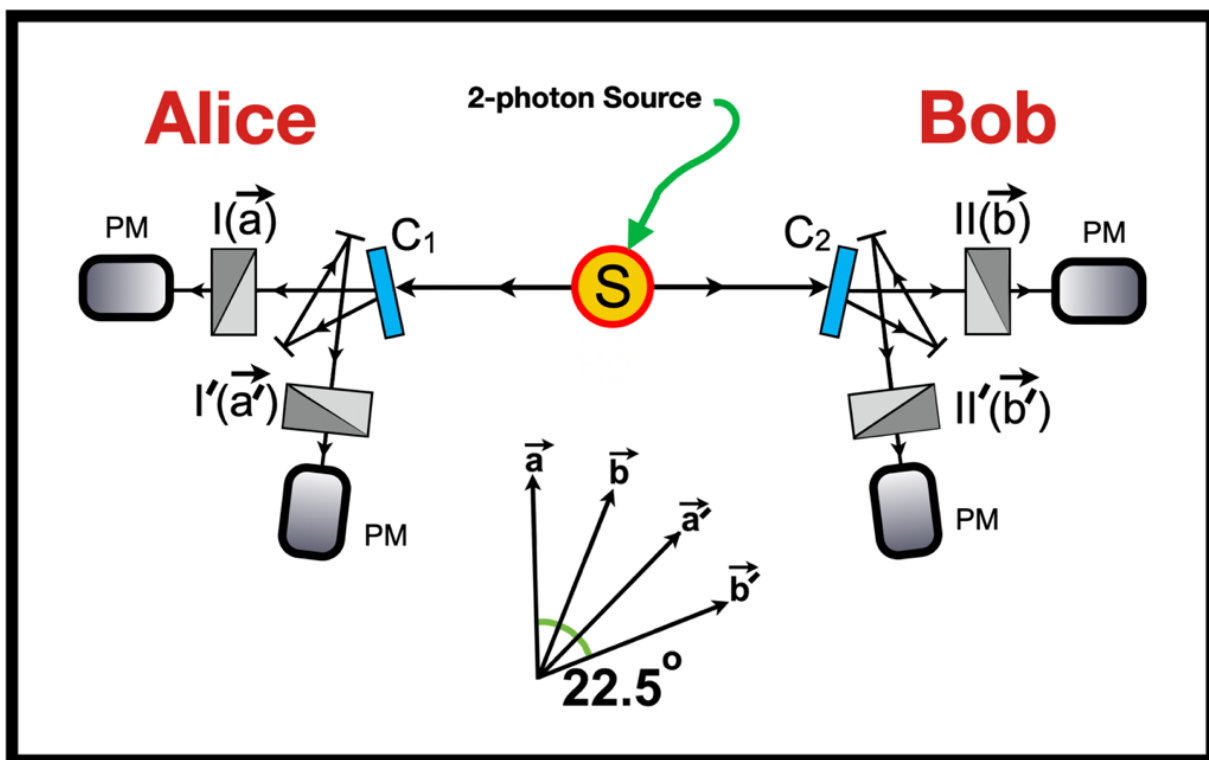


Fig. 41. Equipment used by Aspect, Grangier and Roger in 1982. Entangled photons travel in each direction from the Source. A randomizing device (blue) consisting of a pool of water with standing waves randomly assigns each photon to one of two photomultipliers (PM). The Wollaston prisms (rectangles with a triangle inside) are set at the angles noted. The experimental design is based on the Clauser, Horne, Shimony, and Holt article of 1969.

In Aspect’s 1982 experiment, entangled photons depart the source “S” and are assigned by a randomizing device (C₁ or C₂ shown in blue) to Wollaston prisms (rectangles with a triangle inside) angled at 22.5° increments, and then observed by photomultipliers (PM). The angles of measurement were chosen to maximize the discrepancies between QM and Einstein’s predictions.

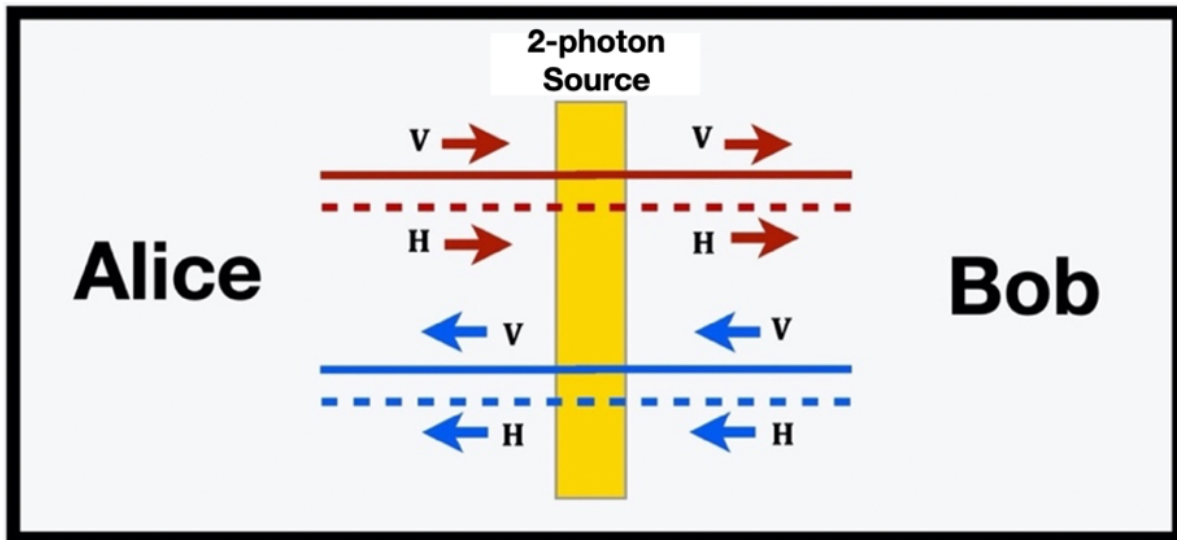


Fig. 42. Using vertical (solid lines) and horizontal (dashed lines) eigenstates of elementary waves, we re-draw Figures 40 and 41. We will use red to denote an elementary ray traveling to the right, and blue for one traveling to the left. These are eigenstates of the individual Elementary Rays, not Bi-Rays.

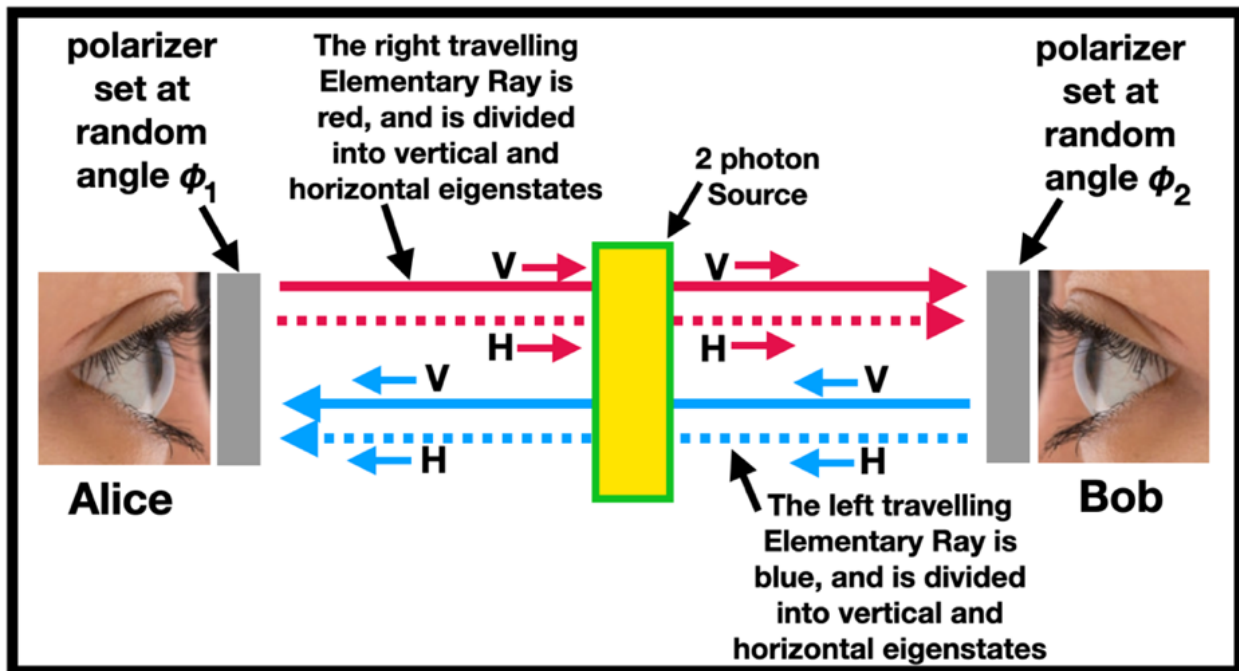


Fig. 43. This elaborates the previous Figure. Each photon follows both Elementary Rays, i.e., each photon follows all the red and all the blue arrows. Notice that the vertical and horizontal eigenstates (V, H, V and H) of the four Elementary Rays, are different than the eigenstates of the Bi-Rays, which will be named (α , β , γ and δ) as in the next Figure.

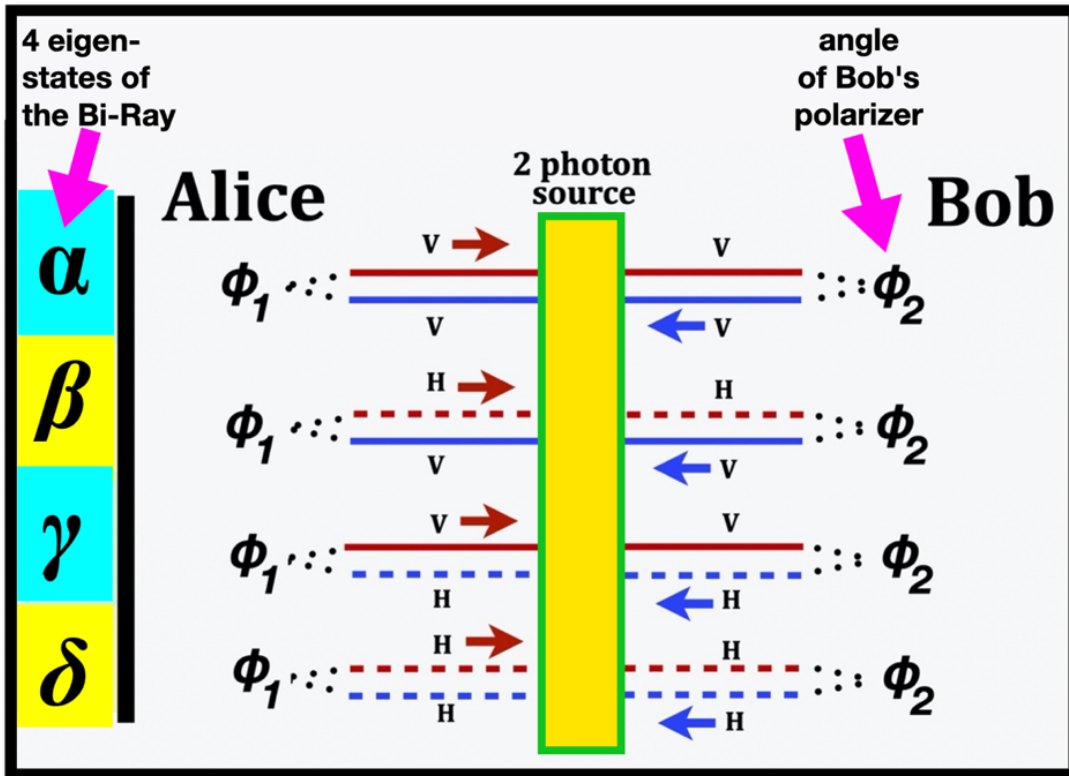


Fig. 44. We define four new eigenstates (α , β , γ and δ) of the Bi-Ray between Alice (whose polarizer is set at random angle ϕ_1) and Bob (polarizer set at ϕ_2).

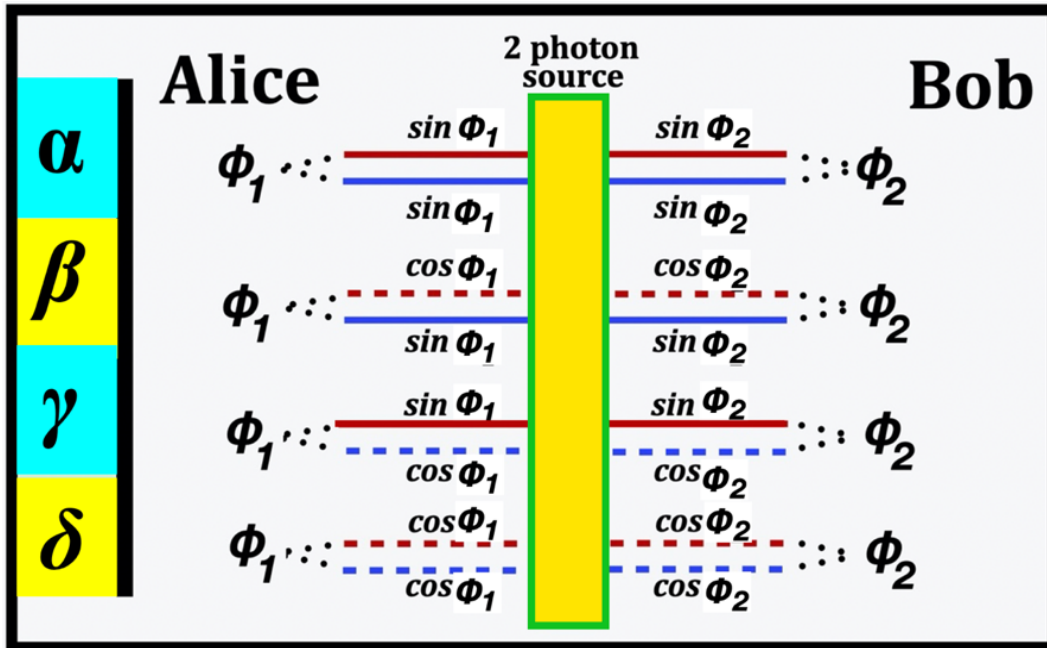


Fig. 45. These sines and cosines show the amplitude for a photon from the source being detected by Alice or Bob in a specific eigenstate. The diagram implicitly assumes that Alice and her equipment never know anything about Bob's photon, nor about Bob's equipment, and vice-versa.

The probability of both Alice and Bob simultaneously seeing a photon (the so-called "coincidence rate") in the α eigenstate is the probability of Alice seeing a photon ($\sin(\phi_1) \sin(\phi_1)$) times the probability of Bob seeing a photon ($\sin(\phi_2) \sin(\phi_2)$). This provides the first line of our equation:

location of the
2-photon Source

$$P = \sin(\phi_1) \sin(\phi_1) \times \sin(\phi_2) \sin(\phi_2) \dots$$

To find the probability of Alice and Bob simultaneously seeing a photon we add together the probability in each of the four of the eigenstates (α , β , γ and δ) in Figure 45:

$$\begin{aligned} P &= \sin(\phi_1) \sin(\phi_1) \times \sin(\phi_2) \sin(\phi_2) \leftarrow \text{(within eigenstate } \alpha) \\ &+ \cos(\phi_1) \sin(\phi_1) \times \cos(\phi_2) \sin(\phi_2) \leftarrow \text{(within eigenstate } \beta) \\ &+ \sin(\phi_1) \cos(\phi_1) \times \sin(\phi_2) \cos(\phi_2) \leftarrow \text{(within eigenstate } \gamma) \\ &+ \cos(\phi_1) \cos(\phi_1) \times \cos(\phi_2) \cos(\phi_2) \leftarrow \text{(within eigenstate } \delta) \end{aligned}$$

When we add those four lines together, the result can be factored:

$$\begin{aligned} &= [\sin(\phi_1) \sin(\phi_2) + \cos(\phi_1) \cos(\phi_2)] \\ &\times [\sin(\phi_1) \sin(\phi_2) + \cos(\phi_1) \cos(\phi_2)] \end{aligned}$$

There is a trigonometry relationship that allows us to compress that into:

$$\begin{aligned} &= \cos(\phi_2 - \phi_1) \times \cos(\phi_1 - \phi_1) \\ &= \cos^2(\phi_2 - \phi_1) \end{aligned}$$

This is how TEW accounts for the Bell test data. Our prediction is that the coincidence rate will be $P = \cos^2(\phi_2 - \phi_1)$. If the 2-photon-Source were changed so it emitted photons orthogonal to one another, then the final coincidence rate would be

$$P = \sin^2(\phi_2 - \phi_1).$$

Wave-function collapse (which is located at the 2-photon source and consists of entangled photons attaching themselves to the same Bi-Ray) occurs as the photons are emitted, not when the photons are measured by Alice and Bob’s detectors.

QM experts have told us they define TEW as “nonlocal realism.” We don’t agree. The distinction between local and nonlocal must be determined before we discuss what constitutes “local” and “nonlocal realism.” TEW starts when Elementary Waves leave the detectors, which is long before a particle leaves the particle source. Therefore, the light cones with TEW are twice as large as the light cones of QM: twice as long temporally and twice as wide spatially. Our theory would be classified as “nonlocal” by QM, but “local” by TEW.

The Bell test experiments have various “loopholes” by which Einstein’s local realism might have survived. Over the course of fifty years, elegant experiments closed all the loopholes. Melissa Giustina, for example, led a research team that conducted a loophole-free Bell test experiment in the basement of science labs in the heart of the City of Vienna. In her video, Giustina discusses loophole-closing at length.(35)

We will not review those “loophole-closing” studies here because they are not relevant.



3.6 Dirac’s “Superposition”

In his book on quantum mathematics, Paul Dirac speaks of the principle of superposition. TEW says particles are never in a superposition. Only waves can add together into a superposition. (30)

3.6.1 Thumbnail Sketch

Paul Dirac was a leading QM mathematician. He says wave-particles are in a superposition that collapses when measured. We disagree. We say that waves can be in a superposition, and often are, as is evident when you look at the ocean, or a pool of water, you can see some waves adding on top of other waves when they crisscross. With TEW, however, we distinguish between the waves and particles because they travel in opposite directions. We say particles are never in a superposition. We will not discuss here how this idea affects our explanation of why quantum computers work so well.



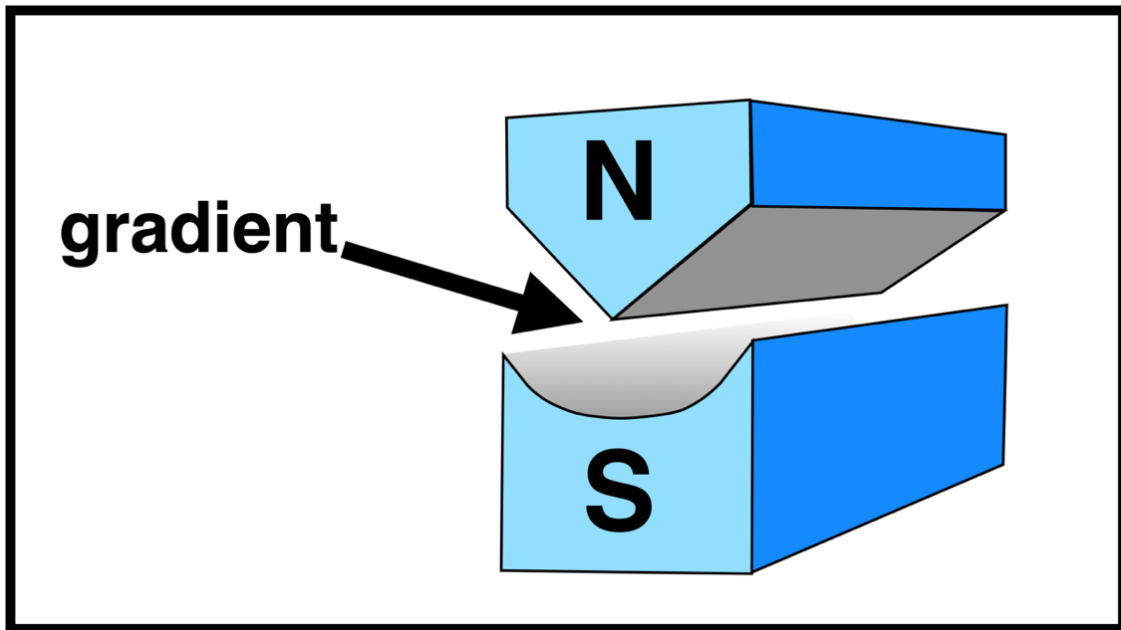


Fig. 46. Like all magnets, a Stern-Gerlach magnet has a **North** and **South** pole. The two poles are connected by a metal bridge not shown here. Unlike other magnets the **North** pole has a sharp edge on its bottom, and the **South** pole has a hollow groove on top. This arrangement causes there to be a gradient to the magnetic field in between, a field that becomes more intense as you move up toward the **North** pole. When a vaporized silver atom is sent through that space, it moves up or down depending on whether its outermost electron has spin is up (+) or down (-).

In a paper published in 1922, Otto Stern and Walther Gerlach of Frankfurt described an experiment in which they fired a narrow beam of silver atoms through this magnetic gradient. The atoms deposited on the target screen in two discrete areas, thus providing the first incontrovertible evidence that individual atoms can have a magnetic moment, and the moment is quantized. That was the first experimental evidence supporting Bohr's theory that things in the quantum world were quantized. In 1922 that was big news.

Stern and Gerlach got a Nobel Prize in 1943 for their experiments proving quantized spin.

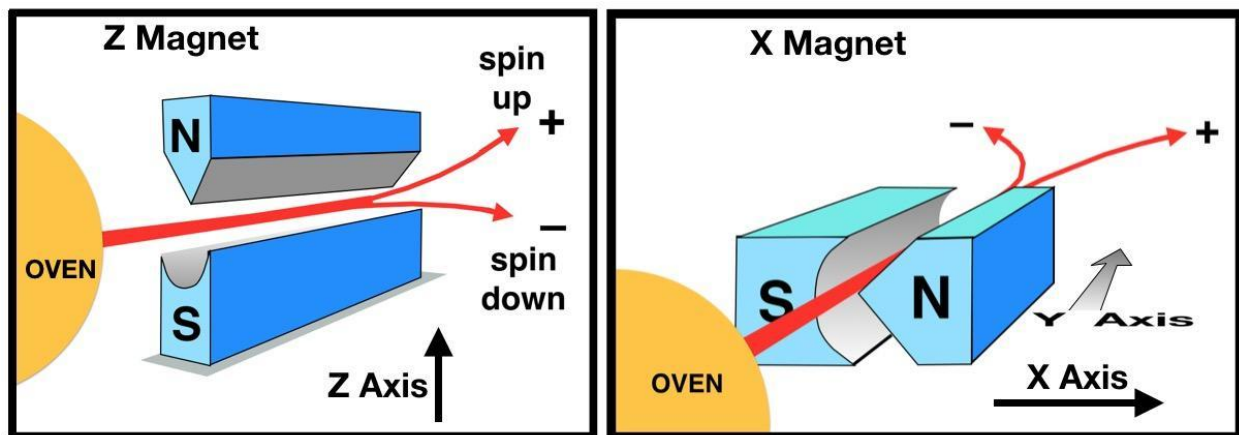


Fig. 47. A Stern-Gerlach magnet can be placed in four positions: up versus down, and oriented to the right or to the left. We name those positions Z^+ , Z^- and X^+ and X^- respectively. Sometimes we will use the words "right" instead of " X^+ " and "left" instead of " X^- ." The "plus" direction is always towards the **North** pole of the magnet. A silver atom (^{47}Ag) is vaporized in an oven on the left, then moves following the curved red arrows through a Stern-Gerlach magnet.

3.7.2.1 Overview of the Stern-Gerlach Experiments

A series of four Stern-Gerlach magnets in a row (a "train" of magnets) will be used to study the spin of vaporized silver atoms traveling through all four in sequence. The main emphasis will be on the middle pair of magnets, which are shown in this Figure. Spin is the central issue.

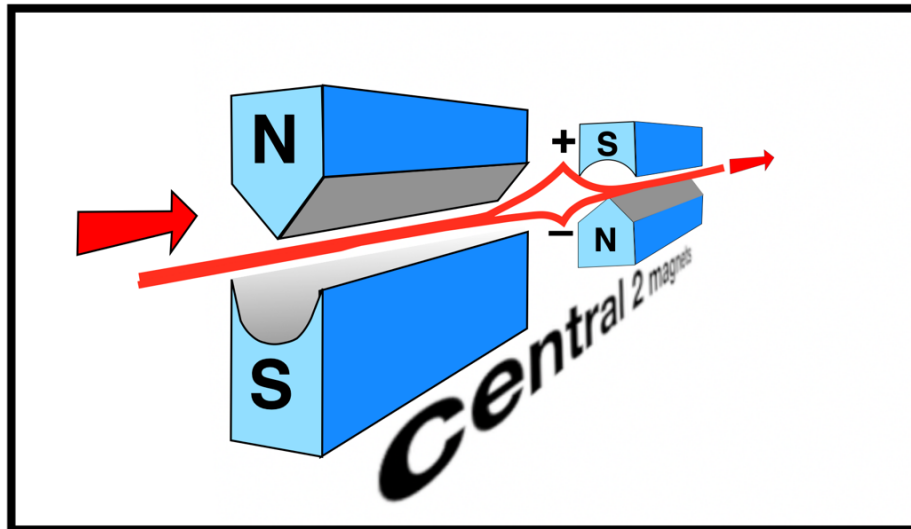


Fig. 48. Two magnets (Z1 and Z2) are arranged as a pair, such that when a silver atom crosses both, whatever the one magnet does, the second magnet undoes. Therefore, the silver atom leaves with the same characteristics as it had before it entered. The pair of magnets behave as if they were absent, having no effect.

A spin right/left atom crossing the two middle magnets continues to have the same spin at the far end, providing we “don’t look”. But if we do “look” at the middle passageway (see the next Figure), suddenly the atom coming out the other end loses its right/left spin and acquires an up/down spin.

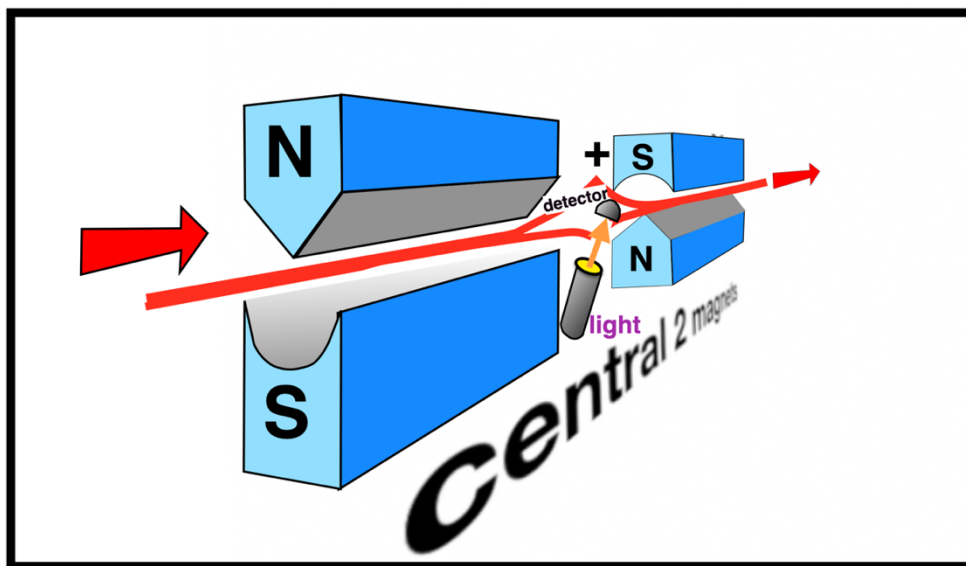


Fig. 49. To “look” inside this experiment, scientists need to introduce a tiny flashlight and detector near one of the passageways. QM says this is of no significance because the energy from the flashlight is insignificant compared to the energy of a massive silver atom (atomic weight 107.9) crossing from the left-front to the right-rear.

Since they think the flashlight has no effect on the silver atoms, therefore they attribute the effect of the flashlight to “being observed” as if human consciousness or observation made a difference in quantum mathematics. Later TEW will offer a more logical explanation.

The train of four magnets in a row is such that the target screen at the far end will have one dot (the right one) if we do not know which trajectory was used in Figure 48 and 49, but two dots if we do know. This is the alleged “observer effect.”

To introduce the reader to the symbolism we are adopting, the next diagram shows only the first two magnets.

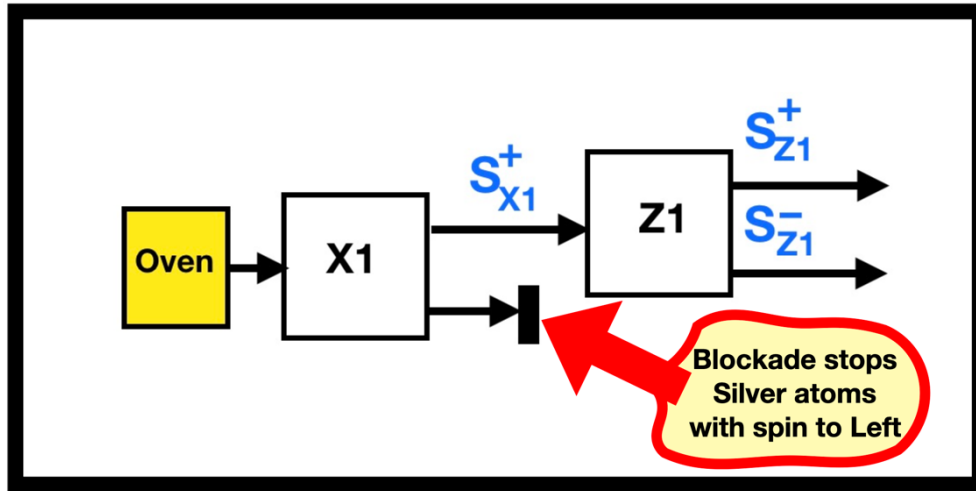


Fig. 50. The silver atom leaves the oven and crosses the X1 magnet which is in the X^+ position (i.e., lying on its right side as in Figure 47-right). If the atom has its outermost electron in a spin-up (“S” for spin, “+” for up, which in this case means “spin to the right”), it comes out the upper exit door of X1. If it has a spin-down, it comes out the lower exit door of X1 which leads to a blockade, which is a dead end. The silver atom with intrinsic spin to the right crosses from the upper exit door of X1 into the entrance to the Z1 magnet.

We use the four Stern–Gerlach magnets shown in the next Figure.

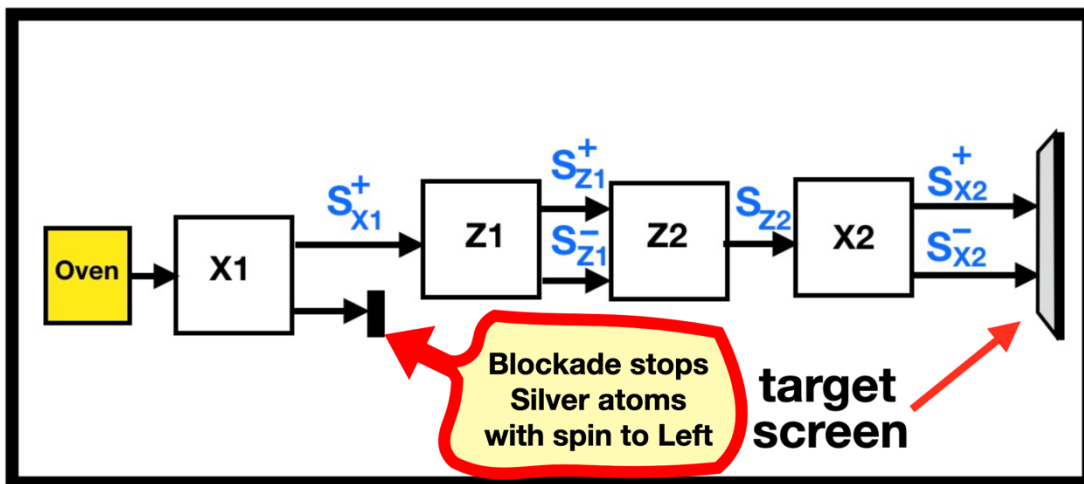


Fig. 51. The experiment involved a train of four Stern Gerlach magnets. The focus is on the middle pair: Z1-Z2. As we said, it makes a difference whether we “know or don’t know” whether a silver atom from the oven went across that pair on the upper trajectory (with spin up) or on the bottom trajectory (with spin down)! On the far right, the target screen will have one dot (the right one) if we “don’t know”, but two dots if we “do know.”

The next Figure shows what it means to say that humans “observe” the middle pair of magnets.

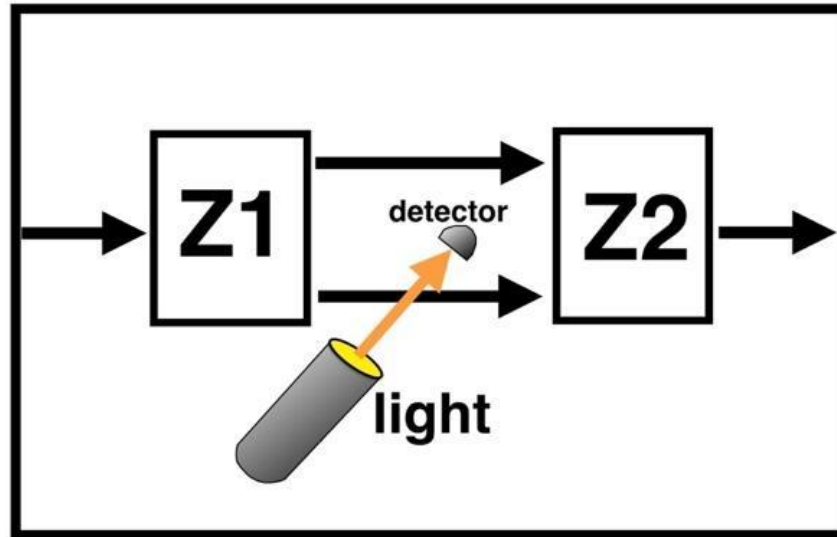


Fig. 52. Humans only know which route a silver atom took if they insert a detector collecting the information. This was shown in Figure 49.

We will develop conditional probabilities, assuming we do not know whether the atom crossed the Z1-Z2 set of magnets with spin up or spin down, as follows.

$$P(S_{Z1} = \frac{1}{2}\hbar | S_{X1} = \frac{1}{2}\hbar) = \frac{1}{2}$$

$$P(S_{Z1} = -\frac{1}{2}\hbar | S_{X1} = \frac{1}{2}\hbar) = \frac{1}{2}$$

If we DO NOT observe the middle pair, then **we add the amplitudes then square them**. The probability of the silver atom emerging in the upper stream on the far right:

$$S_{X2} = \frac{1}{2}\hbar \text{ beam is } P = \left| \Psi_{X2}^+(\frac{1}{2}\hbar) + \Psi_{X2}^-(\frac{1}{2}\hbar) \right|^2 = 1$$

But the probability of the atom emerging in the lower stream:

$$S_{X2} = -\frac{1}{2}\hbar \text{ beam is } P = \left| \Psi_{X2}^+(-\frac{1}{2}\hbar) + \Psi_{X2}^-(-\frac{1}{2}\hbar) \right|^2 = 0$$

On the other hand, if we DO OBSERVE the middle pair of Z1-Z2 magnets, then **we should square the amplitudes then add them**. The probability of the silver atom emerging in the

$$S_{X2} = \frac{1}{2}\hbar \text{ beam is } P = \left| \Psi_{X2}^+(\frac{1}{2}\hbar) \right|^2 + \left| \Psi_{X2}^-(\frac{1}{2}\hbar) \right|^2 = \frac{1}{2}$$

And the probability of the atom emerging in the

$$S_{X2} = -\frac{1}{2}\hbar \text{ beam is } P = \left| \Psi_{X2}^+(-\frac{1}{2}\hbar) \right|^2 + \left| \Psi_{X2}^-(-\frac{1}{2}\hbar) \right|^2 = \frac{1}{2}$$

Those equations mean there is always a dot on the right side of the target screen. But there is only a left-side dot if we “observe” the middle pair of magnets. That left-sided dot vanishes if we don’t observe.

3.7.3 The Elementary Wave Viewpoint

The flashlight-detector emits a tiny amount of energy, which is infinitely greater than the zero-energy in an Elementary Ray traveling right to left. As in the double slit experiments, so also here, the energy of the flashlight destroys the superposition additivity of the Elementary Rays crossing Z1-Z2. It doesn’t stop the Elementary Ray, just modifies it. The flashlight destroys the ability of that Elementary Ray to be interchangeable with the other Elementary Ray crossing Z1-Z2 on the “+” (upper) pathway.

In this Elementary Wave picture of this experiment, we use green arrows starting at the target screen and wending their way through all four magnets to the oven on the left. Iff (if-and-only-if) a continuous green line can

be drawn from the target screen to the oven, will a silver atom from the oven be successful in following that green line backwards to the target screen.

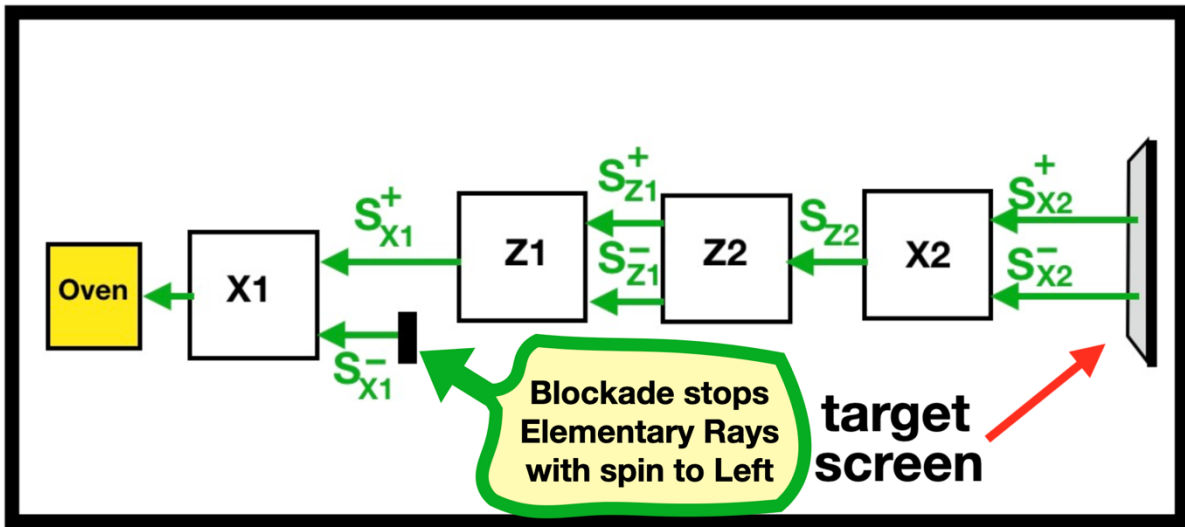


Fig. 53. The first map of elementary rays in the Stern-Gerlach train of four magnets.

The green line is a “flight plan” for the silver atom, analogous to the flight plan of a passenger jet before starting a long flight. A flight plan is needed before an airplane takes off. If the flight plan cannot be drawn from the target screen all the way to the oven, then no silver atom will follow that trajectory backwards, because there is a gap (no flight plan). The main difference between an airplane flight plan and a green arrow is that airplanes never follow the flight plan backwards.

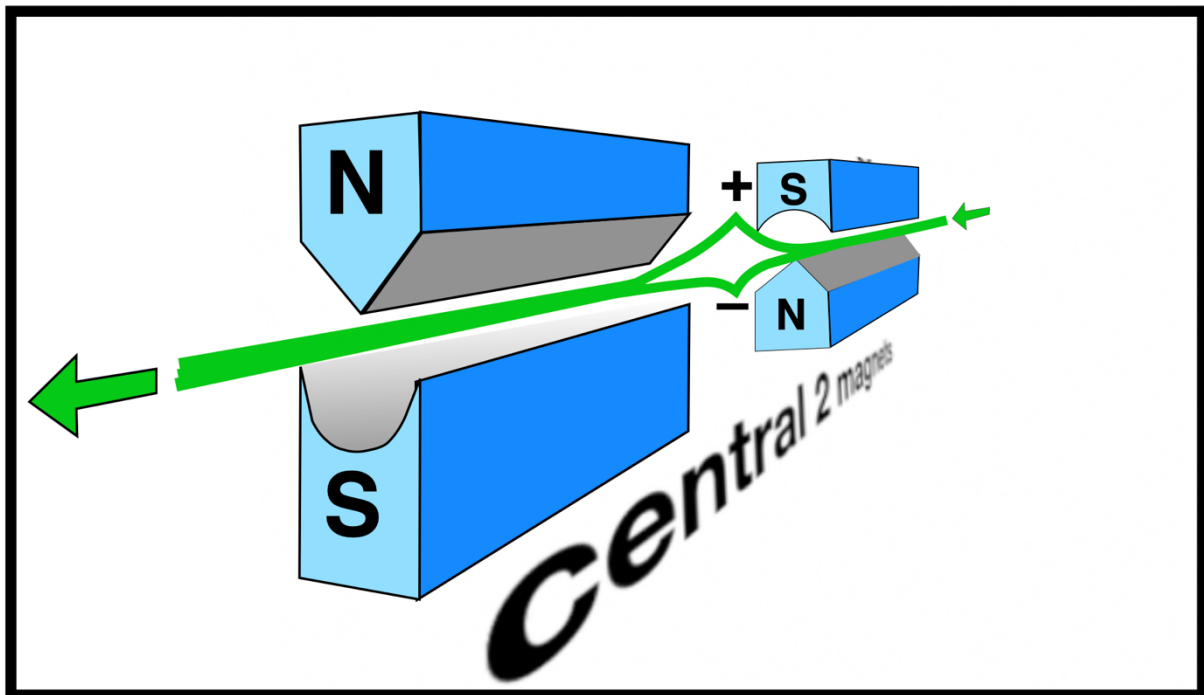


Fig. 54. Elementary Rays cross the middle two magnets in such a way that the two magnets act as if they were absent. Whatever one magnet does, the other magnet undoes. Therefore, a right/left spin is preserved.

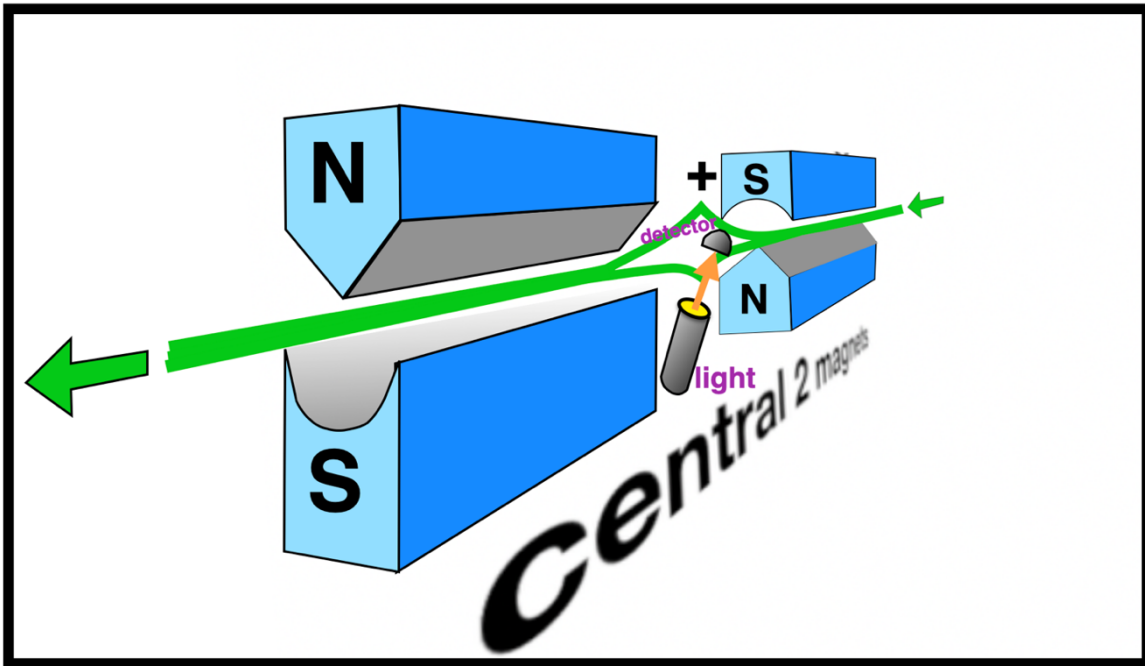


Fig. 55. This is identical to the previous Figure, except that we added a tiny flashlight and detector into the center of the equipment, to see if a silver atom uses the bottom trajectory. This changes the pair of magnets, so now they impose an up-down spin on a crossing silver atom.

This light with small energy, still has infinitely more energy than the zero-energy Elementary Ray. The two trajectories (+ and -) are no longer interchangeable with each other.

The pivotal question, from a TEW viewpoint, is whether there is, or is not a green pathway connecting a point on the target screen and the oven. We claim that, if the flashlight is OFF there IS such a wall-to-wall pathway for the right-hand spot $X2^+$ on the target screen, **but NOT for the left-hand spot $X2^-$** . But if the flashlight is ON then both spots on the target screen can connect with the oven by an uninterrupted green line. As we said before, if-and-only-if there is an uninterrupted green line from the target-screen to the furnace, will a silver atom travel on that route from the oven to the target-screen and make a mark. The next several Figures put those words into pictures.

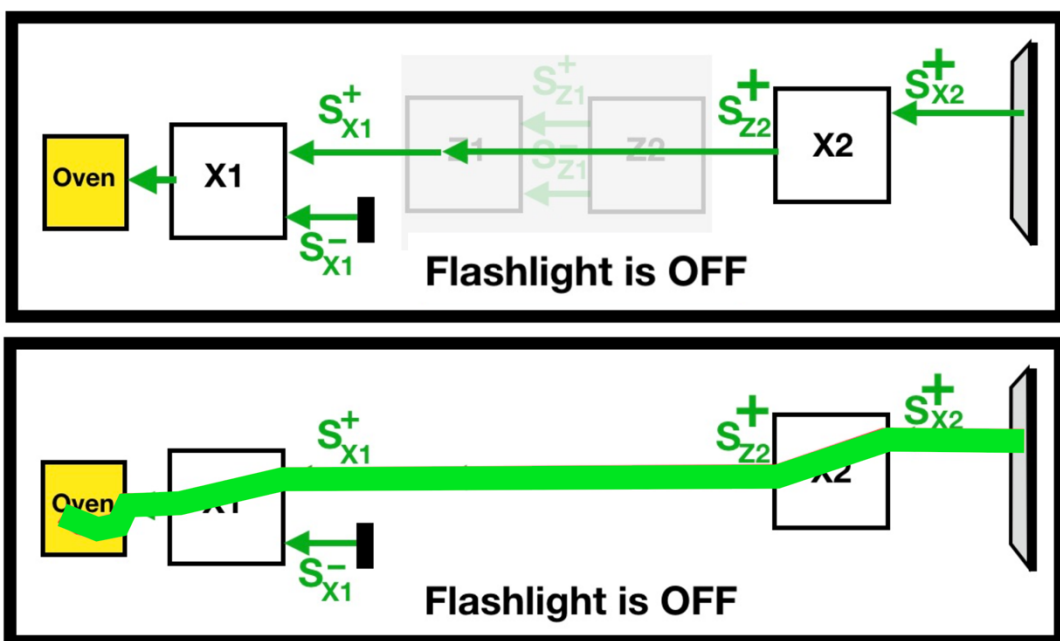


Fig. 56. If the flashlight is OFF, then the middle pair of magnets Z1-Z2 act as if they are not present. A green arrow from the right-hand spot on the target screen CAN reach the oven if the flashlight is off. Therefore, sooner or later a silver atom will come across that green highway and strike the right-hand spot of the target.

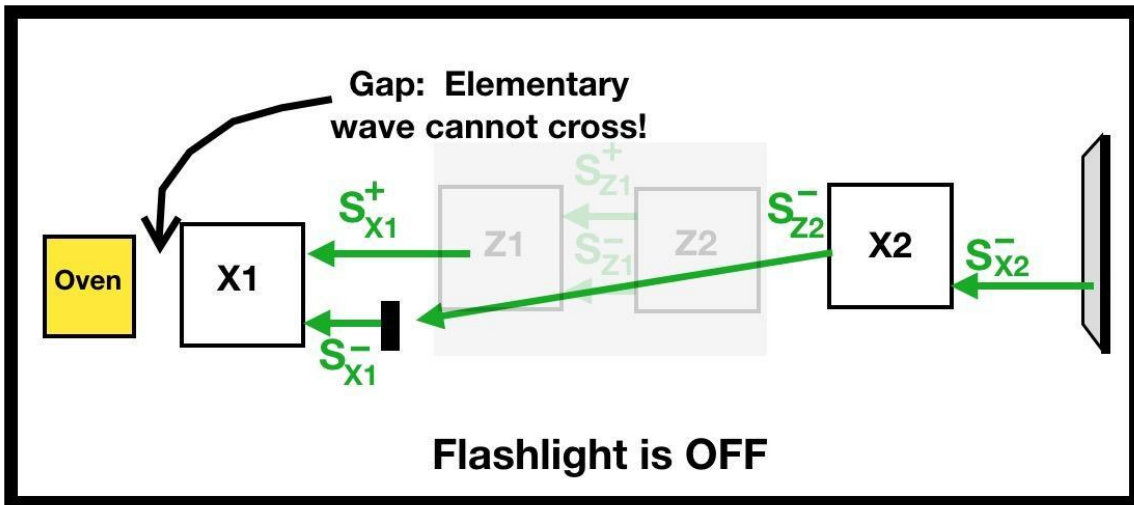


Fig. 57. If the flashlight is OFF, then the middle pair of magnets Z1-Z2 act as if they are not present. A spin-left Elementary Ray starting at the target screen remains spin-left as it crosses three magnets, where it discovers that the spin-left doorway of magnet X1 is blocked, so it cannot enter that X1 magnet and therefore cannot reach the oven.

With no green line from detector to particle source, no silver atom will be able to follow that highway backwards from the oven to the detector. Therefore, there will be no spot at the left-hand side of the target screen. The blockade of the left-handed exit of the X1 magnet is an obstacle that will disrupt everything.

So, the question becomes, what determines whether the Elementary Ray approaches the X1 magnet with a spin right-left, or with a spin up-down? The answer is that it depends how the middle pair of magnets (Z1 and Z2) treat the Elementary Ray. If there is no flashlight then that middle pair act as if they are absent, and the Elementary Ray still carries the left-right spin it acquired in magnet X2, which causes problems when it tries to gain access to the blockaded lower back door to X1.

If, on the other hand, there is a flashlight modifying the middle pair of magnets, then the Elementary Ray acquires an up-down spin from inside Z1-Z2 before it tries to enter X1. Now it is acceptable to X1 and therefore can zip through X1 and into the oven and pick up a silver atom.

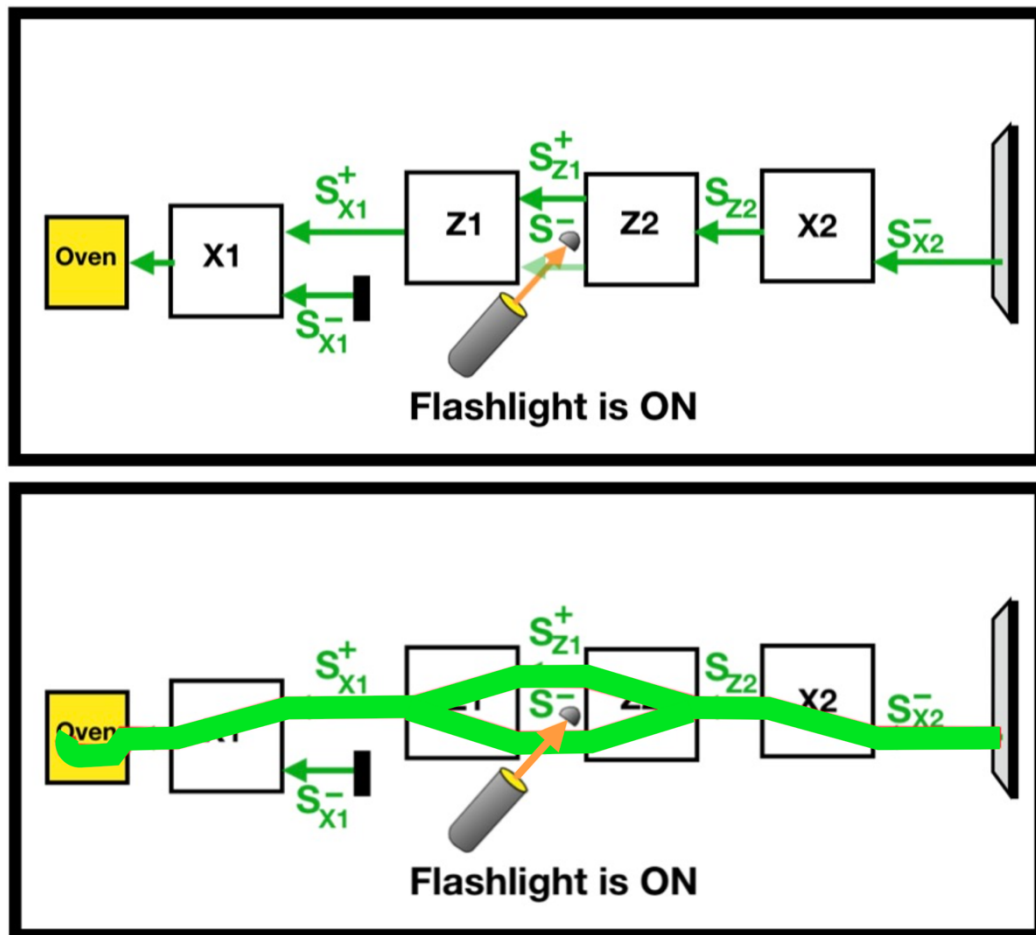


Fig. 58. If the flashlight is ON, then the middle pair of magnets Z1-Z2 process an Elementary Wave from the left-hand spot on the target screen in the way that is shown here. The Elementary Ray moving across the middle pair of magnets acquires a new spin that is either “up” or “down.” Because it has that spin it has no trouble entering the upper doorway of the X1 magnet, and therefore reaching the oven.

We will now formalize the “wall-to-wall” rule. If you can draw an unbroken green line from wall to wall (from target screen to oven) then some silver atoms will eventually follow that passageway backwards and register on the target screen. But if there is a gap in that green line, then no silver atom can take that route because of the gap.

This is like saying you can drive an 18-wheel truck across highway US I-80 from New York to San Francisco if-and-only-if no bridge has collapsed causing a gap in the highway.

As a result, if there is a flashlight in Z1-Z2, then there will be dots at BOTH places on the target screen. If there is no flashlight, then there will only be a right-hand spot on the target screen.

We have accomplished with pictures exactly what QM accomplished with conditional probability equations. The big difference is that we can explain the phenomenon without invoking “observation by humans.”

That which QM attributes to “observation” we attribute to the energy of a flashlight modifying a zero-energy Elementary Wave, so it becomes different from a parallel Elementary Wave crossing Z1-Z2 on the “+” (upper) pathway. Our explanation frees nature from dependence on human observation.

TEW also introduces the idea of a “Butterfly Effect.” The term “Butterfly Effect” comes from chaos theory, which refers to how nature is often ruled by nonlinear differential equations, in which a tiny perturbation can result in unpredictably large results. A butterfly flapping its wings in Beijing can cause major weather changes in New York six months later. Similarly, a tiny change in the behavior of a zero-energy wave can cause major changes in the behavior of massive silver atoms, each of which weighs 200,000 times more than an electron

Something unexpected we discover in this experiment is that **Elementary Waves can CARRY INTRINSIC SPIN!** That is big news! It raises the question whether the “Intrinsic Spin” of electrons is intrinsic to the electron, intrinsic to the Elementary Wave it is following backwards, or both. We think, probably both.



3.7.4 Feynman’s Scattering Experiments

3.7.4.1 Thumbnail Sketch

Feynman’s textbook says that human observation makes a difference in scattering experiments. Once again, we claim humans are irrelevant. It is the Elementary Waves that cause these phenomena. (32)

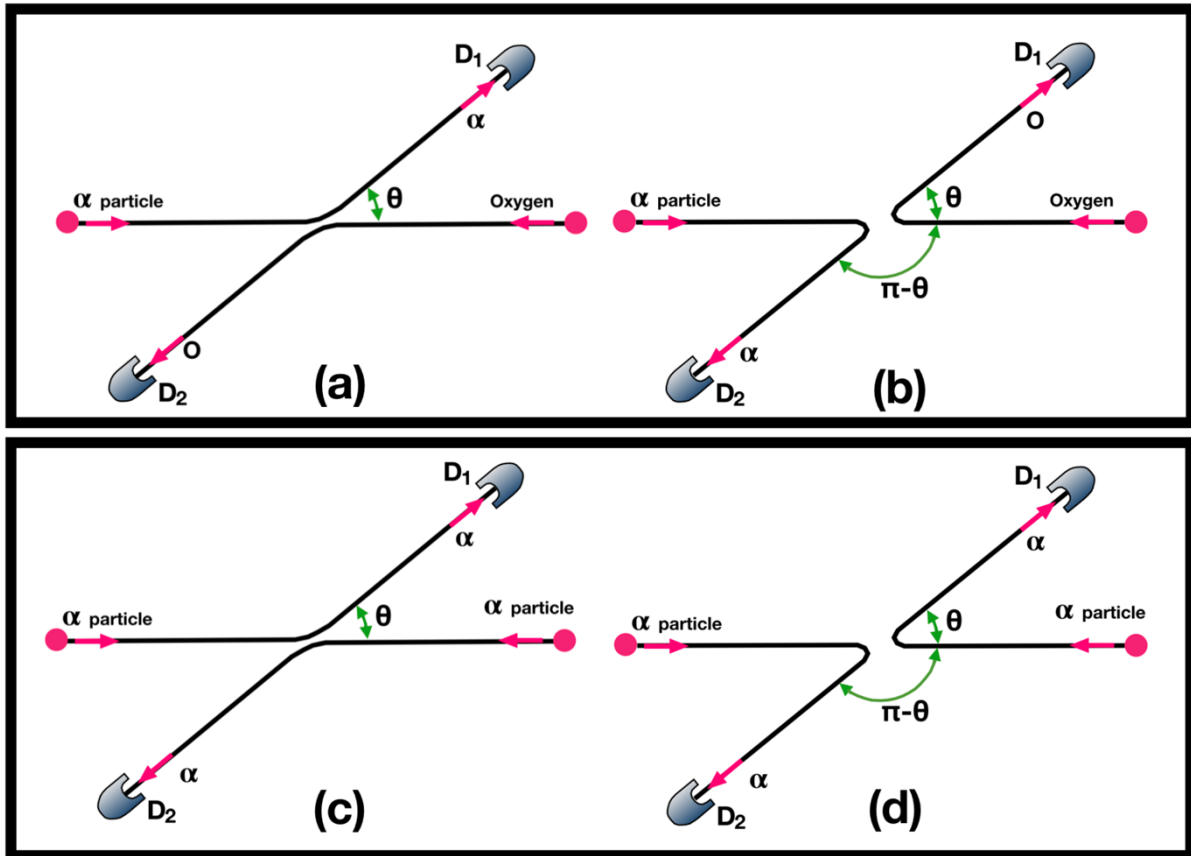


Fig. 59. Scattering diagrams from Feynman (except we added color). Pictures (a) and (b) show the two ways an alpha particle and oxygen atom can collide and scatter to detectors D₁ and D₂. Diagrams (c) and (d) show the two ways that two alpha particles can collide and scatter to D₁ and D₂.

What Feynman demonstrates in these diagrams is that it makes a difference whether the two particles are distinguishable or indistinguishable. The adjective “distinguishable” implies that a human observes or could observe the particles and see that they are different. On a practical level, the difference is how we handle the math. Suppose detectors D₁ and D₂ are designed to click, no matter what kind of particle hits them.

If an oxygen atom scatters at angle θ (Figure 59-b), striking detector D₁, then an α -particle must have scattered at angle $\pi - \theta$, striking detector D₂. So if $f(\theta)$ is the amplitude for α -scattering through the angle θ , then $f(\pi - \theta)$ is the amplitude for oxygen scattering through the angle θ . Thus, the probability of some particles hitting detector D₁ is

$$P(D_1) = |f(\theta)|^2 + |f(\pi - \theta)|^2$$

This shows that if particles are distinguishable, you square the amplitudes before adding them.

On the other hand, Figure c and d illustrate what happens when the particles are indistinguishable. Here an α -particle almost collides with another α -particle. A different math is required: add the amplitudes before you square them. In this case the probability of having some particles hit detector D₁ is

$$P(D_1) = |f(\theta) + f(\pi - \theta)|^2$$

To illustrate how different the second equation is compared to the first, Feynman suggests we set $\theta = \pi/2$. In this case $f(\theta) = f(\pi - \theta)$. Then the probability of any particle hitting D_1 if the particles are indistinguishable is

$$P(D_1) = \left| f\left(\frac{\pi}{2}\right) + f\left(\frac{\pi}{2}\right) \right|^2 = \left| 2f\left(\frac{\pi}{2}\right) \right|^2 = 4\left| f\left(\frac{\pi}{2}\right) \right|^2$$

whereas if the particles are distinguishable the probability is

$$P(D_1) = \left| f\left(\frac{\pi}{2}\right) \right|^2 + \left| f\left(\frac{\pi}{2}\right) \right|^2 = 2\left| f\left(\frac{\pi}{2}\right) \right|^2$$

meaning that it is twice as likely that an indistinguishable particle will hit D_1 as compared to a distinguishable particle.

This is a theme in Feynman’s book: that the observer is implicated in the results. If the observer knows (or could know) that the two particles are distinguishable, you will get one result. Otherwise, you get a different result.

To reiterate, Feynman declares that human consciousness affects the mathematical results of a high-energy scattering experiment. But if we switch from QM to TEW, this absurd idea vanishes.

3.7.4.2. An Elementary Wave Model of Feynman’s scattering

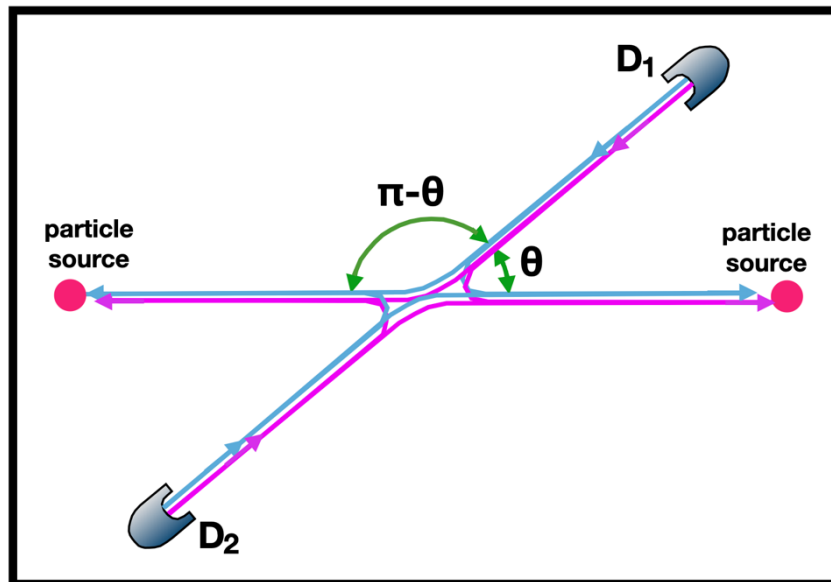


Fig. 60. This shows the two elementary rays (shown in color) emanating from the detectors (D_1 and D_2) and scattering, in an experiment involving two particle sources.

We postulate, for this experiment, that there are different kinds of elementary rays, which we display in blue and pink. Both are available at each particle source.

We propose that an α -particle always follows a blue elementary ray, whereas an oxygen atom follows a pink elementary ray.

The mathematics for these different color elementary rays is different. If two particles follow the same color elementary ray, then the probability of some particle striking detector D_1 requires that we add the amplitudes before we square them.

$$P(D_1) = |f(\theta) + f(\pi - \theta)|^2$$

On the other hand, if two particles follow different color elementary rays then the probability of some particle hitting D_1 is the amplitude squared of one particle hitting D_1 , plus the amplitude squared for the other particle.

$$P(D_1) = |f(\theta)|^2 + |f(\pi - \theta)|^2$$

Thus, the Elementary Ray model produces the same mathematics as the Feynman model, but no observer is involved.

Feynman next discusses the scattering of two electrons.

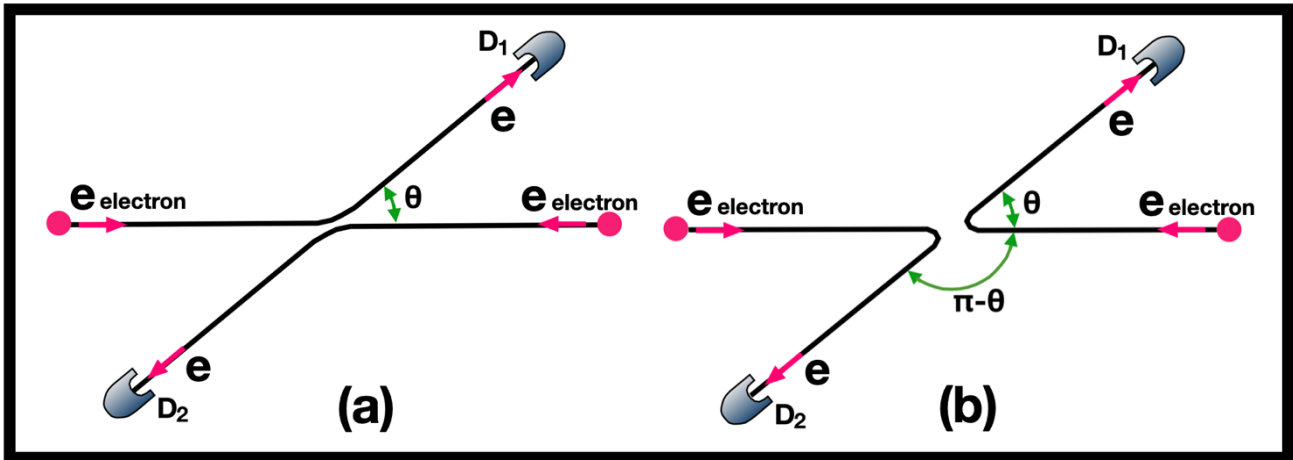


Fig. 61. Feynman’s diagram for two electrons scattering. This is different from two alpha particles, the reason being that two electrons influence one another to avoid occupying the same quantum state (Pauli exclusion principle). Alpha particles don’t behave that way.

Consider what happens if both particles are electrons. In this experiment they interact in a negative way. If they are both trying to occupy the same quantum state, that would violate the Pauli exclusion principle. In the scattering experiment they don’t quite collide, but they do interact in a negative way. The phase of one electron and the phase of the other electron become opposite to each other. By changing their phase in this way, they occupy different quantum states.

As a result, there is a different equation for the probability of an electron hitting detector D₁, which is:

$$P(D_1) = |f(\theta) - f(\pi - \theta)|^2$$

The minus sign in the center of this equation means that you subtract one amplitude from the other before you square them. The minus sign is caused by the Pauli exclusion principle. If they had been alpha particles, we would add the two amplitudes before you square them, but because they are electrons you SUBTRACT the two amplitudes before you square them.

This teaches us something important about **wave-function-collapse**. It does not always happen when a particle leaves the source. Sometimes, it is modified halfway between the particle-source and the detector.



4. Untangling the Mysteries of TEW

In this fourth section of our article, we will use TEW to drill down into the depths of nature, to discover how the foundations of Elementary Waves work. These are not easy waves to think about. We use published experiments to investigate them.

We will examine the Purcell effect where Elementary Waves are clearly visible, develop wave equations, and discuss cosmological issues.



4.1. Purcell effect

4.1.1 Thumbnail Sketch

The Purcell effect concerns how quantum systems behave differently depending on their environment. An atom in a cavity will decay and emit a photon faster in a cavity of one diameter versus a cavity of another diameter. This proves the existence of Elementary Waves carrying information about the size of the cavity into the atom, and photons following the Elementary Waves backwards. We have an interest in the Purcell effect, because it is one place where we see Elementary Waves in plain sight. However, Purcell research has gone off in many



different technological directions unrelated to our interest. We wish some Purcell experts would take an interest in TEW.

3.4.2 Specifics of the Purcell Effect

In 1946 Edward M. Purcell discovered an increase in the spontaneous emission rate of Rydberg atoms when they are injected into a resonant cavity. If λ is the wavelength of the emitted photon,

$$\text{The Purcell factor} \equiv F_p \equiv \left(\frac{2g}{\Gamma_{cav}}\right)\left(\frac{2g}{\Gamma_{atom}}\right) = \frac{3\lambda^3 Q}{4\pi^2 V}$$

$$g = \frac{\mu}{\hbar} \sqrt{\frac{2\pi\hbar\omega}{V}} = \text{the vacuum Rabi frequency}$$

$$Q = \frac{\omega}{\Gamma_{cav}} = \text{the cavity quality factor}$$

A Rydberg atom (such as sodium, cesium, beryllium, magnesium, or calcium) is heated in an oven, then a laser excites the outer electron to a higher energy state, and the atom is injected into a microcavity or nanocavity. The outer electron will drop to a lower energy level and emit a photon hundreds of times faster if the cavity is resonant than if it is not.

If the diameter of the cavity is a multiple of $\lambda/2$ then the cavity is a perfect size for that atom, and we say that it is “resonant” or that it has an “available state” or a “mode of the cavity” which is resonant.

The pivotal question is: “How does the atom know the size of the cavity in which it is located?” Information is flowing into the atom, which is a direction that QM cannot explain if the information flow is carried by quantum waves. Information penetrates from the environment into the atom, whereas quantum waves would need to travel in the opposite direction.

Information about the diameter of the cavity is transmitted into the atom with no transfer of energy. We hereby rename the “available states” and call them “Elementary Waves” that reside inside that cavity. They travel in the opposite direction as quantum waves would travel.

Purcell research today does not focus on these issues. Therefore, scholars who are steeped in the technology some branch of Purcell research (such as NV-center photoluminescence, Mie scattering, nano-antennas, photonics and plasmonics, Fermi’s golden rule, etcetera) could make a major contribution vis-à-vis our understanding of Elementary Waves.



4.2. Proposed Experiments

We now design four experiments, never done by anyone, which will yield different results depending on whether TEW or QM is true.

4.2.1 Thumbnail Sketch

Elementary Waves are new to science and hard to understand. Are there experiments that prove such waves exist? Here we will now give you four experimental designs that will produce different outcomes if TEW is correct versus if wave-particle duality is correct. One is a variation on the neutron interferometer we described at the beginning of this article. The other three experiments are variations on a double slit experiment. This author has no plans to conduct these experiments himself, and he knows of no one else with such plans.

4.2.2 Variation on Neutron Interferometer Experiment

The Kaiser neutron interferometer experiment (see above, section 2.1) inspires many questions. Some young scientists could easily modify that experiment to answer those questions. The next Figure shows how to add another sample of bismuth (“sample A”) to the incoming neutron beam. By varying the width of Sample A, questions could be answered, such as whether there are invisible waves (Elementary Waves) traveling in the opposite direction as the neutrons.



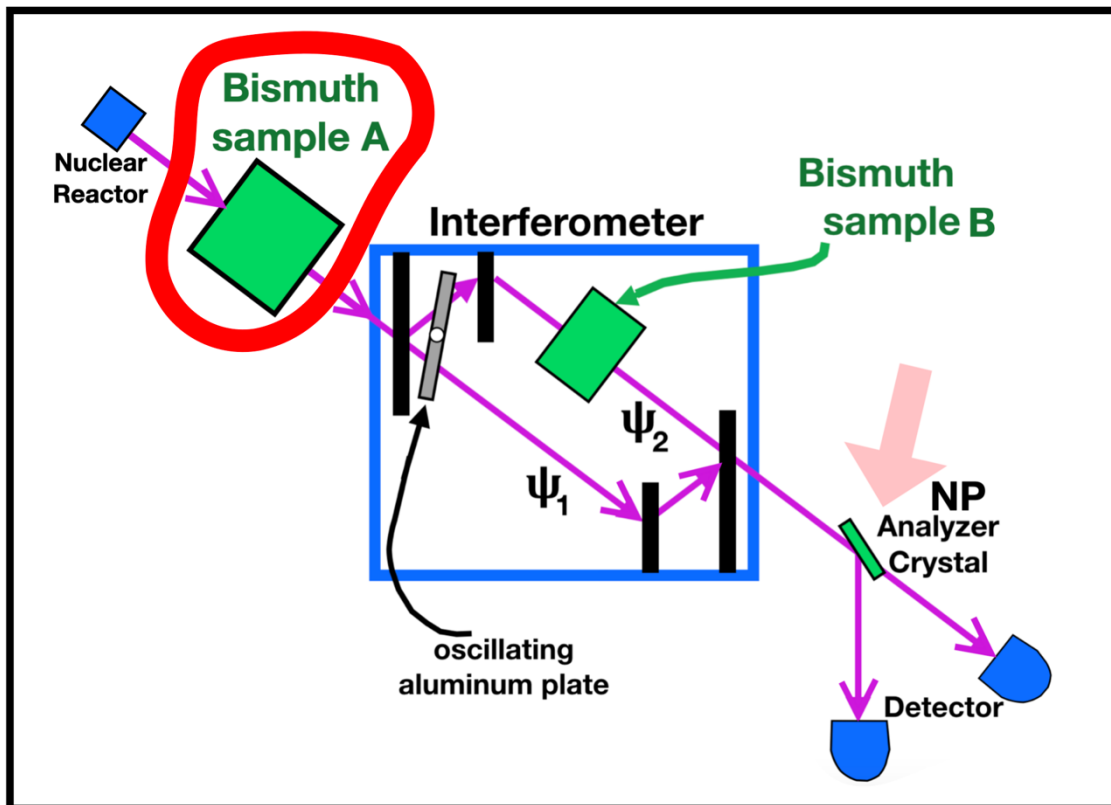


Fig. 62. Another sample of bismuth (sample A, upper left) is added to the Kaiser neutron interferometer experiment. This second sample of bismuth answers many questions.

For example, we said before: the NP Analyzer Crystal increases the coherence length of a wave-packet from 86.2 Å to 3450 Å. A maximum sample of 20 mm bismuth delays a wave packet for 435 Å. If we assume that Elementary Waves are traveling up towards the nuclear reactor, with a wave-packet coherence length of 3450 Å, and we make sample A of bismuth sufficiently thick, then we should be able to block all interference, and we can study the number of centimeters of bismuth required to do this.

You might contact the Helmut Kaiser research team at the University of Missouri Research Reactor, to ask whether their equipment still exists, and whether you could borrow it for a new experiment.

One could also place other samples of bismuth in the exit beams, downstream from the NI. Many questions about invisible waves could be investigated. Everything you discover about this would be publishable.

4.2.3 Variations with Double-Slit Experiments

Now we will propose three experiments based on a double-slit experiment with moving parts. None of these experiments has ever been done. To divide wave-particle-duality from TEW we ask the following question. When does interference occur relative to the firing of a particle gun in a double-slit experiment? TEW says interference occurs prior to or during firing; QM says it occurs after the gun is fired. Therefore, if we devise a way to **divide time** when the particle is fired, we should be able to produce divergent outcomes.

To conduct these experiments, we need to fire one particle at a time, with a delay for the equipment to be reset before the next particle is fired. The equipment in the next Figure is designed so both slits are open until that nanosecond when a particle is fired. At that instant a powerful laser fires straight down, blocking the right slit. TEW says there will be an interference fringe pattern (as shown in this Figure) skewed toward the left. QM says there will be a single vertical line on the target screen, no interference fringe pattern.

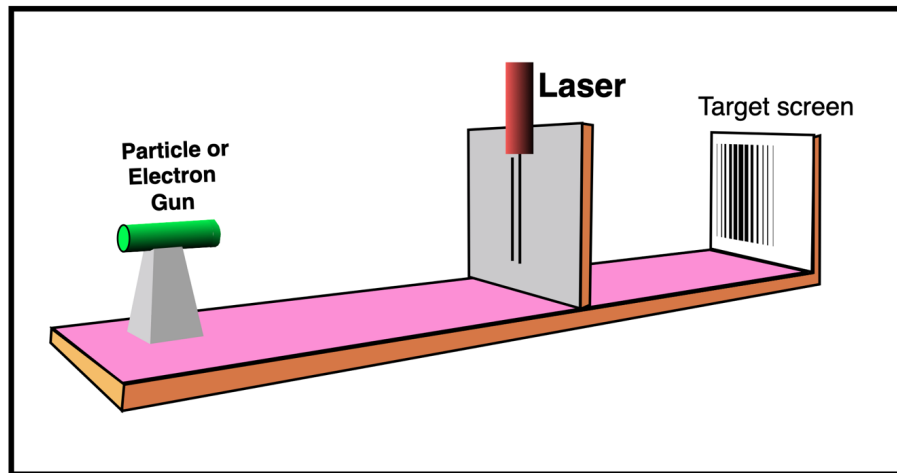


Fig. 63. Particles are fired one at a time, and at the same instant a powerful laser fires down and closes the right-hand slit. TEW predicts the target screen will display an interference-fringe pattern shifted to the left.

The TEW prediction is based on when interference occurs, namely before particle emission. At that time both slits are open. Therefore, there will be interference among the different Elementary Rays moving toward the gun. That interference will be encoded in the trajectories of particles emitted following Elementary Rays backwards. Since the right slit is closed when a particle gets there, only the left slit will be open for particles to inscribe that pattern on the target screen.

If this proves to be true, it will refute a claim of wave-particle-duality: that it is impossible to simultaneously see an interference fringe pattern and know which slit a particle used.

The next two experiments are based on the apparatus shown in the next Figure. In the following two experiments both slits are always open. A “vanishing screen” is inserted in front of the target screen. The vanishing screen is designed so it is opaque to particles until the nanosecond that a particle is fired, and then becomes transparent. Alternatively, it needs to be transparent until the particle is fired, and then it becomes opaque. Particles are fired one at a time, with a pause in between.

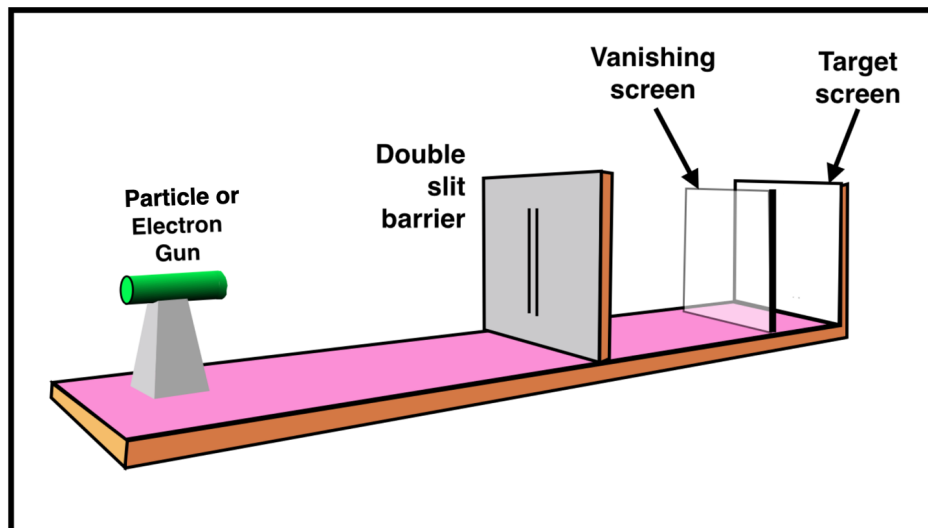


Fig. 64. A screen that switches between opaque and transparent is inserted into a double slit experiment. This will be used in the next two experiments, shown in the next two Figures.

Starting with an opaque “vanishing screen,” elementary rays emanating from all points of that screen will penetrate backwards through the two slits and interfere near the particle gun. Then the gun is fired. If a particle chooses to follow an elementary ray backwards, it is programmed to strike the vanishing screen (if it were opaque) in the familiar aqua-blue pattern. But we trick nature. The vanishing screen is nowhere to be found, having become transparent.

Those particles travel along straight green trajectories until they hit the “target screen” where they inscribe the orange pattern. This is a screwy pattern: not what we would expect. For example, in the center of the screen there is a valley (a white area), where we had expected the tallest probability mountain.

The equipment is designed so nature can vote for one theory or the other. The next figure shows what TEW predicts the outcome data (in orange) to look like. If TEW is wrong and QM is correct, then the target screen will have on it a traditional double-slit pattern like the one shown in aqua blue on the transparent screen.

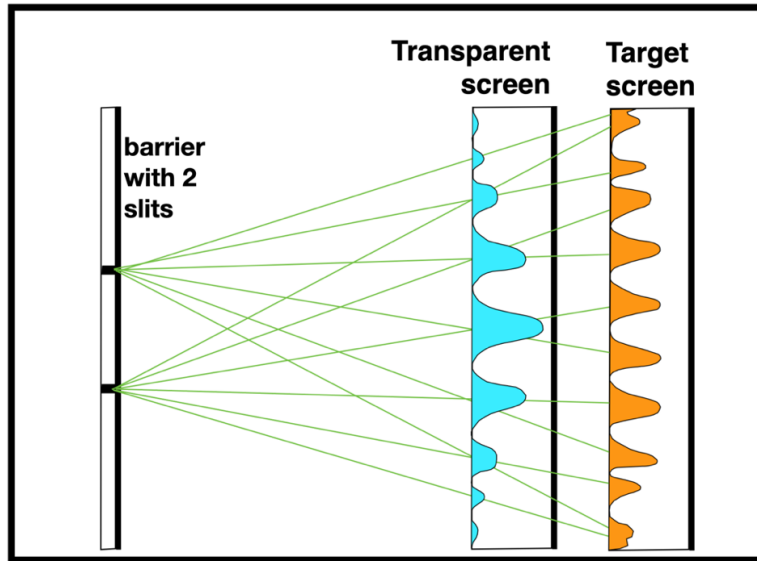


Fig. 65. When the vanishing screen starts opaque then becomes transparent, the orange pattern appears like this on the always-opaque target screen. If the final pattern on the target screen has an orange mountain range like that shown, then TEW is correct, and QM is wrong. If on the other hand the orange mountain range has a familiar pattern with the tallest peak in the center, then QM is correct and TEW is wrong.

In the next experiment the “vanishing screen” starts out transparent. Elementary rays start at the target screen on the far right, pass left through the transparent “vanishing screen” and interfere between the double slit barrier and the particle gun. The particles that follow these rays backwards are programmed to make the blue curve on the target screen. But we trick nature again. We abruptly insert a barrier that wasn’t there before: the vanishing screen suddenly becomes opaque. When the particles hit that screen they inscribe another screwy pattern, as shown in orange. But only if TEW is correct and wave-particle-duality wrong.

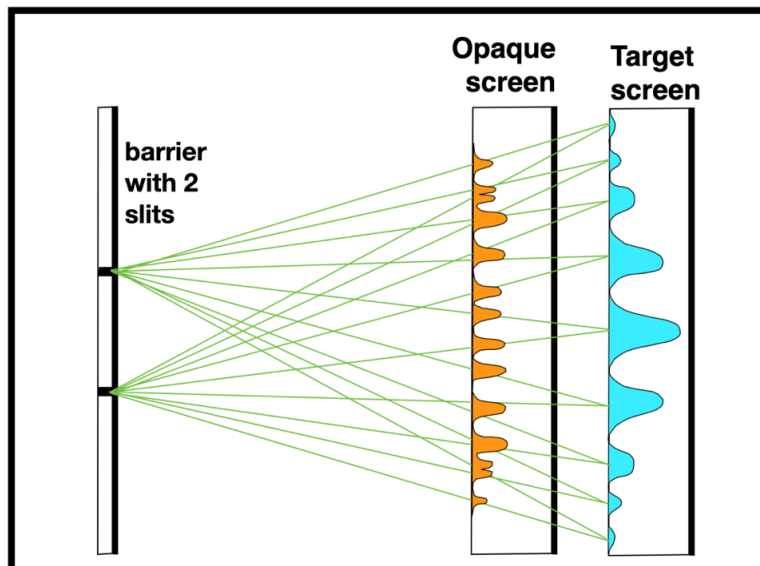


Fig. 66. When the vanishing screen starts transparent then becomes opaque, the orange pattern appears like this. Again, it is the orange pattern that is the pivotal focus that tells us whether wave-particle-duality or TEW is correct, given that they cannot both be correct.

Thus, nature can vote for one theory or the other.



4.3 Wave-Equations

4.3.1 Thumbnail Sketch of the Wave-Equations We Will Now Derive

We will now develop wave-equations to explain how a quantum particle could follow a zero-energy wave backwards. This is no easy trick. If you think of a beach ball thrown into ocean waves, the waves carry the ball in the same direction as the waves. How could a wave-equation explain a particle traveling in the countervailing direction? Our trick is to introduce a U-turn, so that a plane wave (Elementary Wave) flowing out of a detector reverses direction and then transforms from a zero-energy plane wave into a Schrödinger wave-packet capable of transporting a particle toward the detector from which the Elementary Wave is continuing to flow. If you fast-forward to Figures 70-72 at the bottom of this section you will see the three pictures this author is most proud of, which explain our model. That is a theme in this article: pictures speak to the human imagination in a way that equations fail to do. Ordinary humans (non-mathematicians) think in pictures and videos, more than they think in equations.

4.3.2 Deriving Wave-Equations

We will now derive one-dimensional wave equations that would allow a particle to follow a zero-energy Elementary Wave backwards. What we build is not necessarily the way nature does it. We seek only to demonstrate that it is possible.

The following Figure is a roadmap so the reader can keep track of our equations.

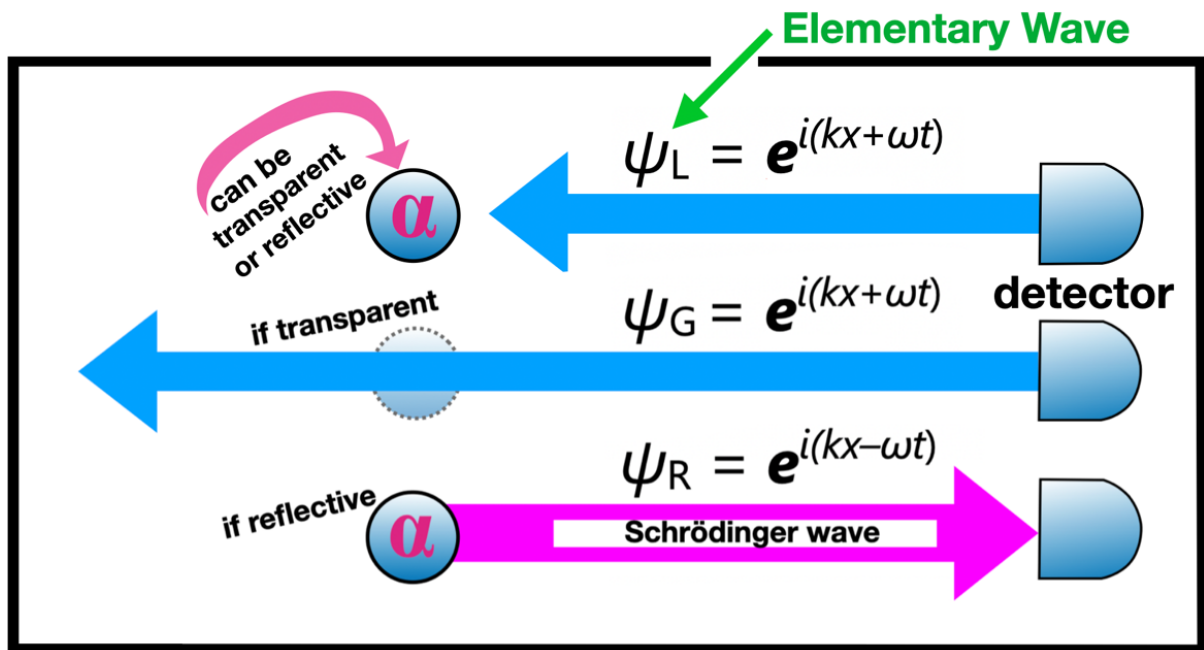


Fig. 67. Top: zero-energy plane wave ψ_L emanates from a detector toward particle α . Middle: the wave almost always passes through the particle without interacting. We call such waves ψ_G where “G” is for “ghost.” The overwhelming majority of waves are “ghosts”, meaning they don’t connect with physical nature. Bottom: Sometimes the particle will reflect the wave ($\psi_L \rightarrow \psi_R$), so it becomes a zero-energy plane wave ψ_R moving to the right. As the wave reflects it blossoms from a plane into a Schrödinger wave capable of carrying a photon or the particle from point α to the detector. The equations below give mathematical symbols illuminating the previous sentence.

We will start with a wave equation, which yields two plane waves (ψ_L and ψ_R).

A standard wave equation is

$$\Psi = e^{ik \pm \omega t}$$

So, the wave to the left (“L”) is

$$\Psi_L = e^{ik + \omega t}$$

and to the right (“R”) it is



$$\Psi_R = e^{ik-\omega t}$$

Usually, two solutions to a linear PDE can be added together to produce a third solution. But in this case the wave traveling to the left ψ_L is a plane wave, while the one traveling to the right ψ_R instantly transforms from a plane into a Schrödinger wave by methods we are about to describe. So, ψ_L and ψ_R are not of the same species, and should not be added.

The subscript “_R” in these equations no longer means “Reverse” as it did in the Feynman path integral equations. Now “_R” means “right”, and “_L” is “left.”

Someone might wonder why the point particle α isn't washed away by the wave, rather than causing the wave to reflect. Well, it is a zero-energy wave, incapable of washing anything away. Our purpose is not to build the equation most people would expect, but to build an equation that mimics nature.

When Murray Gell-Mann and George Zweig proposed equations showing three quarks in each proton and neutron, those were equations that no one expected, nor was it comfortable to think that way. What they proposed was more ludicrous than our idea of plane waves reflecting off a point particle α and flowering into a Schrödinger wave. Our point is that we are not seeking to derive wave equations that look respectable. We are seeking equations that imitate nature.

What we see in nature is that Elementary Waves usually pass through a particle without interacting (middle of Figure 67). It was Einstein who coined the term “ghost waves” for waves that don't interact with physical reality. Einstein thought that a zero-energy wave would not have enough energy to make a detector “click,” and therefore we would never know it was there. TEW deals with this problem by saying that it is particles that make detectors “click.” The reason zero-energy waves interact with the physical world is that quantum particles have an intrinsic capacity to be triggered by a zero-energy wave, and then follow that wave backwards. Thus, it is the particles that do the heavy lifting.

The reason zero-energy waves impinge on physical reality at all, is because quantum particles have a vulnerability to or unmet need for them.

Side comment: given that there are 17 particles in the Standard Model, how many different species of Elementary Waves are there? Answer: we don't know.

Particle α is almost always “transparent” and almost never “reflective.” If it is reflective, we move to the bottom of Figure 67 where the wave makes a “U” turn as it interacts with the particle.

As the plane wave ψ_L reflects off the particle α it immediately blossoms from a plane into a Schrödinger wave. Here are the equations to show how that might happen.

We define

$$\lambda = \frac{2\pi\hbar}{mv}$$

where m and v are the mass and velocity of the particle. We define

$$k = p/\hbar \quad \text{and} \quad p = mv$$

where p is the momentum of the particle. We define $E = \text{kinetic energy} + \text{potential energy}$.

$$E = \frac{1}{2}mv^2 + u = \frac{p^2}{2m} + u$$

Taking the second derivative $\partial^2/\partial x^2$ of the wave function $\psi_R = e^{i(kx-\omega t)}$ we get:

$$\frac{\partial^2\psi_R}{\partial x^2} = \frac{\partial^2}{\partial x^2}(e^{i(kx-\omega t)}) = (ik)^2\psi_R = -k^2\psi_R = \frac{p^2}{\hbar^2}\psi_R$$

$$\hbar^2 \frac{\partial^2\psi_R}{\partial x^2} = p^2\psi_R$$

Multiplying both sides of $E = (p^2/2m) + u$, by ψ_R , we get:

$$E\psi_R = \frac{p^2\psi_R}{2m} + u\psi_R$$

Inserting the earlier equation, we get the **Time Independent Schrödinger Equation (TISE)**:

$$E\psi_R = -\frac{\hbar^2}{2m} \frac{\partial^2\psi_R}{\partial x^2} + u\psi_R = \mathbf{TISE}$$

The time dependent equation can easily be derived by differentiating our wave equation

$$\psi_R = e^{i(kx-\omega t)} \quad \text{by } \partial/\partial t:$$

$$\frac{\partial\psi_R}{\partial t} = -i\omega\psi_R$$

We define $E = \hbar\omega$. Multiplying that by ψ_R we get:

$$E\psi_R = \hbar\omega\psi_R$$

$$-\frac{i}{\hbar}E\psi_R = -i\omega\psi_R = \frac{\partial\psi_R}{\partial t}$$

$$E\psi_R = -\frac{\hbar}{i} \frac{\partial\psi_R}{\partial t} = i\hbar \frac{\partial\psi_R}{\partial t}$$

We can substitute that into the TISE, and that gives us

$$i\hbar \frac{\partial\psi_R}{\partial t} = -\frac{\hbar^2}{2m} \frac{\partial^2\psi_R}{\partial x^2} + u\psi_R = \mathbf{TDSE}$$

which is the **Time Dependent Schrödinger Equation (TDSE)**.

As expected, the Schrödinger equation has a “+” sign, not a “-” sign. Why is that what we want? You must appreciate that our wave makes a “U” turn. There is no word available to describe a “U” shaped arrow that makes a hairpin curve. Consider the following Figure.

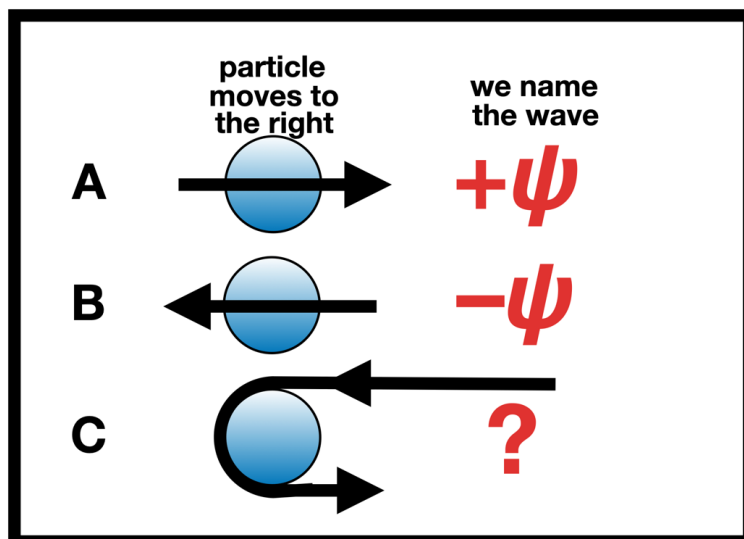


Fig. 68. In these diagrams a particle (blue) is moving to the right. By convention, the direction of the wave is in reference to the particle. In the top row we name a wave moving to the right “ $+\psi$ ”. Middle row, we name a wave moving left “ $-\psi$ ”. Bottom row: what do we name a wave that makes a “U” turn? We have no term “ $-\psi$ ”.

In the bottom row of the last Figure, the wave travels in both directions relative to the particle. The next Figure describes that third arrow in more detail:

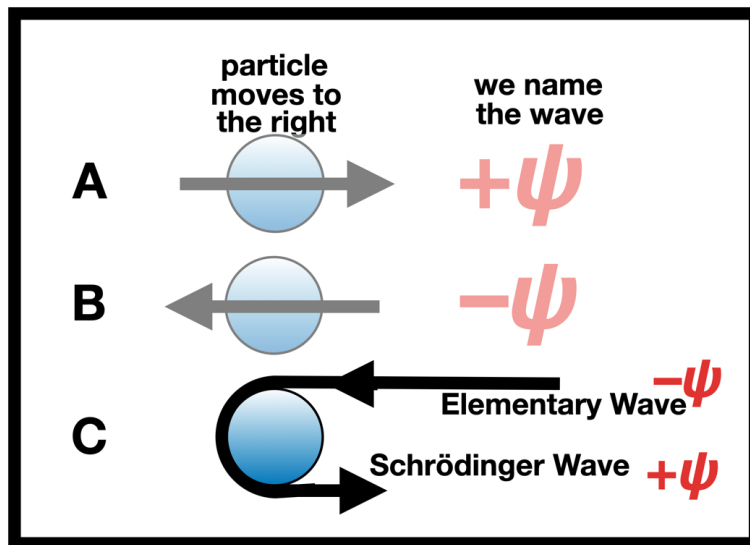


Fig. 69. This reproduces the preceding Figure but clarifies which is the “Elementary Wave” and which is the “Schrödinger wave.”

Figure 69 makes it clear why our Schrödinger wave should have a “+” sign. That does not contradict our thesis, namely that nature uses $-\psi$ in quantum equations (referring to the “Elementary Wave” before the “U” turn). We say that particles follow zero-energy waves backwards, and overall, we name it $-\psi$.

We are choosing the $-\psi$ Elementary Wave as more important than the $+\psi$ Schrödinger wave.

The bedrock upon which this article rests is what we call the “Max Born asymmetry $|\psi|^2 = |\psi|^2 = \text{probability}$.” We claim that nature is on one side of that asymmetry, and garden-variety QM is on the other. A mountain of experimental data says we are right. For these reasons we assert that Figure S61-C should be interpreted as “ $-\psi$ ”, meaning that the Elementary Wave is more important than the Schrödinger wave in Figure 69.

If the reader disagrees and insists that the Schrödinger wave is the more important of the two, and therefore the “U” shaped wave in Figure 69-C should be named “ $+\psi$ ”, that means that the “U” shaped wave name is indistinguishable from the straight “ $+\psi$ ” wave in the top of Figure 68. That makes no sense. That interpretation would ignore the “U-turn” reversal of direction, and it would ignore the mountain of empirical evidence presented in this article.



4.3.3 Visualizing Elementary Waves

4.3.3.1 Thumbnail Sketch of How Elementary and Schrödinger Waves Interact

It is one thing to derive a Schrödinger wave equation, but it is more compelling if we can give you a video of how it works in real life. We provide the next 3 Figures to explain how Elementary Waves cause Schrödinger wave-packets to travel toward the detector at two different times, T1 and T2. The following diagrams summarize this article. We start with a Figure that explains quantum tunneling from our point-of-view.

Below are three snapshots of a zero-energy Elementary Wave (“ $-\psi$ ”) followed backwards by a Schrödinger wave-packet (“ $-\psi$ ”) moving across a one-dimensional line. Halfway across each line is an obstacle: a barrier, well, or wall.

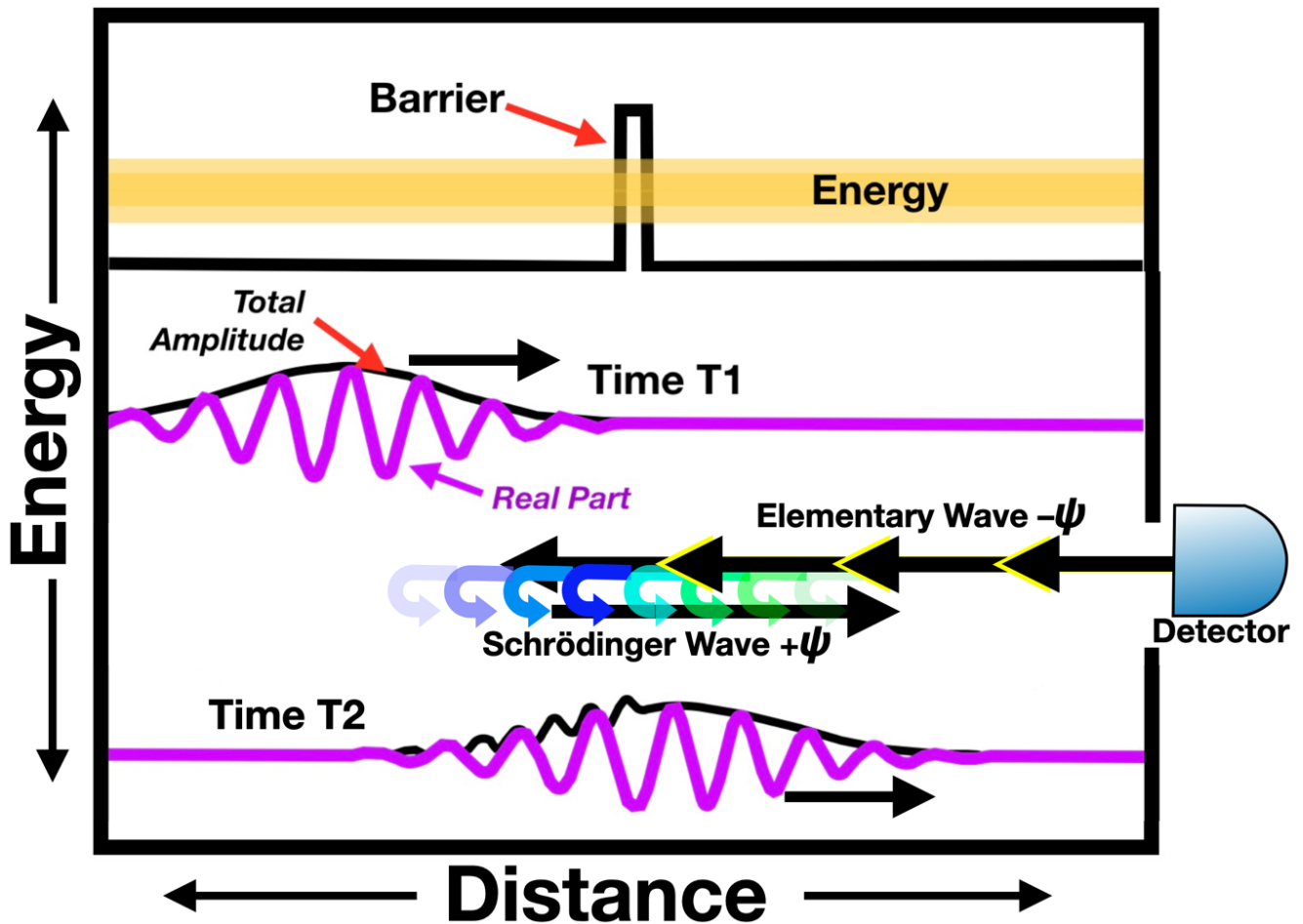


Fig. 70. Tunneling: A thin barrier is at the top center. A Schrödinger wave-packet ($+\psi$) follows backwards an Elementary Wave ($-\psi$) coming from a detector on the right. At time T1 (middle) the Schrödinger wave approaches a barrier. At time T2 (bottom) most but not all the Schrödinger wave tunnels through the barrier and keeps moving to the right.

What is “tunneling”? Consider your smartphone. Tunneling is used by the memory cells inside your smartphone. In a charge-trap-flash memory unit, electrons tunnel through a wall of dielectric material to enter an energy well, where they remain trapped, for hours, days, or years. This is how your smartphone stores information. For example, if you snap a picture to post online, the picture is stored inside your smartphone in thousands of such charge-trap-flashes, each based on tunneling. Engineers who design charge-traps follow the tunneling equations developed by Ralph Fowler and Lothar Nordheim in the 1920’s. There are millions of these charge-trap-flash units inside your phone.

We said earlier that the classical and quantum world are governed by the same rulebook except for size. Some critics object, saying that tunneling is found in the quantum but not in the classical world. We disagree. We claim that a human, if downsized to quantum size, would be able to walk through a wall. Unfortunately, the person might suffer catastrophic damage from the downsizing process.

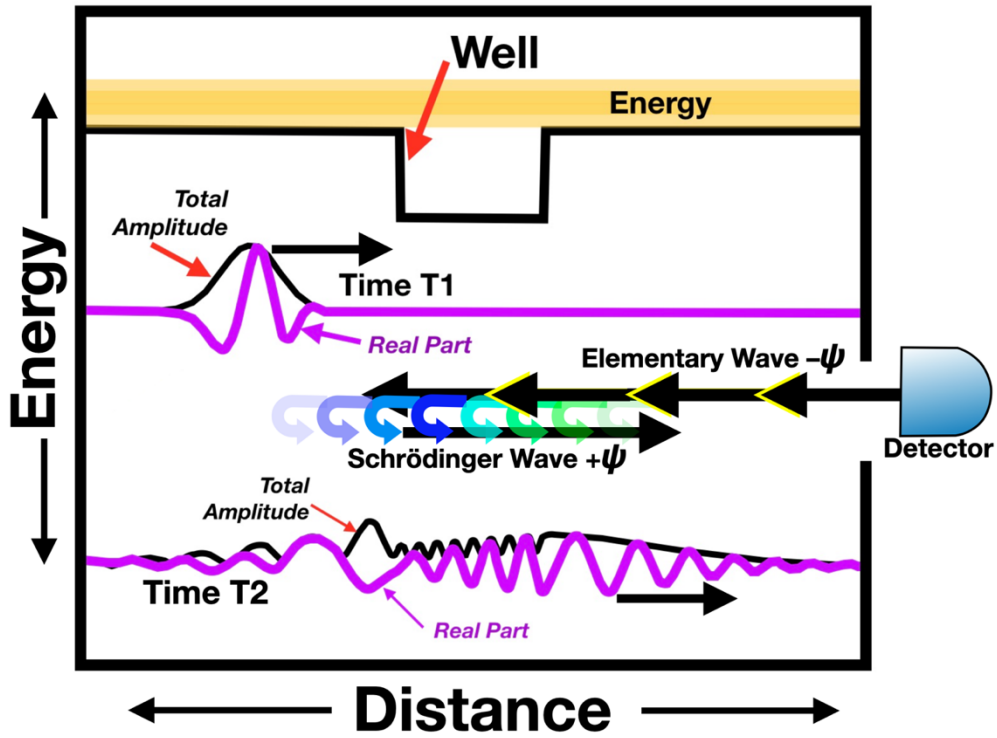


Fig. 71. Here is a one-dimensional potential energy well in the center at the top. A Schrödinger wave-packet ($+\psi$) follows backwards an Elementary Wave ($-\psi$) coming from a detector on the right. At time T1 (middle) the Schrödinger wave approaches the energy well. At time T2 (bottom) much of the wave packet crosses the well, some of it is reflected by one or the other side of the well, and waves are found inside the well. Some of the wave reflects off the right side of the well and then reflects off the left side also, like an echo chamber. A few reflected waves move to the left.

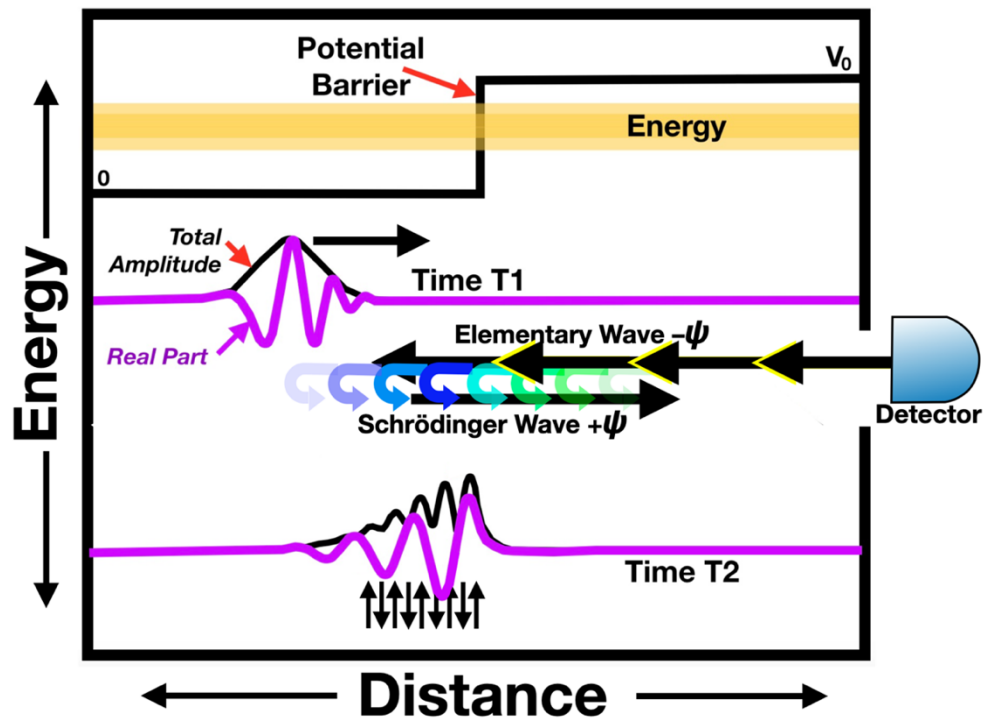


Fig. 72. Here is a one-dimensional potential energy barrier in the center at the top. A Schrödinger wave-packet ($+\psi$) follows backwards an Elementary Wave ($-\psi$) coming from a detector on the right. This diagram shows snapshots at two different times: T1 in the middle, as the Schrödinger wave approaches the barrier it loses

References:

1. J. Baggott, *The Quantum Story: a history in 40 moments*, Oxford University Press, (2011). ISBN:978-0-19-956684-6
2. M. Born, "On the quantum mechanics of collisions," in J. A. Wheeler and W. H. Zurek (eds.), *Quantum Theory and Measurement*, Princeton, 50-55, (1983). ISBN 978-0-691-08316-2.
3. J.H. Boyd, "The Max Born asymmetry topples the Many-Worlds Theory," *Journal of Advances in Physics*, 20, 143-169, (2022). DOI: 10.24297/jap.v20i.9114
4. J.H. Boyd, "Common-sense rejected by physicists: a level-headed approach to time and quantum physics," *Journal of Advances in Physics*, 19, 233-280, (2021). DOI: 10.24297/jap.v19i.9115
5. J.H. Boyd, "PDE boundary conditions that eliminate quantum weirdness: a mathematical game inspired by Kurt Gödel and Alan Turing," *Journal of Advances in Mathematics*, 20, 211-213, (2021). DOI: 10.24297/jam.v20i.9042
6. J.H. Boyd, "Six reasons to discard wave-particle duality," *Journal of Advances in Chemistry*, 18, 1-29, (2021). DOI: 10.24297/jac.v18i.8948
7. J.H. Boyd, "The Periodic Table needs negative orbitals in order to eliminate quantum weirdness," *Journal of Advances in Chemistry*, 17, 88-125, (2020). DOI: 10.24297/jac.v17i.8865
8. J.H. Boyd, "There are two solutions to the equations of Feynman's Quantum Electrodynamics (QED)," *Journal of Advances in Physics*, 18, 39-57, (2020). DOI: 10.24297/jap.v18i.8831
9. J.H. Boyd, "If the propagator of QED were reversed, the mathematics of Nature would be much simpler," *Journal of Advances in Mathematics*, 18, 129-153, (2020). DOI: 10.24297/jam.v18i.8746
10. J.H. Boyd, "A tiny, counterintuitive change to the mathematics of the Schrödinger wave-packet and Quantum Electro-Dynamics could vastly simplify how we view Nature," *Journal of Advances in Physics*, 17, 169-203, (2020). DOI: 10.24297/jap.v17i.8696
11. J.H. Boyd, "New Schrödinger wave mathematics changes experiments from saying there is, to denying there is quantum weirdness," *Journal of Advances in Mathematics*, 18, 82-117, (2020). DOI: 10.24297/jam.v18i.8656
12. J.H. Boyd, "Decrypting the central mystery: 1. The double-slit experiment," *Journal of Advances in Mathematics*, 17, 255-282, (2019). DOI: 10.24297/jam.v17i0.8475
13. J.H. Boyd, "Decrypting the central mystery: 2. A mountain of empirical data supports TEW," *Journal of Advances in Mathematics*, 17, 283-314, (2019). DOI: 10.24297/jam.v17i0.8489
14. J.H. Boyd, "Decrypting the central mystery: 3. A non-Einstein, non-QM view of Bell test experiments," *Journal of Advances in Mathematics*, 17, 315-331, (2019). DOI: 10.24297/jam.v17i0.8490
15. J.H. Boyd, "Decrypting the central mystery: 4. In what medium do Elementary Waves travel?" *Journal of Advances in Mathematics*, 17, 332-351, (2019). DOI: 10.24297/jam.v17i0.8491
16. J.H. Boyd, "The quantum world is astonishingly similar to our world," *Journal of Advances in Physics*, 14, 5598-5610, (2018). DOI: 10.24297/jap.v14i2.7555
17. J.H. Boyd, "The von Neumann and double-slit paradoxes lead to a new Schrödinger wave mathematics," *Journal of Advances in Physics*, 14, 5812-5834, (2018). DOI: 10.24297/jap.v14i3.7820
18. J.H. Boyd, "The Boyd Conjecture," *Journal of Advances in Physics*, 13, 4830-4837, (2017). DOI: 10.24297/jap.v13i4.6038
19. J.H. Boyd, "A symmetry hidden at the center of quantum mathematics causes a disconnect between quantum math and quantum mechanics," *Journal of Advances in Mathematics*, 13, 7379-7386, (2017). DOI: 10.24297/jam.v13i4.6413
20. J.H. Boyd, "Paul Dirac's view of the Theory of Elementary Waves," *Journal of Advances in Physics*, 13, 4731-4734, (2017). DOI: 10.24297/jap.v13i3.5921
21. J.H. Boyd, "A paradigm shift, 1: The Theory of Elementary Waves (TEW)," *Journal of Advances in Mathematics*, 10, 3828-3839, (2015). DOI: 10.24297/jam.v10i9.1908
22. J.H. Boyd, "A paradigm shift, 2: A new local realism explains Bell test and other experiments," *Journal of Advances in Mathematics*, 10, 3828-3839, (2015). DOI: 10.24297/jam.v10i9.1884

23. J.H. Boyd, "A paradigm shift, 3: A mirror image of Feynman's quantum electrodynamics (QED)," *Journal of Advances in Mathematics*, 11, 3977-3991, (2015). DOI: 10.24297/jam.v11i2.1283
24. J.H. Boyd, "A paradigm shift, 4: Quantum computers," *Journal of Advances in Mathematics*, 17, 315-331 (2019). DOI: 10.24297/jam.v17i0.8490
25. J.H. Boyd, "A new variety of local realism explains a Bell test experiment," *Journal of Advances in Physics*, 8, 2051-2058, (2015). DOI: 10.24297/jap.v8i1.1541
26. J.H. Boyd, "Re-thinking a delayed choice quantum eraser experiment" *Physics Essays*, 26, 100-109, (2013). DOI: 10.4006/0836-1398-26.1.100
27. J.H. Boyd, "Re-thinking Alain Aspect's 1982 Bell test experiment," *Physics Essays*, 26, 582-591 (2013). DOI: 10.4006/0836-1398-26.1.100 10.4006/0836-1398-26.4.582
28. J.H. Boyd, "Rethinking a Wheeler delayed choice gedanken experiment," *Physics Essays*, 25, 390-396, (2012). DOI: 10.4006/0836-1398-25.3.390
29. C.J. Davisson and L.H. Germer, "Scattering of electrons by a single crystal of nickel," *Nature* 119, 558-560 (1927). DOI: 10.1038/119558a0
30. P.A.M. Dirac, *The Principles of Quantum Mathematics*, Oxford University Press, New York, 1991. ISBN 0-19-852011-5.
31. R.P. Feynman, *QED: The Strange Theory of Light and Matter*, Princeton University Press, (1985). ISBN 978-0-691-12575-6
32. R.P. Feynman, *Feynman Lectures on Physics*, 3. New York: Basic Books, (1966). ISBN 0-20102114-9-H.
33. R.P. Feynman and A.R. Hibbs, *Quantum Mechanics and Path Integrals*, Mineola, NY: Dover Publications, (c1965). ISBN-13 978-0-468-47722-0.
34. M. Giustina, "Significant loophole-free test of Bell's-theorem with entangled-photons". <https://www.youtube.com/watch?v=tgoWM4Jcl-s>
35. V. Jacques, et.al., "Experimental verification of Wheeler's delayed-choice gedanken experiment," *Science*, 315, 966-8 (2007). DOI: 10.1126/science.1136303
36. H. Kaiser, et.al., "Coherence and spectral-filtering in neutron-interferometry." *Physical Review A*, 45, 31-42, (1992). DOI: 10.1103/PhysRevA.45.31
37. Y.H. Kim, et.al., "A delayed-choice quantum-eraser." *Physical Review Letters* 84, 1-5, (2000). DOI: 10.1103/PhysRevLett.84.1
38. L.E. Little, "Theory of Elementary Waves," *Physics Essays*, 9, 100-134, (1996). DOI: 10.4006/1.3029212
39. R.L. Pfleegor and L. Mandel, "Interference of independent photon beams," *Physical Review*, 159, 1084 (1967). DOI: 10.1103/PhysRev.159.1084
40. E. Schrödinger, *Collected Papers on Wave Mechanics*, Montreal: Minkowski Institute Press, (2020), ISBN: 978-1-927763-81-0.